University of Southampton
Faculty of Engineering and Applied Science
Electronics

STIMULATED RAMAN PROCESSES IN METAL VAPOURS

by

WALTER H.W. TUTTLEBEE

Thesis submitted for the Degree of
Doctor of Philosophy

December 1977

CONTENTS

UNIVERSITY OF SOUTHAMPTON

ABSTRACT

FACULTY OF ENGINEERING AND APPLIED SCIENCE

ELECTRONICS

Doctor of Philosophy

STIMULATED RAMAN PROCESSES IN METAL VAPOURS

by Walter H.W. Tuttlebee

Recent work has demonstrated the potential of stimulated electronic Raman scattering, SERS, as a tunable IR source. The current work has aimed at an extension of the performance of SERS in the two areas of tuning capability and narrower linewidth; to this end a variety of stimulated electronic Raman schemes have been investigated.

Initially the theoretical background of SERS and of various possible competing processes is reviewed. The construction and performance of the dye lasers and heat pipe ovens used for the work are then described, followed by a presentation and discussion of the experimental work performed; this work falls into four main areas.

Firstly the potential of pump and SERS feedback schemes to extend the tuning ranges of an existing alkali metal SERS system, Cs 6s-7s, has been investigated, under non-optimum conditions; results from this appear promising for future work.

Secondly, we have demonstrated for the first time the possibility of obtaining a tunable IR output from a fifth order nonlinear process, stimulated hyper-Raman scattering, SHRS, in Na vapour. Various aspects of theory and behaviour of this process are described.

The advantages of obtaining SERS from an excited initial state have been considered; preliminary results have proved disappointing and have led us to consider possible limiting mechanisms in such processes.

Finally SERS in alkaline earths is considered; only few such schemes would appear to be viable for various reasons. One such scheme in Ba has however yielded a $0.2cm^{-1}$ system-limited SERS linewidth, a narrower SERS linewidth than has previously been attained; indications are that narrower linewidths still may be attainable, although further work will be necessary to verify this. These results also suggest that the optical Stark effect and power broadening have less influence on the Raman linewidth than has previously been thought.

ACKNOWLEDGEMENTS

I wish to gratefully acknowledge the oversight, help and encouragement given to me during this research by my supervisor, Dr D C Hanna.

Through much informative discussion and practical assistance, thanks have been earned by Dr R Wyatt. Dr M A Yuratich has been most patient with me in my efforts to theorise and I am indeed very grateful for his aid in many such areas. Dr D Cotter collaborated in the work using Na, constructing the heat pipe oven and sharing in the experimental measurements, for which I am most grateful.

Thanks also go to Mr A J Turner, for giving of his knowledge of electronics particularly, and to Mr G G Wills and Mr A R Henderson for coating mirrors and etalons for me. I should also like to express my thanks to my other colleagues in the Electronics and Chemistry Departments who have given so freely of their time, advice and practical aid at various times during the work.

For the construction of heat pipes and dye laser components my thanks go to the members of the Electronics Department workshop.

My deep appreciation is also expressed to my flatmates and close friends in the Community Church, particularly to David and Ruth Spencer and family, who have encouraged and supported me so much during the writing of this thesis.

Finally I wish to thank Sue Meen for her patient efforts in typing this work for me.

CHAPTER 1

Introduction

Advances in tunable laser sources over the last ten years or so have been accompanied by a complementary increase in specific applications in widely varying fields. Tunable infrared radiation in particular has been recognised as a powerful tool, since most molecules have vibration-rotation bands falling in this region of the electromagnetic spectrum. Recent work has indicated the capabilities and potential of tunable infrared lasers in areas of linear and non-linear spectroscopy (Walther 1975, Letokhov and Chebotayev 1977), laser induced photochemistry, including time resolved measurements (West 1977, Mooradian et al 1976) and remote atmospheric pollution monitoring (Hinkley 1976, Mooradian et al 1976) amongst others. With such a large realm of potential applications much research has gone into the understanding and development of devices capable of producing tunable coherent radiation in the infrared by various methods; thus, we shall briefly consider some of these approaches, including that of stimulated electronic Raman scattering, SERS, in metal vapours, in order to set the current work in context.

1.1 Tunable Laser Sources

There have been some comprehensive reviews of tunable lasers over the last few years (Colles and Pidgeon 1975, Kuhl and Schmidt 1974) from which some of the following information has been taken; more recent work has been described in the proceedings of the Loen conference in Norway 1976 (Mooradian et al 1976) and in other recent literature, cited where appropriate.

Perhaps the most familiar and widespread tunable laser in use today is the dye laser. Since its invention in 1966 by Sorokin its development has been both rapid and diverse in expression, resulting in cw or pulsed operation, laser pumped or flashlamp pumped, broad- or narrow-band, modelocked or otherwise. The dye laser has become widely used because of the vast fields of experiments opened up by a high power and brightness tunable source; its versatility and, in some forms, relative cheapness and simplicity have also contributed to its proliferation. Whilst used in its own right for original research, considerable effort has still been put into further extensions of its capabilities.

The fundamentals of dye lasers are well discussed in Schäfer 1973, and the more recent developments can be essentially divided into three areas - engineered designs, new dyes and new pumping methods. Cw devices in particular are readily available now as fairly expensive yet reliable engineered systems; recent progress in laboratory set-ups in terms of power and tuning is reported by Anliker 1977 and Romanek 1977. More recently laser pumped pulsed systems have reached the engineering stage and come onto the commercial market; Kato 1976, reports the performance of a pulsed Nd:YAG second harmonic pumped system, typically characterised by the high power attainable. Progress in flashlamp pumped designs has again been in the areas of power and tunability (see eg Schäfer 1976).

It was recognised early on that laser dyes fell into distinct chemical families, eg the xanthenes, oxazones etc, and more recent work especially has concentrated on the synthesis of new dyes by a modification to an established dye structure. This approach, combining theory with 'scientific intuition' is resulting in new dyes still being discovered for laser pumped, pulsed and cw, and flashlamp pumped use (eg Basting 1976, Schimitschek 1976 and Rullière 1976).

The term 'new pumping methods' refers to the advent of high power excimer lasers, notably XeF emitting at 350nm and KrF at 248nm. The potential of these lasers for dye laser pumping is just beginning to be explored, but at first sight would appear to be great, providing high pump powers in the ultraviolet at high repetition rates. Preliminary work pumping new dyes with a KrF device has been carried out by Rullière 1977; Bücher and Chow 1977 have obtained powers up to 1MW of dye laser radiation tunable between 320-365nm pumping with 8MW at 248nm.

A less common and less versatile tunable source is the semiconductor diode laser. This device has a relatively low power emission line, cw or pulsed, somewhere in the region 0.3-30μm, the wavelength being determined by its band gap (which is composition dependent); tuning of the output is then effected by modifying the band gap and/or the longitudinal modes of the optical cavity - current (temperature) tuning is probably the most widely used. The need to operate at liquid nitrogen or helium temperatures has been a drawback although recent developments seem to be overcoming this and also resulting in wider tuning ranges (see Mooradian 1976). This device has been used in

Table 1.1

Representative mixing experiments with dye laser sources

Source	Nonlinear crystal	Infrared tuning range (μm)	Output power (peak) and linewidth	Reference
Ruby laser and ruby pumped dye laser (0.84–0.89 μm)	$LiNbO_3$	3–4	6 kW 3–5 cm^{-1}	*C.F. Dewey, Jr, L.O. Hocker*: Appl. Phys. Lett. **18**, 58 (1971)
Ruby laser and ruby pumped dye laser (0.73–0.75 μm)	Ag_3AsS_3 (proustite)	10–13 4.9	0.1 W 6 W	*D.C. Hanna, R.C. Smith, C.R. Stanley*: Opt. Commun. **4**, 300 (1971)
Ruby laser and ruby pumped dye laser (0.8–0.83 μm)	$LiIO_3$	4.1–5.2	100 W	*D.W. Meltzer, L.S. Goldberg*: Opt. Commun. **5**, 209 (1972)
Ruby laser and ruby pumped dye laser (0.79–0.78 μm)	Ag_3AsS_3 (proustite)	3.2–6.5	100 W	*C.D. Decker, F.K. Tittle*: Appl. Phys. Lett. **22**, 41 (1973); Opt. Commun. **8**, 244 (1973)
Ruby laser and ruby pumped dye laser (0.74–0.808 μm)	$AgGaS_2$	4.6–12	0.3 W	*D.C. Hanna, V.V. Rampel, R.C. Smith*: Opt. Commun. **8**, 151 (1973)
Flashlamp pumped dye laser (0.58–0.62 μm)	$AgGaS_2$	8.7–11.6	10^{-4} W	*D.C. Hanna, V.V. Rampel, R.C. Smith*: IEEE J. QE-**10**, 461 (1974)
Q-switched Nd:YAG laser at second-harmonic dye laser (0.635–0.66 μm)	$LiIO_3$	2.8–3.4	80 mW	*H. Tashiro, T. Yajima*: Opt. Commun. **12**, 129 (1974)
Flashlamp pumped dye lasers (0.44–0.62 μm)	$LiIO_3$	1.5–4.8	0.4 W 0.5 cm	*H. Garlach*: Opt. Commun. **12**, 405 (1974)
Q-switched Nd:YAG laser at 1.06 and 0.532 μm (0.575–0.640 μm)	$LiIO_3$	1.25–1.60 3.40–5.65	70 W 0.5 W 0.08 cm^{-1}	*L.S. Goldberg*: Appl. Opt. **14**, 653 (1975)
Ruby laser and ruby pumped dye laser (0.72–0.76 μm)	GaSe	9.5–17	300 W (0.5 cm^{-1})	*G.B. Abdulaev, L.A. Kulevskii, P.V. Nickles, A.M. Drokhorov, A.D. Savel'ev, E. Yu Salaev V.V. Smirnov*: Sov. J. Quant. Elect. (to be published)
Argon ion laser and cw dye laser (0.56–0.62 μm)	$LiNbO_3$	2.2–4.2	1 μW (cw) (5×10^{-4} cm^{-1})	*A.S. Pine*: J. Opt. Soc. Am. **64**, 1683 (1974)
More recent work:				
Two Ruby pumped dye lasers (0.84-1μm)	Ag_3AsS_3 (proustite)	11-23μm	40W at 11μm 3W at 19μm	L O Hocker, C F Dewey Jr., Appl.Phys. **11**, 137, 1976.
Cw Nd:YAG and dye laser (0.58-0.64μm)	$LiIO_3$	1.3-1.6μm	35μW(cw)	W Lahmann et al., Opt.Commun, **17**, 18, 1976.
Argon ion laser and cw dye laser (0.58-0.62μm)	$LiIO_3$	2.3-4.6μm	4μW(cw)	B Wellegehausen et al., Appl.Phys. **11**, 363, 1976.

(Taken partly from Byer 1977)

preference to others when it has been desired to monitor, say, a specific molecular line (eg Max 1977, Hanson 1977); when different wavelength ranges are required, however, a range of diodes to cover all the regions of interest could prove to be expensive.

Progress in spin flip Raman lasers is also discussed by Mooradian 1976. These devices, needing magnetic fields, cryogenic temperatures and a laser pump are inherently complex; increasing sophistication in the associated technology is gradually resulting in the SFRL becoming more of an engineered device and research tool, as evidenced by recent work by chemists at Newcastle University, Poliakoff et al 1977. The use of an ammonia laser at 12.8μm as the pumping source has also increased the tuning capability of the device (Patel 1976).

Other recent developments receiving attention include optically pumped high pressure gas lasers (Kildal and Deutsch 1976), colour centre lasers (Mollenauer 1975, Gusev 1977) and fibre Raman oscillators (Lin 1977).

One other very important device also warrants mention at this stage, namely the optical parametric oscillator. Using a fixed frequency laser pump (ω_p) the OPO generates a signal (ω_s) and idler (ω_i), such that $\omega_s + \omega_i = \omega_p$, due to the interaction of the pump field and the OPO medium, an optically nonlinear crystal. Early work on the OPO was done as far back as 1965 and devices with good performance were developed (eg Hanna 1972) but further progress was hindered by the practical difficulty of obtaining high quality crystals. Recently however the availability of good quality lithium niobate has resulted in the construction of some sophisticated high performance systems (eg Byer 1977, Wyatt 1977); difference frequency mixing of the signal and idler waves in another nonlinear crystal enables the tuning range to be extended out to beyond 20μm (Wyatt 1977 (private communication) cf Hanna 1974). Fundamentals of the OPO are reviewed by Byer 1977.

Frequency conversion of dye laser radiation in nonlinear crystals has also been widely studied and table 1.1 shows typical results until a few years ago, together with some recent experiments to give some feel for progress since then. Due to the number of stages in such an infrared generation scheme the overall output and efficiency is low; however for

applications requiring medium power and wide tunability this can be a good scheme, although careful consideration needs to be given to factors such as getting good quality co-spatial beams in the crystal.

Both difference mixing and the OPO have suffered in the past with problems associated with the nonlinear crystals, those of optical quality and damage at high laser intensities; this has led to a search for other nonlinear media which could be used instead.

The use of atomic vapours was the new concept which first began to arise as an alternative to crystals. Acentric crystals have a non-zero second order susceptibility $\chi^{(2)}$ which renders them useful for nonlinear optics; in an atomic vapour $\chi^{(2)}$ is zero and the third order susceptibility $\chi^{(3)}$, non-zero for all media, is generally utilized. Normally $\chi^{(3)}$ is very much smaller than $\chi^{(2)}$ in a crystal; also the density of atoms/molecules is much lower in an atomic vapour than a crystal. However $\chi^{(3)}$ can be greatly increased in magnitude by tuning near to an atomic energy level resonance; once this fact was recognised interest in vapours dramatically increased.

Stimulated Raman scattering between electronic energy levels, fig 1.1, was one of the first processes to be discovered in a metal vapour, independently, in 1967 by Sorokin et al and by Rokni and Yatsiv; both experiments used fixed frequency sources. Work by Harris et al at Stanford on third harmonic generation in alkalis followed (Miles and Harris 1973). In the same year Sorokin, Wynne and Lankard at IBM proposed and demonstrated the four wave mixing scheme illustrated in fig 1.2; using a dye laser (ω_p) tuned near to resonance between the ground state and an excited state, SERS occurs producing a wave at ω_s; the mixing of these two waves with a second collinear dye laser (ω_L) results in the generation of the infrared output $\omega_{IR}(= \omega_p - \omega_s - \omega_L)$. Experimentally Wynne et al 1973 reported tuning of this output from 2-4μm in potassium, 2.9-5.4μm in rubidium and from 2-25μ in sodium/potassium mixtures. Further work on this process at Southampton resulted in similar large tuning ranges, although fundamental limitations of the mixing efficiency were revealed; various ASE outputs were also observed, hampering the use of the process for spectroscopy (Kärkkäinen 1975, 1977).

It was at this time that the role of SERS in metal vapours as a process in its own right for generating infrared was appreciated and studied in our own laboratories. Experiments using a high power dye laser and caesium vapour were reported by Cotter 1976a, and a careful

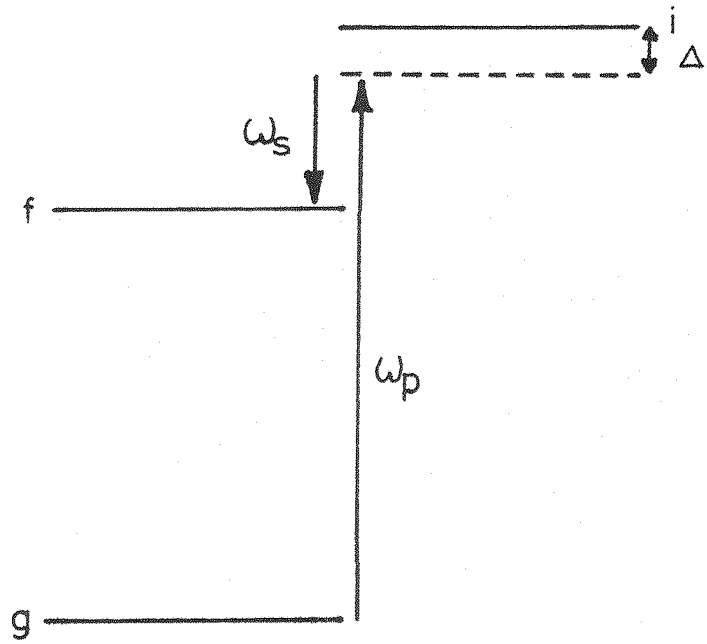

Fig 1.1 The SERS process

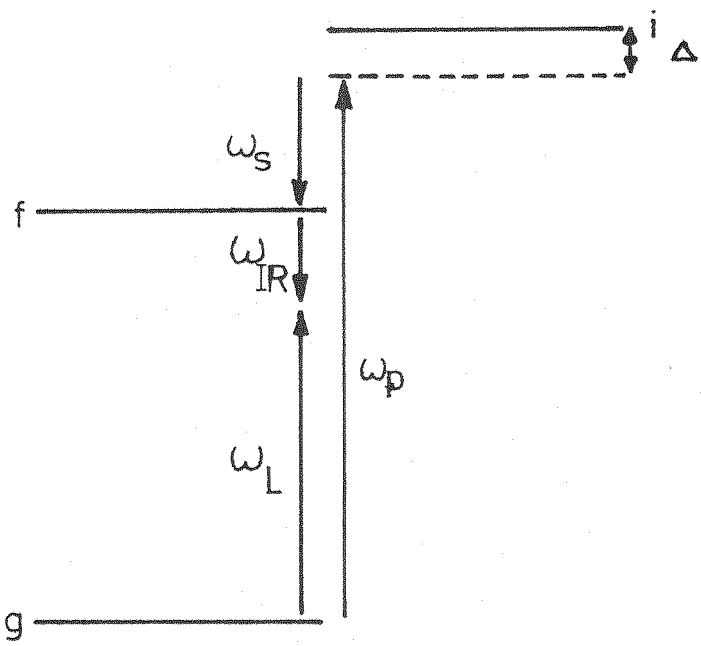

Fig 1.2 Four wave mixing

characterisation of 6s-7s scattering in that metal vapour using a low power pump was subsequently done by Cotter 1976b; this work will be more fully discussed below.

At the time of writing, one further development should be mentioned, namely a great increase in interest and experiments involving stimulated Raman scattering and parametric processes in molecular systems. Liquid nitrogen and high pressure hydrogen and other liquids have been used for a long while for SRS of fixed frequency lasers to provide a high power Raman shifted beam (see eg Grasyuk 1974), but just recently it has been appreciated that tunable SRS and parametric processes such as observed in metal vapours and crystals can also be usefully demonstrated in these media. Frey and Pradère 1976 using a 20-60MW(!) dye laser and successive Stokes shifts in H_2 or CH_4 have yielded 1-20MW from the visible to 4.5μm; this source has recently been used for pumping SRS in liquid N_2 (Frey et al 1977). Four wave mixing type experiments in H_2 are reported by Brosnan 1977 and Loy 1977; the potential for efficient THG in molecules has also been recently demonstrated by Kildal 1977. With metal vapour sources beginning to be well characterised in terms of capabilities, effort is now going into discovering the possibilities of molecular systems.

1.2 SERS in Metal Vapours

SERS metal vapour systems can provide high peak powers, should be readily scalable, have no damage or availability problems like crystals and have advantages of simplicity and cheapness; they can enable a laboratory with a pulsed dye laser to simply extend its capability to regions of the infrared.

The achievements of SERS, prior to this work, are presented in table 1.2, indicating the limitations of tuning and energy; this includes work done at Southampton and also the results of Carlsten and Dunn 1975 using barium. Recently published work using potassium and rubidium by Wynne and Sorokin is also included. From this it can be seen that wide ranges of the spectrum have been covered with high peak powers with a single metal vapour, caesium; the observed linewidth of the radiation is broad, typically $>0.3cm^{-1}$, a restricting factor for some applications.

Table 1.2 - Summary of prior work on tunable SERS in metal vapours

Metal	Transition	Pump power	Tuning range	Power output	Linewidth	Reference
K	4s-5s	25kW	2.56-3.5μm	1kW	$0.4cm^{-1}$	Wyatt 1976, Cotter et al 1975a
Cs	6s-7s	750kW	2.5 -4.75μm	25kW		
	6s-8s	400kW	5.67-8.65μm	7kW	0.3 - $1.4cm^{-1}$	Wyatt 1976, Cotter et al 1976a
	6s-9s	250kW	11.7-15μm	2kW		
	6s-7s	20kW	2.67-3.47μm	1.5kW	$0.3cm^{-1}$	Cotter 1976b
Ba	6^1S_o-$5^3D_{1,2}$	8MW	2.87-2.97μm	1MW	-	Carlsten and Dunn 1975
K	4s-5s	80kW	2.4-3.25μm	-	-	Wynne and Sorokin 1977
Rb	5s-6s	40kW	2.63-2.86μm	-	$0.4cm^{-1}$ dye laser limited	Wynne and Sorokin 1977

Consequently the aims of the current work have been ...

1. to extend the current tuning ranges in the systems already tried;
2. to generate infrared in new regions of the spectrum; and
3. to gain further insight into the linewidth behaviour, with a view to narrowing it.

These have been pursued with a desire to understand the basic physics involved and also to produce a useful infrared device. Although these three objectives have not been fully achieved in the work presented herein, significant progress has been made - useful understanding has been gained from the experiments which did not work as expected, as well as from those which did.

Investigations using a variety of metal vapours pumped by a high power dye laser system are described. In the second chapter the fundamentals of SERS are presented, comprising an approach to threshold calculations and expected tuning ranges, various competing and limiting processes and a comparison of the theory with experiment. Chapter three describes experimental details of pump sources, dye lasers and metal vapours. The experiments performed and their results are discussed individually in subsections of chapter four whilst the final chapter presents general conclusions from the research, providing an assessment of the role of SERS and guidelines for future study.

CHAPTER 2

Fundamentals of SERS

In this chapter the formalism used to calculate the Raman gain, and hence threshold and tuning range, is presented. The limitations of the simple theory are illustrated by a comparison with previous experimental results using caesium. The effects of atomic and pump depletion are described. Finally, a number of mechanisms which could be responsible for the observed broad linewidth output are considered.

2.1 Gain Calculations

A semiclassical approach for deriving an expression for the gain is adopted, starting from the wave equation for the growth of the Stokes wave,

$$\nabla_T^2 E(\omega_s) + \frac{\partial^2 E(\omega_s)}{\partial z^2} + k_s^2 E(\omega_s) + \mu_o \omega_s^2 P(\omega_s) = 0 \qquad \ldots 2.1$$

where s subscript refers to Stokes (p, used later, refers to pump)

k - wave vector

∇_T^2 - transverse component of ∇^2 (Laplace operator)

$E(\omega_s)$ is the complex Fourier amplitude of the Stokes field, related to the latter by

$$E_s(t) = \frac{1}{2}\left[E(\omega_s) \exp i\,(k_s z - \omega_s t) + cc\right] \qquad \ldots 2.2$$

where we have defined $E_s(t)$ as a travelling wave propagating in the $+z$ direction*. The pump field $E_p(t)$ and the nonlinear Stokes polarisation $P_s(t)$ are similarly defined. The Fourier amplitude of $P_s(t)$ may be related to the nonlinear optical susceptibility, $\chi^{(3)}$, by

$$P(\omega_s) = K(-\omega_s;\omega_p,-\omega_p,\omega_s)\varepsilon_o\chi^{(3)}(-\omega_s;\omega_p,-\omega_p,\omega_s)E(\omega_p)E^*(\omega_p)E(\omega_s) \qquad \ldots 2.3$$

---

* Another equally valid definition, $E_s(t) = \frac{1}{2}\left[E_s \exp i\,(\omega_s t - k_s z) + cc\right]$, is used by Cotter 1975b, 1976b; our definition is chosen for consistency with Yuratich and Hanna 1976 and Yuratich 1977a. The effect of using the other definition is a change in sign in some of the equations.

K is a numerical factor related to the symmetry properties of the process and has the value $\frac{3}{2}$ for the case of Raman scattering.

For the case of exact two photon resonance, $\omega_p - \omega_s = \Omega_{fg}$, the susceptibility can be shown to be purely imaginary, ie

$$\chi^{(3)}(\omega_s;\omega_p,-\omega_p,\omega_s) = i\chi_R, \text{ with } \chi_R \text{ real} \quad \ldots 2.4$$

Incorporating these definitions into eqn 2.1, the wave equation becomes

$$\nabla_T^2 E_s + 2ik_s \frac{\partial E_s}{\partial z} - ik_s G_R E_s = 0 \quad \ldots 2.5$$

where

$$G_R = -\frac{3}{2}\omega_s^2 \chi_R E_p E_p^* / k_s c^2 \quad \ldots 2.6$$

is the plane wave power gain.

Replacing the field by the cycle-averaged intensity ($I_p = \frac{1}{2}\varepsilon_o c \eta_p E_p^2 P$ and using the relationship* $\alpha\hbar c = \frac{e^2}{4\pi\varepsilon_o}$, where α is the fine structure constant, this expression becomes

$$G_R = \left(\frac{8\pi\alpha\hbar}{c}\right)\left(\frac{-\chi_R}{e^2}\right). I_p. \omega_s \quad \ldots 2.7$$

2.1.1 Calculation of $\chi^{(3)}$

The third order nonlinear susceptibility has been derived for specific cases by several authors making various simplifying assumptions (eg Miles and Harris 1973). More recently, using the techniques of irreducible spherical tensors and Racah algebra, Yuratich and Hanna 1976 have developed expressions for the generalized n-th order atomic susceptibility incorporating fine structure and general field polarisations. Using their results, the Raman susceptibility may be quite generally expressed as

---

* Incorporating α, the fine structure constant, $\frac{1}{137}$, enables us to drop ε_o and μ_o; thus the equations presented are equally valid for CGS or SI units without ambiguity.

$$\chi^{(3)}(-\omega_s;\omega_p,-\omega_p,\omega_s) = \frac{2\pi\alpha c N}{3\hbar^2\epsilon^2}\frac{1}{(\Omega_{fg}+\omega_s-\omega_p)+i\Gamma}\sum_{\text{deg of } g}\sum_{\text{deg of } f}(\bar{\rho}^0_{gg}-\bar{\rho}^0_{ff})\,|\mathcal{M}_{SRE}|^2$$

... 2.8

where

$$\mathcal{M}_{SRE} \equiv \sum_i\left(\frac{\langle f|\epsilon_s^*.Q|i\rangle\langle i|\epsilon_p.Q|g\rangle}{\Omega_{ig}-\omega_p}+\frac{\langle f|\epsilon_p.Q|i\rangle\langle i|\epsilon_s^*.Q|g\rangle}{\Omega_{ig}+\omega_s}\right).$$

... 2.9

a sum representing the contribution of all the possible intermediate states, i.

N is the density of atoms, Γ is a phenomenological damping term representing the spontaneous Raman linewidth (HWHM) , $\bar{\rho}$ refers to the fractional population of the levels, $\underline{\epsilon}$ is a polarisation vector and $\underline{Q}$ the dipole moment operator, $\underline{Q} = e\underline{r}$. Usually $\bar{\rho}^0_{ff} = 0$ and $\bar{\rho}^0_{gg} = [J]^{-1} = (2J+1)^{-1}$, where J is the degeneracy of the level, and we define

$$\overline{|M_{SRE}|^2} = \sum_{\text{deg } g}\sum_{\text{deg } f}\bar{\rho}^0_{gg}\,|M_{SRE}|^2 \qquad \ldots 2.10$$

The calculation of $\overline{|M_{SRE}|^2}$ now involves examining the term diagram of the element in question and determining the important levels contributing to the susceptibility and summing over these. For example, in the alkalis if $g = |n^2S_{\frac{1}{2}}>$ the dominant contribution would come from the $i = |n_2{}^2P_{\frac{1}{2},\frac{3}{2}}>$ states nearest resonance with ω_p; the sum thus simplifies on application to a sum over just the nearest one or two levels. If more than one final level f exists, it may be necessary to calculate $\overline{|M_{SRE}|^2}$ for each case in order to deduce to which level(s) scattering will dominate. Yuratich and Hanna 1976 have obtained the following general expressions for $\overline{|M_{SRE}|^2}$ for the above example, where f may be one of three levels:

For $f = |n_1{}^2S_{\frac{1}{2}}>$

$$\overline{|\mathcal{M}_{SRE}|^2_{LS}} = \frac{e^4}{3}\left|\sum_{n_2}\left[\tfrac{2}{3}\Phi(n_2p\tfrac{3}{2}0)+\tfrac{1}{3}\Phi(n_2p\tfrac{1}{2}0)\right]\right|^2\Theta^{(0)} + \frac{2e^4}{81}\left|\sum_{n_2}\left[\Phi(n_2p\tfrac{3}{2}1)-\Phi(n_2p\tfrac{1}{2}1)\right]\right|^2\Theta^{(1)} \qquad \ldots 2.11$$

For $f = |n_1\,^2D_{\frac{3}{2}}\rangle$

$$\overline{|\mathcal{M}_{SRE}|^2_{LS}} = \frac{e^4}{81}\left|\sum_{n_2}[\Phi(n_2p\tfrac{3}{2}1) - \Phi(n_2p\tfrac{1}{2}1)]\right|^2\Theta^{(1)} + \frac{4e^4}{75}\left|\sum_{n_2}[\tfrac{1}{6}\Phi(n_2p\tfrac{3}{2}2) + \tfrac{5}{6}\Phi(n_2p\tfrac{1}{2}2)]\right|^2\Theta^{(2)} \qquad \ldots\ 2.12$$

And, for $f = |n_1\,^2D_{\frac{5}{2}}\rangle$

$$\overline{|\mathcal{M}_{SRE}|^2_{LS}} = \frac{2e^4}{25}\left|\sum_{n_2}\Phi(n_2p\tfrac{3}{2}2)\right|^2\Theta^{(2)} \qquad \ldots\ 2.13$$

where we have defined, for convenience,

$$\Phi(n_2l_2J_2K) \equiv \langle n_1l_1|r|n_2l_2\rangle\langle n_2l_2|r|nl\rangle\left(\frac{1}{(\Omega_{n_2l_2J_2nlJ} - \omega_p)} + \frac{(-1)^K}{(\Omega_{n_2l_2J_2nlJ} + \omega_s)}\right) \qquad \ldots\ 2.14$$

a combination of radial matrix elements and resonant and anti-resonant frequency denominators.

The factor $\Theta^{(k)}$ containing the angular dependance of the fields is tabulated in Yuratich and Hanna 1976.

For SERS from an excited state, $g \neq n^2S_{\frac{1}{2}}\rangle$, the more general formula may be used

$$\overline{|\mathcal{M}_{SRE}|^2} = \frac{1}{[J]}\sum_K\left|\sum_{n_2l_2J_2}\begin{Bmatrix}J_1 & K & J\\ 1 & J_2 & 1\end{Bmatrix}\Phi(n_2l_2J_2K) \times \frac{\langle n_1l_1\tfrac{1}{2}J_1||Q||n_2l_2\tfrac{1}{2}J_2\rangle\langle n_2l_2\tfrac{1}{2}J_2||Q||nl\tfrac{1}{2}J\rangle}{\langle n_1l_1|r|n_2l_2\rangle\langle n_2l_2|r|nl\rangle}\right|^2\Theta^{(K)}$$

$$\ldots\ 2.15$$

where the sum $\sum_{n_2 l_2 J_2}$ is over the intermediate contributing levels; $\begin{Bmatrix}J_1 & K & J\\ 1 & J_2 & 1\end{Bmatrix}$ is a 6-j symbol, a numerical factor available from tables, and $\langle\,||Q||\,\rangle$ is a reduced matrix element, related to $\langle\,|r|\,\rangle$ by a numerical factor times the electronic charge.

The radial matrix elements necessary for the calculation may be readily available or may need to be derived from the corresponding z-matrix elements or oscillator strengths, using the appropriate

interrelationships given in Yuratich and Hanna, equations (32-36). The 'Bibliography on Atomic Transition Probabilities' compiled by Miles and Wiese (1970) is a useful reference for this data.

Frequently one can consider the contribution to $\chi^{(3)}$ from just one intermediate level and neglect all others; also, when not tuned too close to a doublet, its fine structure may be neglected. The formulae then simplify and the most important considerations become more apparent.

Thus we find that, if a single intermediate level i is involved,

$$\chi_R \propto \frac{N}{\Gamma} \quad \frac{f_{gi}}{\omega_{gi}} \quad \frac{f_{fi}}{\omega_{fi}} \quad \frac{1}{(\Delta\omega)^2} \qquad \ldots 2.16$$

where f_{gi}, f_{fi} are oscillator strengths
and $\Delta\omega = \omega_{gi} - \omega_p$, the detuning of the pump from resonance. Thus for SERS processes involving similar level schemes a quick estimate of possible performance may be found by comparison of the oscillator strengths and frequencies involved with those of a system for which the performance is known.

Thus $\chi^{(3)}$ may be evaluated for the Raman process either by direct calculation, ab initio, or by comparison with another system. Using the direct approach, considering exact two photon resonance, equation 2.8 collapses to

$$\chi^{(3)}(-\omega_s;\omega_p,-\omega_p,\omega_s) = N\left(\frac{2\pi}{3}\right)\left(\frac{\alpha c}{\hbar^2}\right)\left(\frac{1}{2e}\right)\left(\frac{-i}{\Gamma}\right)\overline{|M_{SRE}|^2} = i\chi_R \qquad \ldots 2.17$$

as described earlier, and the expression for the gain becomes (from 2.7),

$$G_R = gI_p = \left(\frac{4\pi\alpha}{3\hbar}\right)^2 \quad \frac{N\omega_s}{\Gamma} \quad \frac{\overline{|M_{SRE}|^2}}{e^4} \cdot I_p. \qquad \ldots 2.18$$

2.1.2 Gain Focussing and Diffraction Loss

A further refinement of the calculation, necessary when considering large Stokes shifts, is to consider the effect of a focussed pump beam. The profile of the Raman gain, $G \alpha I_p$, now varies spatially as the pump intensity. This results in the generation of a Stokes wave with a beam waist defined by the pump, thus the generated radiation will diffract into a larger angle than the pump, since it is of longer

wavelength, and only that portion remaining in the pumped region will experience gain. This diffraction effect can be a serious loss mechanism, particularly when long wavelengths are generated.

Following the gain focussing theory developed by Kogelnik, Cotter 1975b has developed an approach which allows this effect to be simply incorporated into the gain calculation.

In the earlier expressions we replace E_p by $E_{po} \exp(-r^2/w_p^2)$, where w_p = pump spot size, and then approximate the consequent Gaussian r-dependence of G_R, $G_R = G_{RO}\exp(-2r^2/w_p^2)$, by a parabolic one. With this approximation the problem becomes soluble for E_s, giving a solution which yields the beam parameters R_s, w_s of the Stokes beam; it can be shown that a 'matched mode' exists, whose parameters R_m, w_m remain constant throughout the medium whilst propagating in it, and that the Stokes beam parameters quickly converge to these values. Also we may derive an expression for the growth of the amplitude, A, of the wave

$$\frac{1}{A}\frac{dA}{dz} = \frac{G_{RO}}{z} - \frac{1}{R_s} \qquad \ldots 2.19$$

Integrating over a length L and assuming a matched mode gives the overall field gain as

$$\frac{A(L)}{A(0)} = \exp\left(\tilde{P}_p - 2\sqrt{\tilde{P}_p}\right) L/2k_s w_p^2 \qquad \ldots 2.20$$

where we have defined a 'normalised' pump power

$$\tilde{P}_p = G_{RO} k_s w_p^2 \qquad \ldots 2.21$$

which may also be expressed as

$$\tilde{P}_p = 24\,\alpha\hbar \frac{\omega_p^2}{c^2} K^2 \left(\frac{-\chi_R}{e^2}\right) \cdot P_p \qquad \ldots 2.22$$

for the case of a gas or vapour, whose refractive index $\simeq 1$;
$K = k_s/k_p$.

This analysis has assumed a constant w_p throughout the medium, rather than the real situation. Assuming the pump beam is focussed, with a confocal parameter b_p, at the centre of the cell, it is

possible to modify the above procedure and arrive at an equation analogous to 2.20, valid for large $\frac{A(L)}{A(O)}$, viz.

$$\frac{A(L)}{A(O)} = \exp\left[(\tilde{P}_p - 2\sqrt{\tilde{P}_p}\gamma_2 K \quad] \arctan (L/b_p) \right. \qquad \ldots 2.23$$

Equations 2.20, 2.23 display a fundamental gain threshold effect, ie the gain is positive only for $\tilde{P}_p > 4$. In practise in order to amplify up the signal from noise to a detectable level, detector threshold, it is necessary to have a field gain of $\sim\exp(15)$, hence a somewhat larger P_p. From 2.22-23, to generate a power $P_s(L)_{th}$ from a starting signal of P_{so}, we find we need a threshold power $P_{p_{th}}$ of

$$P_{p_{th}} = \frac{\left[1 + \left\{1 + \left[K/\arctan (L/b_p)\right] \ln \left[P_s(L)_{th}/P_{so}\right]\right\}^{\frac{1}{2}}\right]^2}{24\, \alpha\hbar \frac{\omega_p^2}{c^2} K^2 \left(\frac{-\chi_R}{e^2}\right)} \qquad \ldots 2.24$$

A theoretical curve of threshold versus pump frequency may be derived using this result.

The analysis may be further extended to incorporate the effect of the real part of the susceptibility, representing a contribution to the Stokes refractive index proportional to pump intensity, the optical Kerr effect. The induced pump focussing/defocussing has the effect of modifying the exact frequency of maximum Stokes gain; thus as the intensity of the pump varies in time during the pulse a frequency pulling, or chirp, of the output may be expected, of magnitude comparable to Γ the spontaneous Raman linewidth.

This analysis is covered in greater depth in Cotter 1976b, and also in Cotter et al 1975b, but note the change in definition - $P(\omega_s) = \frac{3}{2}\varepsilon_o \chi$ ... is replaced by $P(\omega_s) = \varepsilon_o \chi$ ... - in this latter reference; also ε_o, μ_o are retained instead of α in both references. These references also contain further application of the theory to the possibility of using a Raman oscillator cavity; the diffraction effect is a severe loss mechanism when using small beam waists and the conclusion was that one would need to use a large spot size, with correspondingly higher pump powers, to gain advantage from an oscillator configuration. Use of an oscillator cavity could however alleviate problems associated with atomic depletion (see section 2.3).

2.2 Limitations of the Simple Theory

To illustrate the use and limitations of the theory outlined above and to provide a platform from which to discuss the causes of these limitations we shall compare the theory with the experimental results obtained by Wyatt 1976 (see also Cotter et al 1976a). These experiments using caesium pumping from the 6s ground state used 7p, 8p and 9p intermediate levels and scattered correspondingly to the 7s, 8s and 9s levels, see fig 2.1.

Initially to predict tuning ranges, we evaluate $\chi^{(3)}$, by inserting the relevant data. The atomic number density N is simply calculable from the vapour pressure/temperature (see chapter 3); the frequencies ω_p, ω_s and Ω_{fg} are readily deduced from fig 2.1, a partial term diagram of Cs, taken from Moore 1949. The matrix elements needed for the calculation were taken from Eicher 1975, although Warner's calculations 1968 of gf-values are those which we have generally used, after comparison with various other experimental and theoretical sources has shown them to be fairly reliable. The spontaneous Raman linewidth was taken to be the Doppler width of the transition calculated as

$$\Gamma_D = \omega_o \left[\frac{2\ln 2\ kT}{Mc^2}\right]^{1/2} \quad \text{(HWHM)} \qquad \ldots 2.25$$

where Γ_D, ω_o are (angular) frequencies, k is Boltzman's constant, T is the absolute temperature, M is the atomic mass and c the velocity of light. For a two photon SERS transition ω_o is $\omega_o = \omega_p - \omega_s$ for forward scattering or $\omega_o = \omega_p + \omega_s$ for backward (Wyatt 1976). Thus Γ_D is calculated to be of the order of $0.015 cm^{-1}$. The theory then predicts that using a 10kW dye laser with linewidth less than Γ_D, confocally focussed over the length of the vapour column, with Cs at 10 torr vapour pressure, using enhancement from the levels already mentioned, complete coverage of the range 2-20μm should be possible with outputsexceeding 1W.

In practice this optimistic prediction was not fulfilled; using a much higher power dye laser significant tuning ranges were obtained, though not covering all of 2-20μm, see the Cs results listed in table 1.2 . The calculated thresholds were found to be nearly two orders of magnitude too low, even when the $0.1 cm^{-1}$ linewidth of the dye laser was allowed for. The linewidth of the Stokes output was measured as $0.3-1.4 cm^{-1}$, depending upon experimental conditions, rather than $0.1 cm^{-1}$ which might be expected if it were limited by the

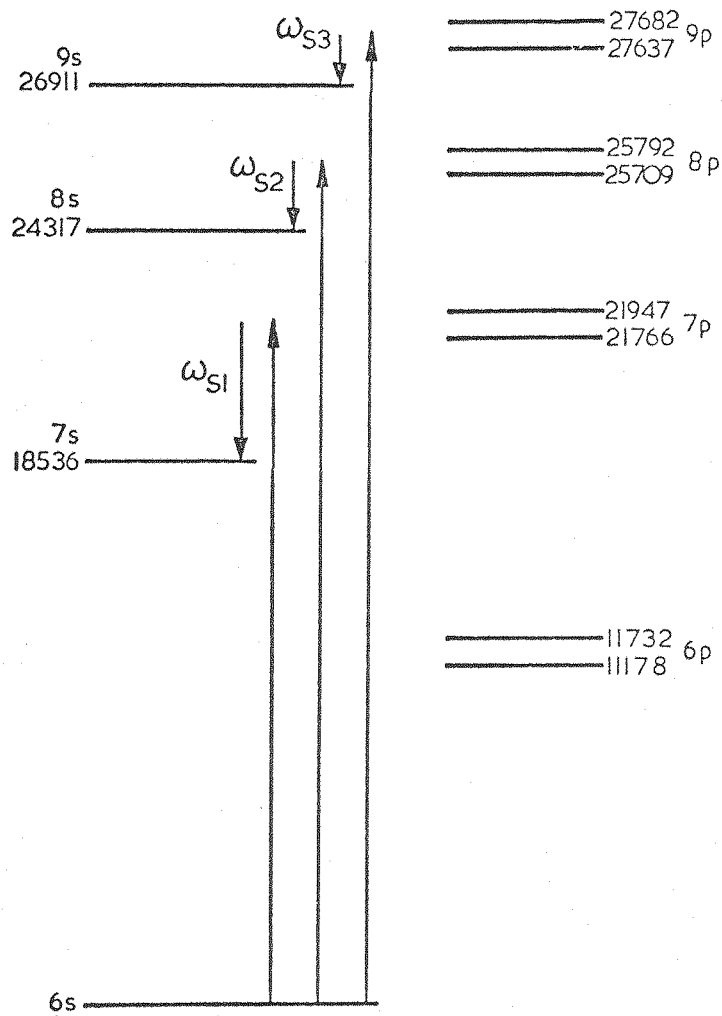

Fig 2.1 Partial energy level diagram of Cs showing SERS transitions investigated by Cotter et al 1976a

dye laser linewidth. These observations imply a much larger Γ than that assumed, ie the presence of some line-broadening mechanism(s) - some possible processes are assessed in section 2.4.

The theory as already outlined has not discussed the magnitude of the energy output nor the shape of the output versus tuning curve. The mechanisms relating to these factors are considered in the next section.

2.3 Atomic and Pump Depletion

Ideally one would like every pump photon to be scattered into a Stokes photon, the ratio of output to input energies would then be given by the ratio of photon energies, ω_s/ω_p. This corresponds to the so-called Manley-Rowe limit, 100% photon conversion efficiency. Experimental peak photon conversion efficiencies of 50% have been obtained near the centre of the tuning range (Cotter et al 1977a); away from resonance the output is observed to fall off with detuning.

Initially the SERS radiation grows exponentially with a small signal gain coefficient already calculated and may quickly reach a regime where the gain saturates to a lower value, limited by one of these two mechanisms, atomic or pump depletion, where the output is limited by the number of atoms or pump photons remaining available. The energy/tuning behaviour is adequately accounted for by incorporating these saturation mechanisms. The effects of pump absorption both by atoms and molecules is also a factor which is considered in this section.

2.3.1 Atomic Depletion

When a high intensity dye laser interacts with a short column of low pressure metal vapour the number of pump photons passing through the interaction region may easily exceed the number of atoms present. When a pump photon scatters into a Stokes photon it leaves an atom in an excited state; consequently if the pump pulse is shorter than the relaxation time of the atom back to the ground state, as is usually the case for our experiments, then the number of Stokes photons which may be generated, N_s is limited by the number of ground state atoms available from which to scatter.

Initially the signal grows exponentially from noise over a build up length l until it reaches a level at which either the pump intensity begins to be significantly reduced (pump depletion) or the atomic population of the ground state tends towards zero. The latter condition we refer to as atomic depletion and, from eqn 2.8, it can be seen that the gain falls to a low value in this saturated region. Thus, considering only atomic depletion, the total number of Stokes photons generated will be given by a contribution from the small signal region and a contribution from the saturated region, the latter of the two being dominant for all cases except large l, comparable to L the length of vapour column. For the case of $l \ll L$ this contribution will be of the order $\mathcal{N}_s = \pi w_s^2 L . \frac{N_A}{2}$ where N_A is the atomic number density. The peak photon conversion efficiency is thus limited and the output energy given by $\mathcal{N}_s \hbar\omega_s$. This case of a short build up length corresponds to a high small-signal Raman gain coefficient G_R and thus to the case of near-resonance of the pump to the ground state - intermediate state transition. Further from resonance the gain decreases and thus so does the net volume of atoms contributing to the generation of Stokes photons, thus the output falls with detuning from resonance.

2.3.2 Pump Depletion by SERS

As pump photons are converted into Stokes photons then the number of pump photons and correspondingly the intensity will decrease. Since the gain coefficient G_R is proportional to the pump intensity this implies a decrease in small-signal gain. Thus when $\mathcal{N}_s$ becomes comparable with $\mathcal{N}_p$ the number of Stokes photons generated will be limited by the number of pump photons available, this is often the case by virtue of the metal vapour pressure and focussing conditions used, particularly when operating with a lower power nitrogen pumped dye laser.

2.3.3 Interrelationship of these Saturation Processes

In this section conditions for photon depletion and atom depletion are derived and their interrelationship considered.

Photon depletion occurs as the number of Stokes photons generated $\mathcal{N}_s$ approaches the number of pump photons available $\mathcal{N}_p$, which, assuming equal pump and Stokes pulse lengths, may be expressed as

$$I_s \simeq \frac{\omega_s}{\omega_p} I_p \qquad \ldots 2.26$$

Now, the Stokes wave grows exponentially as

$$I_s = I_{so} \exp (gI_p z) \qquad \ldots 2.27$$

Thus, the condition for photon depletion is approached for $z = l_p$ where

$$l_p = \frac{1}{gI_p} \ln \left(\frac{\omega_s}{\omega_p} \frac{I_p}{I_{so}}\right) \qquad \ldots 2.28$$

I_{so} is the spontaneous Raman noise intensity which may be derived, eg from Loudon 1973, as

$$I_{so} = \frac{\hbar \omega_s^3 \Gamma}{4\pi^3 c^2} \cdot \Delta\Omega \qquad \ldots 2.29$$

where $\Delta\Omega$ is the solid angle subtended by the geometry of the pumped region. Considering this as a cylinder of length L and radius w_o, equal to the beam waist of a confocally focussed beam, we find

$$I_{so} = \frac{\hbar c k_p^2 K^3 \Gamma}{4\pi^2 L} \qquad \ldots 2.30$$

which, quantitatively, we find to be typically of the order $10^{-3} - 10^{-5} Wm^{-2}$.

To derive the condition for atomic depletion we adopt a transition rate approach; depletion of the atomic ground state population will occur if at the end of the pump pulse the probability of an atom having undergone a transition approaches unity, ie if $W.\tau_p \simeq 1$. The transition rate W may be obtained from first principles (cf Loudon 1973) or by comparing the propagation equation for the Stokes wave

$$\frac{\partial I_s}{\partial z} = W N_A \hbar\omega_s \qquad \ldots 2.31$$

with that obtained by differentiating eqn 2.27; hence

$$W = \frac{1}{N_A \hbar\omega_s} \, g I_p I_s \qquad \ldots 2.32$$

Using eqn 2.27 again for I_s, the condition $W\tau_p = 1$ yields the length $z = l_a$ for the onset of atomic depletion, where

$$l_a = \frac{1}{g I_p} \ln \left(\frac{N_A \hbar\omega_s / \tau_p I_{so}}{g I_p} \right) \qquad \ldots 2.33$$

For the case of stimulated hyper-Raman scattering (see chapter four) eqns 2.32-33 are simply modified by $I_p \rightarrow I_p^2$.

For either saturation process to be important we require $l \lesssim L$; assuming this, to determine which process initially dominates we may compare l_p and l_a, eqns 2.28 and 2.33.

For atomic depletion to occur first, $l_a < l_p$, we find

$$\mathcal{N}_p > N_A \frac{\pi w_s^2}{G_R} \qquad \ldots 2.34$$

or, since $\mathcal{N}_p$ and G_R both depend on I_p,

$$I_p^2 > N_A \hbar\omega_p \, \frac{1}{\tau_p} \, \frac{1}{g} \qquad \ldots 2.35$$

Considering the implications of this for a typical case of 6s-7s SERS in C_s, assuming $\Gamma = 1 cm^{-1}$ gives $g = 10^{-8} - 10^{-10} mW^{-1}$ and thence we find limiting intensities of $0.7 - 7 \times 10^{10} Wm^{-2}$. Thus we find that for typical experimental parameters atomic depletion usually begins to occur before photon depletion, ie that the gain exponent required for atomic depletion is less than that required for photon depletion.

We need to consider also the effect of varying the Raman gain gI_p as the pump is tuned near to resonance or as the intensity is varied. From eqns 2.33 and thence 2.27 it may be shown that as gI_p decreases, the build-up length, the gain exponent and the Stokes intensity, I_{ss}, necessary for the onset of atomic depletion all increase in value.

The Stokes output has two contributions, from the build-up length and from the saturation region. The former we may evaluate as

$$E_{sb} \simeq I_{ss} \pi w_s^2 \tau_p \qquad \ldots 2.36$$

and the latter as

$$E_{ss} \simeq \hbar\omega_s N_A \pi w_s^2 (L - l_a) \qquad \ldots 2.37$$

Inserting typical parameters reveals that over all but the extremes of the tuning range $E_{ss} >> E_{sb}$, the output generally being taken as E_{ss}.

The simplified geometry assumed for the pumped region and the constant I_p assumed, independent of z and t, are limitations of this model; also, generally, I_p is not well specified, nor is Γ. Nevertheless rough estimates of these effects may be obtained.

After atomic depletion has begun, photon depletion may subsequently occur also, if the number of atoms remaining with unit probability of undergoing a transition exceeds the remaining number of photons in the pump beam (- this may be taken as the initial number of photons); ie it may occur if

$$\mathcal{N}_p < N_A \pi w_s^2 (L - l_a) \qquad \ldots 2.38$$

More loosely we may state that photon depletion will occur if the number of pump photons is less than the number of atoms in the pumped region, assuming $l_a << L$.

In practice the Stokes output from ~ 20cms of Cs vapour at 10 torr pumped confocally with a 20kW dye laser has been observed to be limited by pump depletion at the centre of the tuning range, the drop in energy with detuning being due to the atom depletion mechanism . Cotter et al, 1977a have treated the atomic and pump depletion mechanisms analytically, and more precisely, incorporating provision for including the effects of the backward wave, diffraction loss etc and find good numerical agreement between experiment and the computer model. The attempt here has been to provide a simple, yet quantitative, model giving a clear physical insight into the saturation behaviour.

2.4 Effects of Pump Absorption

Depletion of the pump beam may occur not only due to conversion of the pump to Stokes photons, but also by molecular and atomic absorption.

This may lead to a depletion of the pump whilst the Stokes wave is still in the small signal regime and the consequent decrease in gain will impede its growth.

We may express the pump absorption as it travels through the medium as

$$I_p(z) = I_{po} \exp(-Kz) \quad \ldots 2.39$$

where K is the absorption coefficient. Integrating the gain coefficient $G_R, \propto I_p(z)$, over the length L of the vapour column gives a total gain exponent of

$$G = G_{RO}\left(\frac{1 - \exp(-KL)}{K}\right) \quad \ldots 2.40$$

For weak absorption, small K, this approximates to the usual $G = G_{RO}L$, whilst for strong absorption it becomes $G = G_{RO}/K$, ie we effectively have a gain of G_{RO} over just one extinction length, as one might expect. In intermediate cases the full expression 2.40 must be used.

Pump absorption will therefore cause a reduction in gain and consequent drop in output energy and tuning range. The behaviour of molecular and atomic absorption differs in some respects and so these will be treated separately.

2.4.1 Molecular Absorption

In an alkali vapour at pressures of a few torr there are present several percent of alkali dimers which have broad absorption bands in the visible, see eg Lapp and Harris 1966. Typical absorption cross-sections for these dimers are $\sigma = 10^{-18} - 10^{-15} cm^2$, leading to an absorption coefficient $K = 5 \times 10^{-3} - 5 cm^{-1}$, assuming an atomic number density of $10^{17} cm^{-3}$ and 5% dimers present; this would imply a heavy loss mechanism with a $1/e$ absorption length of 200 - 0.2cms.

Since however the dimer density is only a few percent of the atomic density it is fairly simple to arrange the focussing such that the dimer absorption is saturated by the first part of the pump pulse, thus reducing the overall absorption. This becomes even less of a problem when a high power pump laser is used, such as was used for much of this work, as this condition is readily fulfilled.

The constraint that tight focussing should be used, resulting in a small confocal parameter b_p, is not troublesome since examination of equation 2.23 shows that, neglecting other effects, this is in fact required anyway for high Raman gain. Other competing nonlinear effects do become important for very tight focussing, but saturation of the molecular absorption occurs before this regime is reached.

2.4.2 Atomic Absorption

To enhance SERS the pump laser is tuned close to an intermediate resonance; thus single photon absorption, SPA, may occur resulting in a population of the intermediate level. This may cause resonance broadening of the final Raman level, see the next section, as well as reducing the pump intensity and hence gain, as considered here.

If the absorption lineshape is assumed to be Lorentzian we may express the SPA cross-section, for an s→p transition, as

$$\sigma_A^{(1)} = \frac{2\pi\alpha\hbar}{m} f_{sp} \frac{\Gamma_{sp}}{(\Delta\omega)^2 + \Gamma_{sp}^2} \frac{\omega_p}{\Omega_{ps}} \qquad \ldots 2.41$$

where m is the electron mass, ω_p is the pump frequency, Ω_{ps} is the transition frequency and $\Delta\omega$ is the detuning from single photon resonance. Γ_{sp} is the linewidth of the transition and may have contributions from a variety of sources, including some of those to be outlined in section 2.5.

Ignoring for the moment any intensity dependent line broadening, it would seem that under typical SERS conditions Γ_{sp} would be predominantly resonance broadened. For this we would expect a Lorentzian lineshape for $\sigma_A^{(1)}$ with Γ_{sp} given by

$$\Gamma_{sp} \simeq \left(\frac{2j_s + 1}{2j_p + 1}\right)^{1/2} \frac{2\pi\alpha\hbar c}{m} N \frac{f_{ps}}{\Omega_{sp}} \quad \text{HWHM (rad s}^{-1}\text{)} \qquad \ldots 2.42$$

where the 'j' refers to the angular momentum of the state (Hindmarsh, 1974). This expression is valid within the 'impact approximation' which, for neutral atom broadening, is limited to within a few cm^{-1} of resonance. Thus, far from resonance, the assumption in equation 2.41 that the lineshape is Lorentzian appears to be in doubt, since a quasi-static model should be used (cf Bloom et al, 1975a).

A numerical example using the above formalism will be given here, for SPA in Na. The low-level absorption of 25cms of Na vapour at 10 torr was measured using a tungsten lamp, monochromator and photomultiplier; this is plotted in fig 2.2. For comparison a 'theoretical' curve is also plotted; this has been derived assuming resonance broadened linewidths, $\Gamma_{3s-3p_{1/2}} = 0.08cm^{-1}$ and $\Gamma_{3s-3p_{1/2}} = 0.12cm^{-1}$ calculated from eqn 2.42, and a Lorentzian lineshape as per eqn 2.41. Although the impact approximation is not valid over most of the range shown, neverless it is observed from the figure that this approach does give some idea of the importance and behaviour of the SPA; similar fortuitous agreement is observed also near the Sr $5^1S_o - 5^1P_1$ resonance line. The example taken of Na is extreme in fact, due to the very large oscillator strength involved, and was used because of availability of data as an illustration. The SPA for a more typical SERS candidate is much less; for example in Cs, at 10 torr, for the $6s-7p_{3/2}$ transition we calculate $\Gamma_{6s-7p_{3/2}} = 4 \times 10^{-3}cm^{-1}$ and a $1/e$ absorption length of 25cms for a detuning of $\sim 8.5cm^{-1}$; for such a case the impact approximation is valid over much of the range of interest.

It is interesting to note the behaviour of the Raman gain in the presence of strong SPA, for which we find from equation 2.40, that

$$G = \frac{G_{RO}}{\sigma_A^{(1)}{}_N} \qquad \ldots 2.43$$

Assuming once more a Lorentzian behaviour of $\sigma_A^{(1)}$ then, since G_{RO} depends similarly on detuning from resonance, we find G to be independent of detuning. This feature will be further considered in connection with the specific case of SERS in strontium. An analogous result may be derived for single photon absorption by the intermediate level in stimulated hyper-Raman scattering, considered later.

2.5 Linewidth of the SERS Radiation

Our preliminary theory assumed a Doppler-broadened linewidth, Γ for spontaneous Raman scattering and used this in the calculation of $\chi^{(3)}$; the initial experiments by Wyatt 1976, in caesium revealed a much broader SERS linewidth than was expected, of the order of $0.3-1.5cm^{-1}$. His experimental results on the 6s-8s and 6s-9s transitions indicated

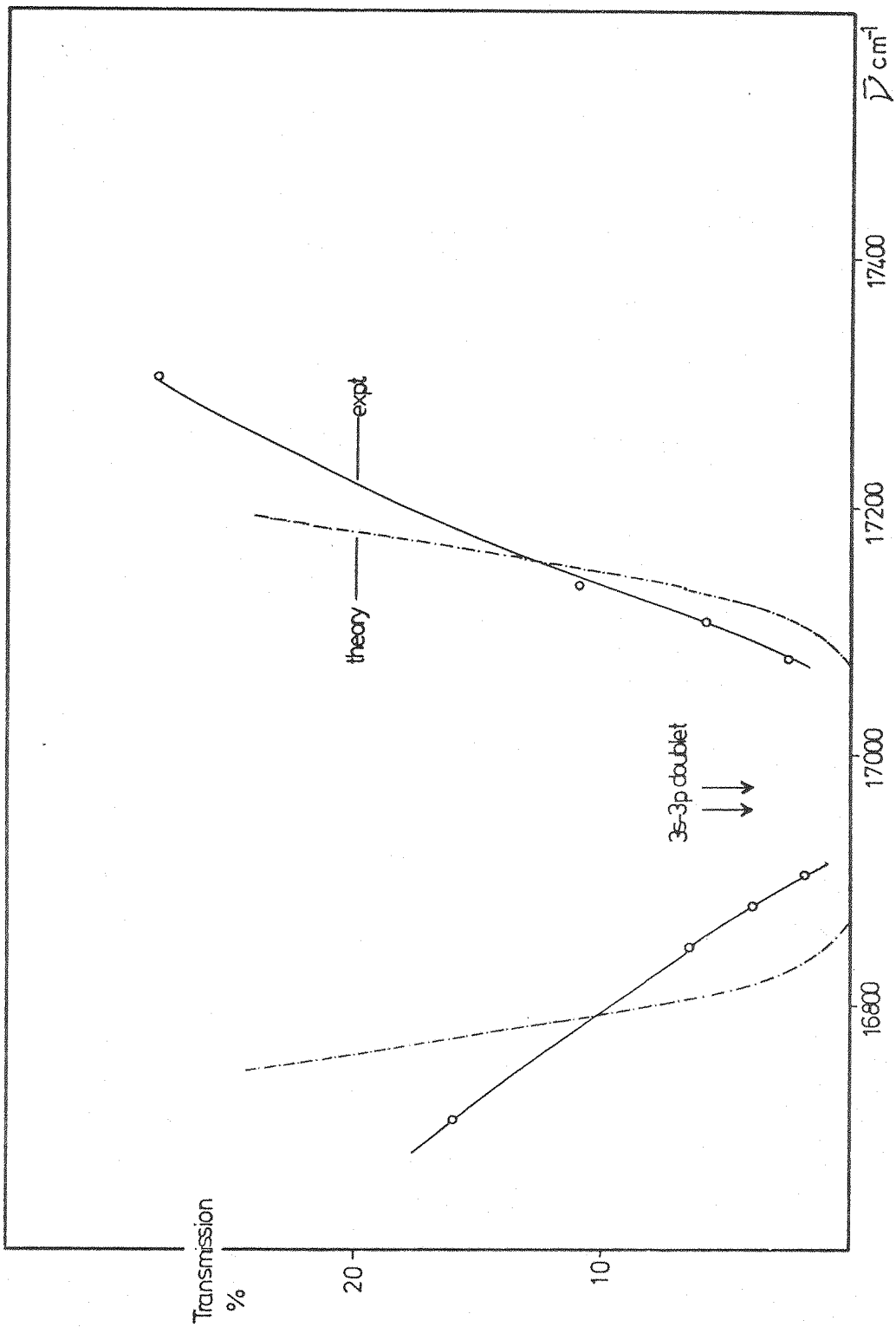

Fig 2.2 Transmission of 25cms of Na at 10 torr

the presence of an intensity dependent line broadening mechanism under some conditions; these results are summarized in table 2.1, along with some measurements by Cotter 1976b relating to the 6s-7s transition, taken using a lower power pump system.

2.5.1 Relation of Output Linewidth to Pump Linewidth and Spontanous Raman Linewidth

The stimulated Raman scattering process may be viewed as a four wave parametric mixing process involving, in the limit of monochromatic radiation and precise energy levels, two waves of frequency ω_p and two of ω_s. If now the pump radiation is allowed to have finite linewidth γ and the levels are considered broadened to a degree expressed by Γ then slightly differing frequency components of the pump will produce slightly differing frequency components of Stokes radiation; these generated frequencies may then further interact in a four wave mixing process to generate other Stokes components. The composite Stokes output thus has a linewidth δ dependent upon γ and Γ. This parametric interaction has been analysed, under a steady-state assumption by Yuratich 1977b for the case of exact two photon resonance, $\omega_p - \omega_s = \Omega_{fg}$, ie a purely imaginary $\chi^{(3)}$. Two special cases of the solution of the problem are worthy of note. For the case of $\Gamma >> \gamma$ the gain exponent G remains as calculated but the linewidth is narrowed towards a value $\delta = \sqrt{\gamma\Gamma}$; for the other extreme of $\Gamma << \gamma$ the gain is modified to $G\,\Gamma/\gamma$ and the linewidth tends towards $\delta = \gamma$. It is interesting to note that the output linewidth is determined by Γ and γ even when using an externally injected signal narrower than Γ or γ as the noise source, at least for high gain conditions, as has been experimentally verified by Cotter 1976b.

Experimentally, we have typically used a value of $\gamma = 0.1\text{cm}^{-1}$ and observed $\delta > 0.3\text{cm}^{-1}$, implying we are in the regime defined by $\Gamma > \gamma$ where the parametric effect results in a linewidth δ tending toward the geometric mean of Γ and γ. Γ represents the linewidth used in the calculation of $\chi^{(3)}$ earlier, equation 2.8, and is obviously larger than Γ_s the spontaneous Raman linewidth, taken as the Doppler width; processes which might be responsible for this broad effective linewidth are outlined below.

Thus in the absence of line broadening mechanisms we would expect $\Gamma = \Gamma_s < \gamma$ and we would expect δ, the output linewidth, to be

Detuning from resonances	FWHM linewidth (cm^{-1})
6s - 9s transition	Relative intensity I x 60
35 cm^{-1} above 6s - $9p_{3/2}$	- 0.77
3 cm^{-1} above 6s - $9p_{3/2}$	- 0.71
5.5 cm^{-1} above 6s - $9p_{3/2}$	0.42 0.84
12 cm^{-1} above 6s - $9p_{3/2}$	0.3 0.92
6s - 8s transition	Focussing (intensity) Loosest .... Tightest
60 cm^{-1} above 6s - $8p_{3/2}$	0.4 0.6 1.36 1.65
8 cm^{-1} above 6s - $8p_{3/2}$	1.1 - - 1.1
15 cm^{-1} below 6s - $8p_{3/2}$	0.35 - - 0.35

From Wyatt 1976
Dye laser pump used for 6s - 9s : 250kW, 0.15 cm^{-1}
6s - 8s : 400kW, 0.15 cm^{-1}

Detuning from resonances	FWHM linewidth (cm^{-1})			
	1 torr	3 torr	10 torr	30 torr
177 cm^{-1} below 6s-$7p_{1/2}$	-	-	0.28	-
97 cm^{-1} below 6s-$7p_{1/2}$	-	-	0.46	-
71 cm^{-1} below 6s-$7p_{1/2}$	-	-	0.47	-
19 cm^{-1} below 6s-$7p_{1/2}$	-	0.40	0.49	0.52
6 cm^{-1} below 6s-$7p_{1/2}$	-	0.54	-	-
65 cm^{-1} above 6s-$7p_{1/2}$	-	-	0.43	-
54 cm^{-1} below 6s-$7p_{3/2}$	0.30	0.34	0.51	-
33 cm^{-1} below 6s-$7p_{3/2}$	0.37	-	-	-
39 cm^{-1} above 6s-$7p_{3/2}$	0.26	0.28	0.35	0.45
164 cm^{-1} above 6s-$7p_{3/2}$	-	-	0.34	-
255 cm^{-1} above 6s-$7p_{3/2}$	-	-	0.29	-

From Cotter 1976b
Dye laser pump used, 6s - 7s : 10kW, 0.1 cm^{-1}

Table 2.1 SERS linewidth data

limited by the pump linewidth, whereas, with broadening mechanisms resulting in a larger Γ we expect an output linewidth broader than the pump, yet less broad than Γ .

Independent of its effect on the parametric interaction, the real part of $\chi^{(3)}$ does have an intensity dependent effect on the Stokes refractive index as mentioned earlier, the optical Kerr effect. This results in a frequency dependent self focussing/defocussing; thus changes in intensity and hence Raman gain with frequency occur, and the Stokes frequency which experiences optimum gain becomes intensity dependent. Since the pump intensity is spatially and temporally varying anyway this should result in a frequency 'chirp', calculated to be of magnitude comparable to Γ . The observed SERS output linewidth is measured as being broader than the spontaneous Raman linewidth expected. This could imply an overall broadened linewidth, in which case the optical Kerr effect will serve to increase the effective broadening. Alternatively this could represent the frequency 'chirping' of an instantaneously narrower linewidth, in which case the contribution of the optical Kerr effect to the observed linewidth would be less important; a more complete analysis however would then be necessary for a full understanding of the behaviour.

2.5.2 Line Broadening and Shifting Effects

A number of mechanisms have been considered which could have contributed to the large value of Γ inferred from the early experiments. Strictly, a dynamic analysis incorporating all these interacting effects is necessary to get a true picture of what is happening from the theory; this was however beyond the scope of this work where an experimental approach to an understanding of the line broadening has been pursued. In the caesium work the relative magnitude of many of the effects appeared comparable and so some of the experiments (chapter 4) were designed to estimate the relative importance of them. In this section the mechanisms are outlined and formulated such that rough estimates of their effects may be made.

(i) Resonance Broadening

As already outlined, single photon absorption of the pump can result in significant population of the intermediate level and consequent resonance broadening of the final Raman level; eqns 2.41, 42

may be used to estimate the magnitude of this effect. Using this approach, Wyatt 1976 has shown that an intermediate state population of only 0.1 - 1% of the total atomic number density is necessary to give resonance broadening of the same order as the Doppler broadening of the level; SPA of the pump radiation would probably yield a population of this order even at very large detunings of the pump from resonance, although eqns 2.41, 42 would be inadequate for quantitatively evaluating the effect under such conditions.

In some circumstances however there may be a loss of intermediate state population due to amplified spontaneous emission, ASE, to lower levels. The effect of this ASE may be considered by estimating the stimulated emission cross-section, σ_{stim}, given at line centre by

$$\sigma_{stim} = \frac{2\alpha\hbar}{m} \frac{f_{ih}}{\Delta\nu_i} \qquad \ldots 2.44$$

where the symbols have their usual meanings, $\Delta\nu_i$ being the HWHM linewidth of the transition i→h on which ASE occurs. Evaluation now of the gain coefficient for ASE over the cell length, $\sigma_{stim} N_i L$, gives an upper limit on the intermediate state population density, N_i, which can be produced before ASE begins to occur.

Considering the case of 6s-7s SERS in Cs, 7p-5d ASE has been observed (Cotter 1976b). For the case of the pump tuned near to the $7s-7p_{3/2}$ resonance, taking the $7p_{3/2}$ level as Doppler broadened, we calculate a value of $\sigma_{stim} \simeq 8 \times 10^{-17} m^2$ for the cross-section for ASE to the $5d_{3/2}$ level. Hence for a 20cm vapour column, we have an upper limit of $N_i \simeq 2 \times 10^{18}$ atoms m^{-3}, for $\sigma NL = 30$, ie ~0.002% of the total atoms present, assuming 10 torr vapour pressure.

From this argument it would seem unlikely that resonance broadening should contribute significantly to the broadening of the final level in cases where ASE from the intermediate level can occur; it could however be of greater significance in systems where such ASE is absent.

(ii) Lifetime Broadening

If the lifetime of the final Raman level is short then its energy spread may be large, in accordance with the uncertainty principle

$$\Delta E . \Delta t \simeq h \qquad \ldots 2.45$$

For Gaussian lineshape and pulseshape we find that

$$\Delta\nu\,\Delta t = 0.44 \qquad \ldots\ 2.46$$

where $\Delta\nu, \Delta t$ are FWHM values. Thus for the frequency spread to be less than $0.1cm^{-1}$ FWHM we would require the final level lifetime to be greater than 150ps; the natural lifetime of the final Raman level certainly exceeds this value.

However as the SERS proceeds atoms are promoted from the ground state to the final Raman state where a large population attempts to build up. If there exists a state of lower energy and opposite parity to the final state then ASE between the two may occur, thus shortening the lifetime of the level; obviously if the level is metastable this situation cannot arise.

For this situation, the linewidth of the level may be expressed as the sum of the spontaneous and stimulated emission rates,

$$\Gamma_f = \sum_l A_{fl} + \sum_l B_{fl}\,\bar{W}(\omega_{fl}) \qquad \ldots\ 2.47$$

where f is the final Raman level, l the lower levels, A and B the Einstein coefficients and $\bar{W}(\omega_{fl})$ the radiation density, $\frac{\bar{I}(\omega_{fl})}{c}$, at the frequency ω_{fl}; the notation and approach have followed Loudon 1973. Considering just one lower level, then the spontaneous and stimulated rates become equal when $A = B\,\bar{W}_o(\omega_{fl})$; this specifies a spectral radiation density $\bar{W}_o(\omega_{fl})$ for which this occurs which, using the definitions for A and B, may be expressed as

$$\bar{W}_o(\omega_{fl}) = \frac{\hbar\omega_{fl}^{\,3}}{\pi^2 c^3} = \frac{4h}{\lambda^3} \qquad \ldots\ 2.48$$

Thus eqn 2.47 may be rewritten as

$$\Gamma_f = \frac{1}{\tau_f}\left(1 + \frac{\bar{W}(\omega_{fl})}{\bar{W}_o(\omega_{fl})}\right) \qquad \ldots\ 2.49$$

where A_{fl} has been rewritten as τ_f^{-1}, the natural linewidth. $\bar{W}(\omega_{fl})$ may be taken as $\frac{1}{\Delta\omega} \cdot \frac{I_{ASE}}{c\eta}$ where I_{ASE} is the ASE intensity and $\Delta\omega$ its linewidth, typically Doppler broadened; η, refractive index, will be taken as unity. Thus we obtain

$$\Gamma_f = \frac{1}{\tau_f}\left(1 + \frac{I_{ASE}}{c\,\bar{W}_o(\omega_{f1})\,\Delta\omega}\right) \qquad \ldots 2.50$$

Since I_{ASE} is initially small and $\Delta\omega$ is, say, Doppler broadened Γ_f may be small. As I_{ASE} increases so does Γ_f; once $\Gamma_f > \Delta\omega$ one might expect the ASE linewidth now to be determined by Γ_f in which case a better estimate for Γ_f might be

$$\Gamma_f = \left\{\frac{1}{\tau_f}\,\frac{I_{ASE}}{c\,\bar{W}\,(\omega_{f1})}\right\}^{\frac{1}{2}} \qquad \ldots 2.51$$

Experimentally such ASE transi tions are observed; eg in Cs, at 10 torr when pumping 6s-7s SERS, $7s\text{-}6p_{1/2,3/2}$ ASE is observed. For the case $7s\text{-}6p_{3/2}$, $\tau_{7s} \simeq 60ns$, $\lambda_{7s\text{-}6p_{3/2}} = 1.47\mu m$, $\Delta\nu_D = 160MHz$ ($5 \times 10^{-3} cm^{-1}$) and taking $I_{ASE} \simeq 10^{8} Wm^{-2}$ we could expect linewidths of the order $0.5cm^{-1}$, ie final level lifetimes of $\sim 5ps$.

Thus this process may contribute significantly to the line-broadening for cases where the final Raman level is not metastable and ASE occurs, eqn 2.51 giving some feel for the magnitude of the effect. A further effect of such ASE might be to introduce an additional Stark shift of the final level; this could be severe, despite the medium intensity of the ASE, due to the resonant nature of the transition.

(iii) Optical Stark Shift

The interaction of a strong electromagnetic field with an atomic system may cause a shifting and broadening of its energy levels; the pump and Stokes intensities typically used for our SERS experiments are sufficient to require consideration of such effects.

The optical Stark shift experienced by levels in the presence of an intense optical field has been considered in a comprehensive review of the Stark effect by Bonch-Bruevich and Khodovoi 1967 and is also discussed by Letokhov and Chebotayev 1977. The frequency shift of a level n by radiation of frequency ω, electric field strength E and polarization $\underline{\varepsilon}$ may be derived from perturbation theory as

$$\delta\omega_n = \frac{e^2E^2}{4\hbar^2} \sum_m \left\{ \frac{\langle m\,|\,\underline{\varepsilon}.\underline{r}\,|\,n\rangle^2}{\omega_{mn} - \omega} + \frac{\langle m|\underline{\varepsilon}.\underline{r}|n\rangle^2}{\omega_{mn} + \omega} \right\} \qquad \ldots 2.52$$

where $\hbar\omega_{mn}$ is the energy difference of the unperturbed energy levels m,n and the sum is over contributing levels m; this expression is valid

provided $\delta\omega_n << \omega_{mn} - \omega$. When this condition is violated, eg at high field intensities, it is still possible to derive an expression for the Stark shift, given explicitly by Liao and Bjorkholm 1976 as

$$\delta\omega_n = \frac{\omega_{mn} - \omega}{2} \left[\left\{ 1 + \sum_m \left(\frac{eE \langle m|\varepsilon.r|n\rangle}{\hbar(\omega_{mn} - \omega)} \right)^2 \right\}^{1/2} - 1 \right] \quad \ldots 2.53$$

In the low intensity limit this reduces to eqn 2.52. For the case of resonance, $\omega_{mn} = \omega$, splitting rather than shifting of the levels occurs as discussed by Bonch-Bruevich; this case will not be further considered here since generally this situation does not occur in our experiments. These formulae enable an estimate of the shifts of the individual levels to be made; usually the summation reduces to considering the influence of just one near resonant level 1, for which $\omega - \omega_{n1} << \omega$.

In their original work on level shifts involving a two photon resonant situation Liao and Bjorkholm 1975 noted that the product of the shifts of the initial and final levels was proportional to the two photon transition rate W; this applies also to the case of SERS where we also have two photon resonance. Thus, using eqn 2.32 for the transition rate,

$$\delta\omega_g \, \delta\omega_f \propto g I_p I_s \quad \ldots 2.54$$

Thus the effects of level shifts become more severe with increasing Raman gain and pump and Stokes intensities.

In practise, the spatial and temporal variation in the field intensities will result in corresponding variations and smearing out of the shifts; thus the Stark effect may be expected to cause an overall broadening of the observed Stokes output, possibly including a frequency chirping effect. Some evidence of this latter effect has been gathered (Wyatt 1976, Cotter 1976b).

Putting eqn 2.52 in a more useful form

$$\delta\bar{\nu}_n = 3.4 \times 10^{-11} \frac{I}{\Delta\bar{\nu}} z^2_{mn} \qquad (cm^{-1}) \quad \ldots 2.55$$

where I is the field intensity Wm^{-2}, $\Delta\bar{\nu}$ the detuning $(\bar{\nu}_{nm} - \bar{\nu})cm^{-1}$, and z the z matrix element, expressed in Bohr radii. Using Miles and Harris' values for z for Cs, 6s-7s scattering and considering

just the 7p state for level m, we find that $\delta\bar{\nu}_g = 4.6 \times 10^{-12} I_p/\Delta\bar{\nu}$ (cm^{-1}) and that $\delta\bar{\nu}_f = 1.8 \times 10^{-9} I_s/\Delta\bar{\nu}$ (cm^{-1}). Thus for a detuning of $\Delta\bar{\nu} = 10cm^{-1}$ we expect $\delta\bar{\nu}_g = 0.23\ cm^{-1}$ and $\delta\bar{\nu}_f = 5.4\ cm^{-1}$ for typical nitrogen laser pumped system intensities of $I_p = 5 \times 10^{11} Wm^{-2}$ and $I_s = 3 \times 10^{10} Wm^{-2}$. Thus, for this case, the Stokes contribution appears to be the more dominant shift; however, the Stokes intensity does not reach such a high value until it is in the saturated regime, by which time one might expect the spectral properties of the radiation to be already defined, although a strong Stokes backward wave could modify the small-signal behaviour.
Thus the numbers indicate that this process warrants consideration, but its precise magnitude and role remain unclear.

(iv) Power Broadening

In considering power broadening as applied to SERS we shall first explain the process in relation to single photon absorption from a level g to a level f. If we monitor the transmission of a weak probe laser as we tune through ω_{gf} we will measure an absorption lineshape width Γ_o. The atomic transition rate W_{gf} will increase with laser intensity until a regime is reached where the population of the ground state g begins to be significantly depleted. As this is exceeded so the transition rate, and hence the absorption, will still be high further from resonance, whilst near resonance, saturation of the transition occurs, leading to observation of an apparently broadened linewidth.

Analagous to the single photon case, two photon resonant power broadening may also occur; this has recently been investigated by Ward and Smith 1975 and Wang and Davis 1975 for the situation of two photon resonant third harmonic generation. The manifestation of the power broadening in these experiments was a broadened third harmonic and fluorescence linewidth, indicating a saturation of the two photon transition.

In SERS the two photon resonance condition is satisfied by virtue of the nature of the process, $\omega_p - \omega_s = \Omega_{fg}$. Saturation of the two photon transition is now another name for atomic depletion, discussed in section 2.3, and occurs as $W\tau_p$ tends to unity. Thus when atomic depletion occurs, so does power broadening of the transition linewidth. Taking over the results of the analysis of Wang and Davis we obtain

a power broadened linewidth Γ_p related to Γ the homogeneous transition linewidth by

$$\Gamma_p = \Gamma (1 + S)^{1/2} \qquad \ldots 2.56$$

where S is the saturation parameter defined as

$$S = 2 \tau' W \qquad \ldots 2.57$$

where W is the two photon transition rate at line centre, given by 2.32; τ' is given either by T_1, the relaxation time of promoted atoms back to the ground state or by $\frac{1}{4} \tau_p$, whichever is shorter. For SERS in the alkalis the atomic population cascades down by ASE to the lowest p level where radiation trapping prolongs the lifetime of this level; in the alkaline earths the final Raman level may be metastable. Thus for our experiments we may take $\tau' = \frac{1}{4} \tau_p$; hence we find

$$\Gamma_p = \Gamma \left\{ 1 + \frac{\tau_p}{2 N_A \hbar \omega_s} g I_p I_s \right\}^{1/2} \qquad \ldots 2.58$$

Putting numbers in appropriate for 6s-7s scattering in Cs again, taking $g = 4 \times 10^{-8} m W^{-1}$ (ie $|M_{SRE}|^2 = 10^{-30} \times 6 \hbar^3 \varepsilon_o$, and $\Gamma = 0.02 cm^{-1}$), $I_p = 5 \times 10^{11} Wm^{-2}$, $I_s = 3 \times 10^{9} Wm^{-1}$, the output Stokes intensity, then we find $S \simeq 70$ which would imply a broadening of $\Gamma_p = 8\Gamma = 0.16 cm^{-1}$, indicating the possible importance of this mechanism.

The power broadening becomes severe only once atomic depletion has begun and the Stokes wave has achieved a significant intensity. As with the optical Stark effect one might think that the spectral width by this stage would already be determined; again, the practical importance of this is not fully clear.

(v) Plasma Broadening

For the alkalis, as already noted, there are a few percent of dimers present in the metal vapour under the conditions used for SERS. At the intensities used not only does linear absorption of the pump by these molecules occur but also subsequent ionization of the dimers. Two photon ionization of the atoms in the vapour may also occur, a process which will be resonantly enhanced by the SERS intermediate level. Thus the environment for SERS generation may contain a significant density of electrons and ions whose presence will broaden the

energy levels of the atoms by the quadratic Stark effect (Hindmarsh 1974).

We shall consider first photoionization of the atoms. A perturbation theory approach has been used to obtain the two photon ionization (TPI) rate for the alkalis by Bebb 1966 and more recently Lambropoulos and Teague 1976 have calculated detailed numerical values of the TPI rate for Na, Cs and Rb. For Cs they calculate a rate, W/F^2 (F is the photon flux), ranging from $\sim 10^{-46} cm^4 s$ near resonance to $\sim 10^{-49} cm^4 s$ off resonance. Recent experimental work by Granneman et al 1975 and Klewer et al 1977 has indicated good agreement with these estimates near resonance, but poor agreement elsewhere, measuring an off resonance rate of $\sim 10^{-47} cm^4 s$. After a pulse length τ_p the probability of an atom being ionized is $(\frac{W}{F^2}) . F^2 \tau_p$; thus for Cs, taking the experimental rates, a 15ns pulse and a pump intensity of $5 \times 10^{11} Wm^{-2}$ we predict a probability of $\sim 2 \times 10^{-2} - 2 \times 10^{-3}$. This implies an ionization of 0.2 - 2% of the atoms during the pulse by this process yielding an electron (or ion) number density of $N_e \simeq 2 \times 10^{20} - 2 \times 10^{21} m^{-3}$ (for 10 torr of Cs) the higher value occuring near resonance.

Ionization rates for alkali dimers are found to be considerably higher than those for atoms. Granneman et al 1976 have investigated ionization processes for Cs_2 dimers, measuring a rate $W/F^2 \simeq 10^{-42} cm^4 s$. Thus we might expect complete ionization of the dimers present, resulting in an electron density of $N_e \simeq 1.5 \times 10^{21} m^{-3}$, a value exceeding the background atomic two photon ionization for this intensity pump. Granneman et al 1976 have also experimented with Rb_2 and have measured rates generally slightly smaller than those for Cs_2.

A charged particle at a distance R from an atom will result in an energy level shift of magnitude $\delta E = C_4/R^4$ through the quadratic Stark effect. C_4 is the appropriate Stark constant given, for the shift of a level n, by

$$C_{4_n} = (\alpha \hbar c)^2 \sum_m \frac{< n|z|m >^2}{E_n - E_m} \quad \ldots 2.59$$

For the alkalis, for the shift of an ns level the summation may be approximated by considering only the dominant contribution to the sum due to the p level of same principal quantum number, for which case the matrix element is large and the energy denominator small. This expression is valid within the impact approximation which, for electron

broadening of a neutral atom, corresponds to energy level shifts up to several hundred wavenumbers. For SERS in Cs we find typically $C_4 \simeq 10^{-55} - 5 \times 10^{-54} Jm^4$. Thus as R takes all possible values a Stark broadened linewidth is deduced (Hindmarsh 1974) given by

$$\Gamma_s = 11.4 \left(\frac{C_4}{\hbar}\right)^{2/3} \bar{v}^{1/3} N_e \quad \text{HWHM} \qquad \ldots 2.60$$

For a typical electron velocity $\bar{v} = 6 \times 10^5 ms^{-1}$ (Cotter 1976b) and an electron density of $N_e = 2 \times 10^{21} m^{-3}$ we may expect a broadening of the order of $0.15cm^{-1}$(HWHM). In the impact approximation the effect of electron broadening is much greater than that due to the ions; at high ion densities however the contribition of quasi-static ion broadening may become important also. A net shift accompanies the line broadening and is given by $\Delta\omega = \Gamma_s \tan\left(\frac{\pi}{3}\right)$ for the quadratic Stark effect, ie $\Delta\omega = \sqrt{3}\,\Gamma_s$. Thus the combined effect of the Stark broadening and shift, varying as the ionization may vary as the pulse evolves, may represent a significant contribution to the line broadening.

Griem 1974 also considers the theory of plasma broadening from a quantum mechanical approach in some detail; he includes tabulations of normalized shifts and widths for several elements incorporating the ionic quasi-static contribution which, as noted by Hindmarsh for our conditions, is general small. For Cs these values give agreement to within a factor of two with calculations following Hindmarsh.

(vi) Hyperfine Structure

For the alkalis the hyperfine structure, HFS, of the ground state can be significant; for Cs this is estimated as $0.3cm^{-1}$ and for Na $0.06cm^{-1}$. Thus HFS was considered when the initial broad linewidth results were obtained with Cs; despite instrumental resolution of $0.1cm^{-1}$ however a monochromator scan of the SERS observed just one broadened line rather than two distinct lines originating from the two HF levels as might have been expected. The significance and role of the HFS in Cs in relation to SERS is not clear at present. For Na the HFS is narrower than the dye laser linewidths used for pumping SERS and so is not considered further. For the alkaline earths, with ground state $ns^2\,{}^1S_o$, no HFS of this state can occur (since the angular momentum $J = 0$).

2.5.3 Concluding Comments on Linebroadening

We have attempted to outline the physical mechanisms which could be responsible for the observed broad SERS linewidth. Whilst providing some order of magnitude for the effects to indicate their possible significance their physical behaviour and interrelationship is by no means clear. Whilst a complete dynamic analysis of the problem has not yet been attempted, such an analysis has apparently been performed for the case of two photon absorption (Elgin 1977) and it might be possible to modify this analysis for our SERS case.

It would seem that the limiting factor for several of the possible mechanisms we have considered is the pump intensity used. In order to obtain efficient SERS over wide tuning ranges such high intensities are necessary; unfortunately this inherently adds to the severity of most of the broadening mechanisms considered. (For comparison we note the 'atomic Rydberg state 16μm laser' operating on the $6d_{3/2} \rightarrow 7p_{1/2}$ levels in K described by Grischkowsky et al 1977; using a pump intensity of $3 \times 10^{4} Wm^{-2}$ the linewidth of their ASE output was less than their $0.2cm^{-1}$ instrumental resolution - a detailed examination of their experiment with respect to line broadening mechanisms has not been performed.)

The crucial question with respect to the line broadening is whether or not it will be possible to obtain a narrow linewidth SERS output whilst using the high intensities necessary to make a useful system.

2.6 Other Processes

The dominant processes occuring in the atomic vapour when pumped to produce SERS have already been covered. However some further nonlinear processes which generally are not of major significance do occur and some of these will be briefly mentioned here for completeness.

In the alkalis, with small continuum matrix elements, it is anticipated that THG of the pump will be inefficient. A similar argument applies for the mixing processes $2\omega_p \pm \omega_s$, provided the energy of the generated photon exceeds the ionization potential. The processes $\omega_p \pm 2\omega_s$ are more likely to occur under suitable conditions; the process $\omega_p - 2\omega_s$ has in fact been previously observed in potasium by Sorokin et al 1973 and, over a broader tuning range accompanying the SERS, by Wyatt 1976. Such four-wave mixing processes have been studied in some detail by Kärkäinen 1975, 1977 where the low conversion

from SERS to the parametric wave is noted. Other four-wave mixing processes involving ASE transitions occuring from the final Raman level have also been reported , Corney and Gardner 1977; they observed the coherent anti-Stokes Raman scattering process $\omega_{UV} = \omega_p - \omega_s + \omega_{ase}$ in Cs vapour.

In Na using two photon pumping, sections 4.2, 4.3, other parametric processes may occur; the process $2\omega_p = \omega_{UV} + \omega_{IR}$ is considered later on.

In the alkaline earths, with their higher ionization potentials and low lying autoionizing levels in the continuum, it is anticipated that under the appropriate conditions THG and four-wave sum mixing could occur quite strongly; indeed it was an attempt at SERS in Sr which initiated Sorokin's work on these processes. Four-wave mixing processes of the type observed in the alkalis may also be expected to occur.

It is possible also at the intensities used that coherent pulse propagation phenomena may occur which could modify the pulse shape; a treatment of these effects has however not been attempted.

CHAPTER 3

Dye Lasers and Metal Vapours

In this chapter the details of construction and performance of the dye lasers and pumping system are considered along with some physical properties of the alkalis and alkaline earths; the design and operation of the heat pipe ovens used for containing the metal vapours are also discussed.

3.1 Dye Lasers

The dye lasers used in this work were based on that used by Wyatt 1976, involving a frequency doubled ruby laser pumping a dye oscillator-amplifier arrangement. This system was inherited and (the oscillator) used for the initial work on Cs and later reconstructed for the Sr work, both experiments requring a blue dye laser, $\lambda_p \sim 460$nm. For the work using Na and Ba some modifications to the dye laser were needed to provide the wavelengths required, ~580nm and ~790nm respectively.

Firstly the primary pump, the ruby laser, and the frequency doubler will be discussed followed by the design and characterization of the dye oscillator-amplifier arrangement.

3.1.1 The Primary Laser

The ruby laser used, shown in fig 3.1, was a 1971 Laser Associates model no 505 design, using a 4" x $\frac{3}{8}$" AR coated ruby rod pumped by a helical Xe-filled flashlamp; the laser head was cooled by circulating cold de-ionized water from an associated refrigeration unit. The optical cavity consisted of a 2.6m curvature concave mirror (R = 100%) and an uncoated heavy-glass etalon (R= 27%), serving as an output coupler, separated by ~50cm. Used as such the laser gave an output of 1J multimode in a relaxation oscillation behaviour over a period of 300μs. For frequency doubling or dye laser pumping the ruby laser was operated Q-switched using a KD*P Pockels cell and a calcite Glan-Taylor polariser between the ruby rod and the 100% mirror. Q-switched operation without the polariser was possible, using the birefringence of the ruby to polarise the radiation; bad hot spots were observed in the beam under these circumstances however and so the laser was usually operated with the calcite polariser. Thus under normal operating conditions we could obtain an energy of 1J in a 30-35ns pulse,

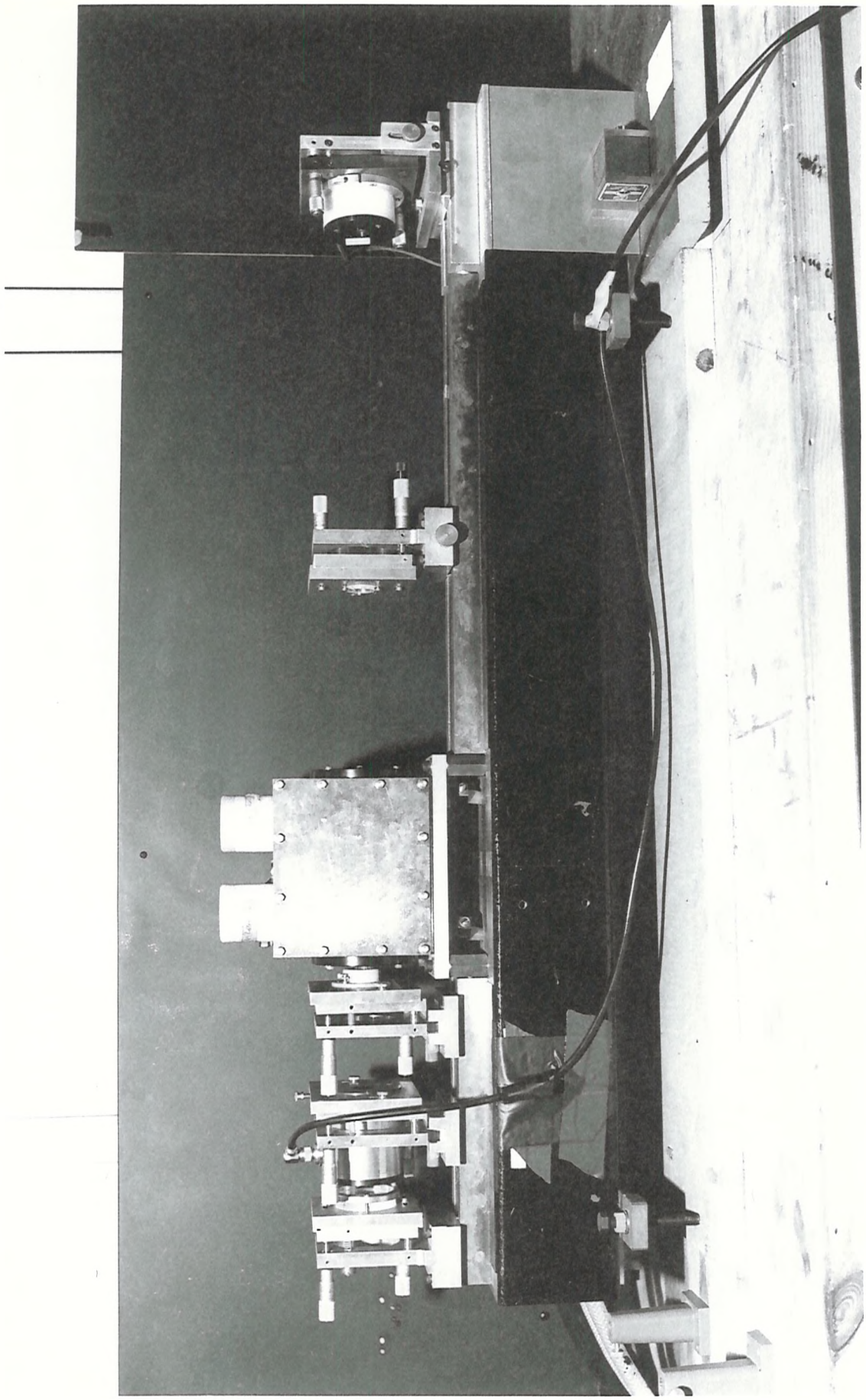

Fig 3.1 The Ruby laser and RDA doubling crystal

a power of ~30MW. This was usually frequency doubled to 347nm to pump the visible dyes, but for the near-IR dye laser direct pumping at 694nm was used.

The multimode output from the ruby laser had a beam divergence of several millirads; consequently the angular acceptance of the frequency doubling crystal was an important factor in determining the second harmonic generation efficiency. A 2cm crystal of RDA, Rubidium Dihydrogen Arsenate, (see Kato 1974) was generally used for SHG; heating in an oven to ~100^{o}C enabled non-critical phase matching and consequently a large angular acceptance. In this manner we were able to reliably obtain ~ 100mJ of second harmonic in a slightly shortened pulse length, 25-30ns. On occasions, room temperature ADP, Ammonium Dihydrogen Phosphate, was also used as the frequency doubler; with its lower angular acceptance this gave ~ 30mJ of UV.

Various problems were encountered with the doubling crystals; these motivated us to be content with the reliable doubling efficiencies quoted rather than to push for higher efficiencies attainable at higher powers. At high UV outputs, Wyatt 1976 observed internal damage of the RDA crystal which he attributed to hot spots in the passively Q-switched beam; this internal damage has since then not increased. However it has become apparent that the index matching fluid 'FClO4' used in the RDA oven begins in time to absorb the UV radiation and decompose; once started the effect accelerates, depositing material on the crystal and the windows. In such cases it has been necessary to strip down and clean the crystal and windows, and on one occasion, to have the crystal repolished. This problem was in some measure overcome by using a modified cell with less distance of liquid between the crystal and the windows; at lower temperatures the effect appears not to be so severe and another alternative would be to use a different cut of crystal 90^{o} phase matchable nearer room temperature. In fact, at room temperature, decomposition of the 'Freon' index matching fluid used with the ADP has also occured on one occasion.

Some comments regarding the limitations of this primary pump system are in order at this point. Firstly, perhaps the prime limitation of the ruby laser used was the repetition rate; 1Hz should be attainable using the refrigeration unit to cool the laser head, but more generally $\frac{1}{4}$ Hz was used in order to prolong the life

of the flashlamp. This repetition rate makes alignment of the dye laser and optics very tedious and, even at 1 Hz, is prohibitively slow for spectroscopic purposes. As the flashlamp aged and its efficiency decreased the output of the laser was observed to drop. (Initial problems were also encountered due to vibrations from the flashlamp misaligning the optical cavity; continuing ones were also met in terms of breakdown of parts of the (somewhat elderly) power supply and refrigerator units.)

The fundamental problem of repetition rate is inherent to the ruby laser, relating to its inefficiency; however, a high power pump source at high repetition rates would be desirable. Using such a system it should be possible to provide a well characterised SERS source, usable for practical sprectroscopy, based on the Cs 6s-8s, 6s-9s transitions around 7μm and 13μm, such as has already been done using the nitrogen laser pumped Cs 6s-7s system around 3μm (Cotter et al 1977b). Two possible candidates exist for the role at present, an excimer laser or a frequency multiplied Nd:YAG system. An excimer system, KrF or ArF, has the advantage of high efficiency high energy UV output, up to a few hundred mJ, directly available to pump a dye (see Sarjeant 1977, Lambda-Physik 1977). It could also pump dyes further into the UV than is possible with a doubled-ruby or nitrogen laser, thereby allowing access to new SERS transitions. The big limitation of such a laser currently is its need for frequent gas refills, eg after every 10,000 shots, which is every $\frac{1}{2}$ hour at 5Hz (Lambda-Physik 1977); improvements in gas life are hoped for in the near future however. A further reservation is that being a recently developed system it is still not yet thoroughly engineered and characterised.

Alternatively, the brightness of the Nd:YAG oscillator has recently been dramatically improved by using an unstable resonator configuration (Laycock 1977). In this way a standard 25J flashtube input Nd:YAG laser has produced a maximum of 50 mJ second harmonic (200mJ of 1.06μm doubled in KD*P). For pumping Rhodamine 6G and longer wavelength dyes this would be a very practical and useful source. For pumping blue and UV dyes a further stage of frequency conversion, tripling or quadrupling the fundamental, would be necessary; use of a Nd:YAG amplifier before the frequency conversion stages should result in the energy output required. From our

experience with ruby doubling in RDA at high powers however reservations exist as to the reliability of the frequency conversion stages; further, such a system would be rather expensive.

3.1.2 The Dye Oscillator

The dye oscillator comprised a small cell containing dye solution inside a resonator, one element of which was an output coupling mirror and the other a diffraction grating to provide tunability. A beam-expanding prism was used to spread out the intracavity beam incident upon the grating; in this way the power density was reduced, preventing damage to the grating, and also the divergence of the beam incident on the grating was reduced thus enabling us to obtain a narrower linewidth. The whole assembly was mounted on a solid metal girder to provide good mechanical stability.

The coupling of the primary pump into the dye oscillator and amplifier is shown in fig 3.2. An uncoated silica beam splitter was used to couple ~14% of the pump to the oscillator, the remainder pumping the amplifier; ~10cm cylindrical silica lenses were used for focussing to give a roughly cylindrical pumped region of dye in the cell.

The physical layout of the oscillator is illustrated in fig 3.3 and the photograph in fig 3.4 shows the set up as used with the near-IR dye; constructional details for the three variations which were used are given in table 3.1.

The dye output mirror for the blue and orange dye lasers was an uncoated, wedged sapphire flat, R = 8%, used originally because we did not have a suitable high damage threshold mirror; for the near-IR a ruby laser mirror having R = 50% at 790nm was found to give increased energy output and so was used. When working up the near-IR dye laser the output mirror was moved nearer to the dye cell and was left in this position during operation.

The diffraction gratings for the blue and orange spectral regions were holographic ones supplied by the NPL and were mounted in an 'Oriel' micrometer adjustable mount; the near-IR grating was also holographic, from Oxford University. Initial adjustment of the grating involved aligning the rulings, its vertical axis and those of the beam-expanding prism and the output mirror all parallel. This was

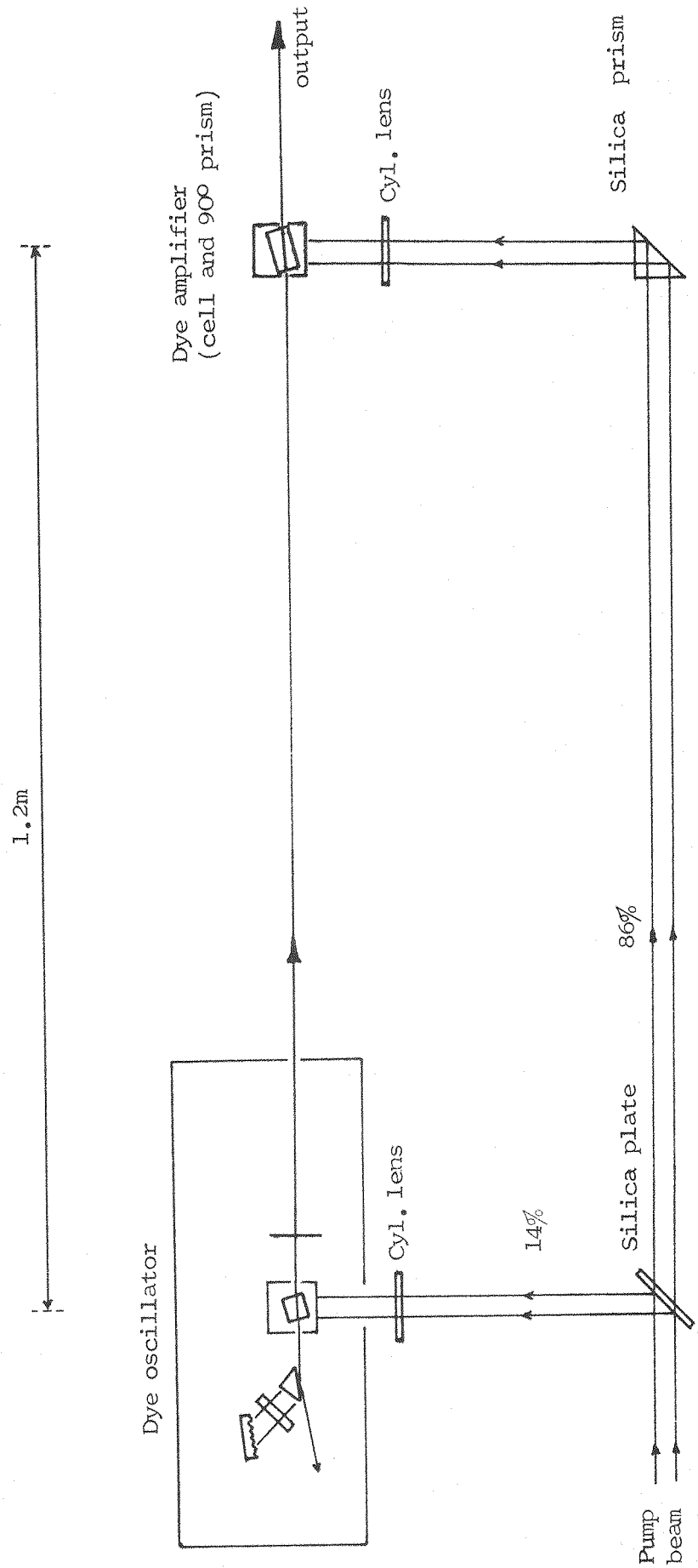

Fig 3.2 Dye laser pumping arrangements

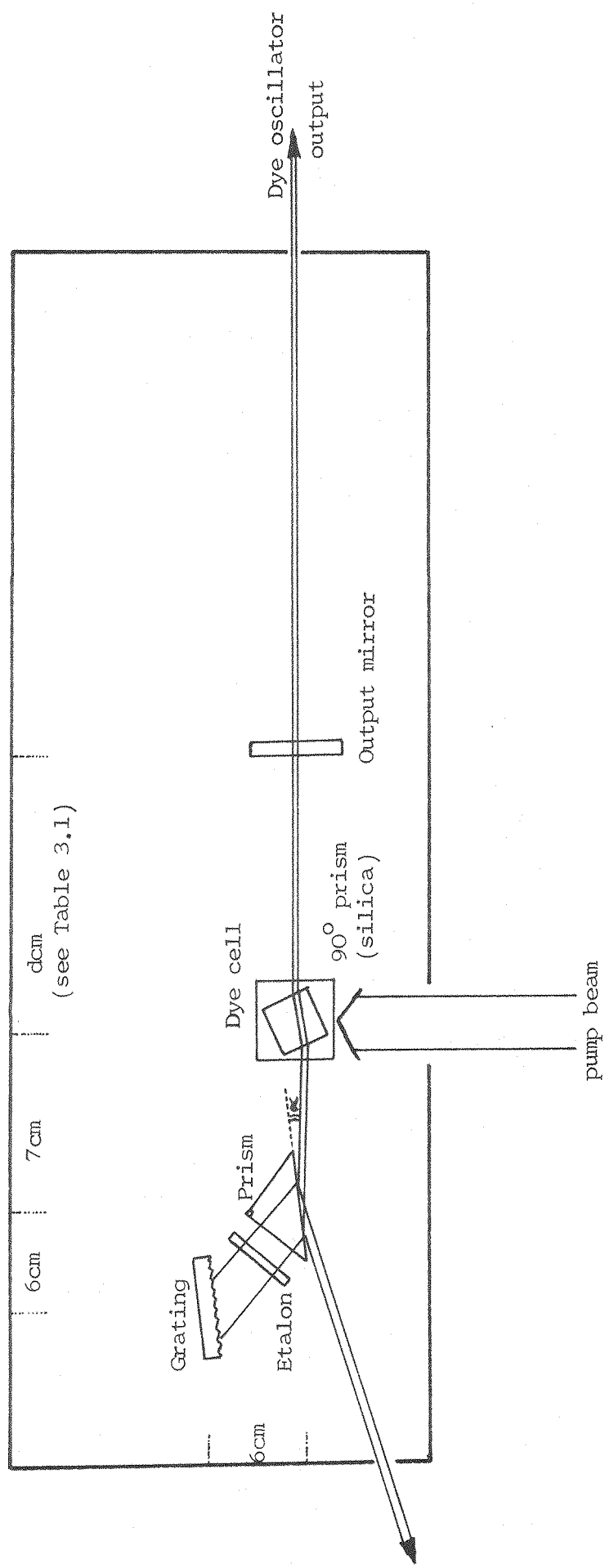

Fig 3.3 Dye oscillator layout

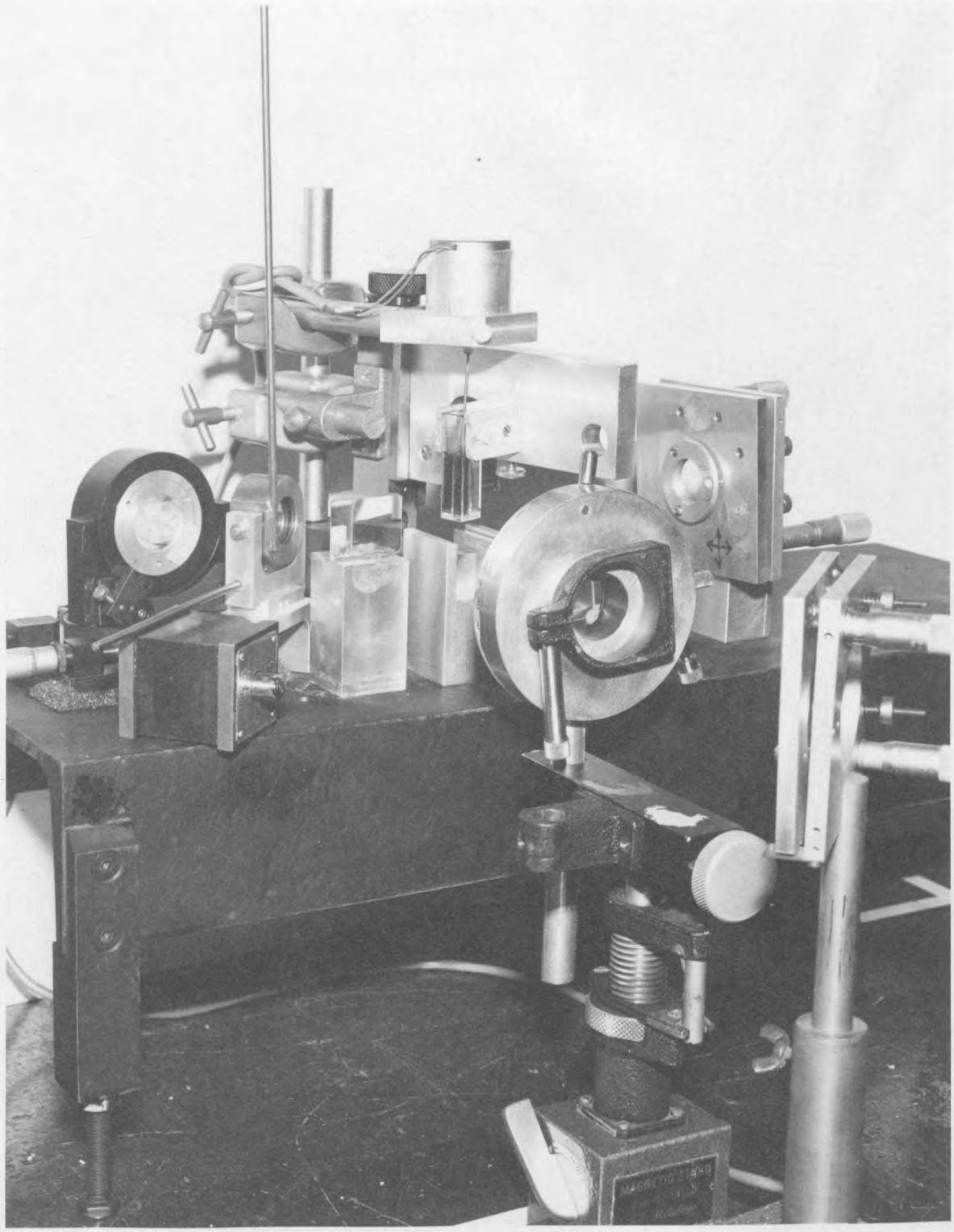

Fig 3.4 Dye laser oscillator

Dye	Grating l/mm	Output mirror R	Output mirror d	Intracavity etalon	Dye cell length	Preferred polarisation	Dye concentration
7D4MC (blue)	3680	8%	28cm	-	1cm	Parallel to pump	10^{-3}M/l in MeOH or EtOH
Rh6G (orange)	2880	8%	28cm	-	2cm	Perpendi-cular	1.5×10^{-3}M/l in EtOH
HITC (near-IR)	1460	50%	13cm	Sometimes used. FSR = $1.7cm^{-1}$ F = 8	1cm	Parallel	5×10^{-5}M/l in EtOH

Table 3.1

Constructional details of the dye oscillator

done using a HeNe laser (for the orange and near-IR) or an Ar laser (for the blue) and observing, and modifying, the relative positions of the zeroth and first order diffractions.

The prism was arranged to have an angle $\alpha \simeq 3^{o}$, see fig 3.3, between the prism face and the beam direction, the optical axis. This corresponded to a prism magnification of M ~ 15; under typical pumping conditions this allowed the beam to be spread out to fill the grating.

With the grating set at an appropriate angle and the position of the pumped region adjusted to be incident on the prism, and thence the grating, an output could be fairly readily obtained. This initial adjustment was more difficult for the near-IR dye since an infra-red viewer was needed to observe the position of the beam. Once working optimisation of several parameters in a systematic way was possible: the transverse and vertical position of the pumped region, its orientation relative to the optical axis and tightness of pump focussing. In this way a good compromise between energy and beam quality was possible.

Some laser dyes have a preferred polarisation, relative to the pump polarisation, for which the gain is higher (see eg Fawcett 1970, McFarland 1976). For many blue dyes, including that used, 7D4MC, the gain is highest for polarisation parallel to that of the pump. The prism-grating combination used in the oscillator is also polarisation sensitive providing higher feedback for horizontally polarised light. Thus in order to pump optimally it was necessary to use a 90^{o} prism to pump the dye cell from underneath. This was also found to be necessary for the near-IR dye, HITC, whereas side pumping was required for the orange, Rh6G, dye.

With the prism-grating arrangement with the visible dyes it was possible to achieve good narrow-linewidth performance, without the use of an intracavity etalon. Typically linewidths of ~ 0.1-0.15cm^{-1} were measured by visual observation of fringes obtained by passing the beam through a Fabry-Perot viewing etalon. The linewidth of the near-IR dye laser however was found to be considerably broader, typically 0.7cm^{-1} but sometimes even broader. This was attributed to the higher pump intensity used, pumping with the ruby rather than second harmonic, which resulted in a somewhat poorer beam quality and higher beam divergence from the oscillator; the shorter cavity length

may also have contributed to this. This higher divergence would result in poorer frequency discrimination by the grating; the lower frequency of the rulings of the grating could also have contributed to the broad linewidth. Using an intracavity etalon, a dielectric coated 2mm substrate, of 1.7cm^{-1} free spectral range and a finesse of 8 enabled linewidths of 0.1-0.2cm^{-1} to be obtained. For the near-IR dye the linewidth was measured by frequency doubling the amplified output in ADP and then observing the FP fringes on a scanning photodiode array, thus providing a more objective method than visual observation. The second harmonic linewidth was taken as being $\sqrt{2}$ times that of the fundamental, a linewidth broadening inherent in the SHG process, assuming the second harmonic linewidth to be given by the convolution of the gaussian fundamental linewidth with itself. Such measurements enabled us to quantify the stability of the dye laser, necessary for the SERS linewidth measurements performed to be unambiguous. Figure 3.5 shows photographs of the photodiode array scan across a section of the FP fringes showing (a) a series of 20 successive shots and (b) a sample of one shot per minute for 15 minutes. Thus the short and long term linewidths were verified as being better than 0.17cm^{-1} FWHM for the 790nm laser. Careful adjustment of the intracavity etalon was necessary to obtain optimum performance, care being taken to eliminate any trace of operation on more than one etalon mode. Further linewidth narrowing was attempted using an extra cavity etalon but did not succeed since the mirrors available for the etalon were not of sufficient quality.

The dye cuvettes used were either 1 x 1 x 4 cm or 1 x 2 x 4 cm fluorimeter cells supplied by Heraeus (Fused Quartz Products) and made of natural or synthetic quartz (both varieties were used). Problems with the optical quality had been observed with earlier cells from another source but none were found with these. A compromise might be expected between cell length, conversion efficiency and competition from amplified spontaneous emission from the dye solution. An interrelationship between these certainly occurs but practically the approach used in deciding which cell length, 1 or 2cm, to use was to experimentally see which gave best results. The blue and near-IR dye oscillators were observed to give considerably more ASE with a 2cm cell and so a 1cm one was used in these cases, for the orange dye the laser operated satisfactorily with the 2cm cell, and was consequently incorporated into the oscillator. A mechanical stirrer was used in

Fig 3.5 HITC dye laser frequency stability (FP fringes)

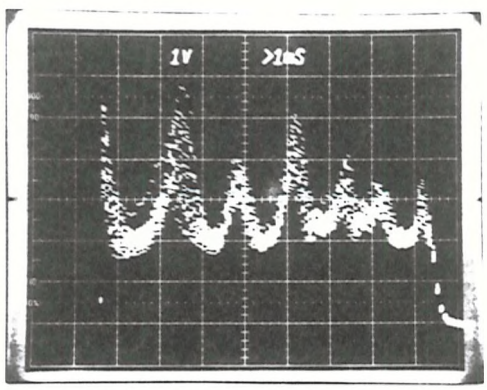

(a) Short term stability

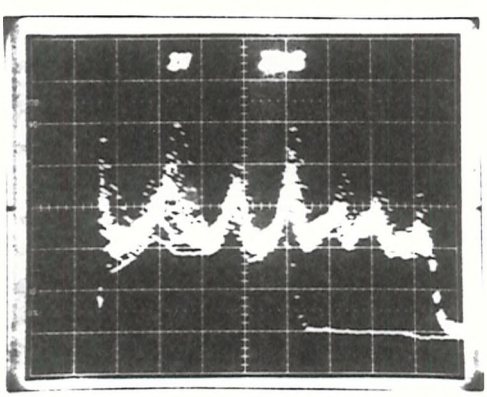

(b) Long term stability

the dye cell to alleviate any thermal effects and to prevent photodissociation products of the dye accumulating in the pumped region; the dye solution was generally renewed daily for similar reasons.

It was for reasons of ASE behaviour that the output was taken through the mirror, see fig 3.3, rather than off the prism, as has been done with the nitrogen pumped arrangement (Hanna et al 1975); with our somewhat higher pump levels the problem of ASE is increased. Coupling the output through the mirror prevented ASE from causing difficulties; only for the Rh6G dye laser did we observe any significant ASE output in the forward direction, and that only at one (lower) extreme of the tuning range. Strong ASE, a few mJ, was observed from the prism face in the backward direction for the near-IR oscillator when the grating was obscured; even so, in the forward direction, this was not sufficiently strong to cause the amplifier to respond and no output at all was observed from the amplifier under such conditions. Nevertheless this serves to illustrate the need to couple the output through the mirror as was done; obviously however considerable dye energy is coupled out of the cavity by the prism, thus reducing the useful efficiency of the oscillator.

The dyes used were 7D4MC (7 Diethylamino 4 Methyl Coumarin, also known as Coumarin 1), Rh6G (Rhodamine 6G) and HITC(1,3,3,1′, 3′,3′ - Hexamethyl - 2,2′ - indo tricarbo cyanine iodide). The tuning range of the blue dye matches well to the tuning range required for pumping Cs 6s-7s SERS, as had been previously shown, and was used for this reason. For the orange dye the original requirement for the wavelength was that we should be able to attain two photon resonance with the Na 3s-4d transition, $\lambda_p \sim 579$nm; it was originally thought that an admixture of Rhodamine B to Rh6G might be needed, but this proved unnecessary. The solvent originally used with the 7D4MC was methanol, but later this was replaced by ethanol, which was also used with the Rh6G. Ethanol was preferred because of its lower toxicity and its reduced ability to transport the dissolved dyes through the skin; its performance as a solvent for lasing was very similar to that of methanol. Around 790nm, HITC was recognised as being a fairly efficient dye (Miyazoe et al 1968, Oettinger and Dewey 1977) and was in fact the dye used by Carlsten and Dunn 1975 for their Ba experiments. In common with other polymethine dyes it is very

concentration and solvent dependent in its behaviour (cf Sorokin et al 1967b). Initial experiments investigated the efficiency and tuning behaviour of the dye at various concentrations in the following solvents - water + 5% 'triton' (a surfactant), DMSO (dimethyl sulfoxide), acetone and ethanol. With our transverse pumping arrangement the best performance at 790nm was obtained with ethanol. The importance of these concentration and solvent effects is noted in that using the one dye HITC it was possible to cover completely the tuning range 770-865nm by varying these factors.

The low observed efficiency of the dye oscillator using HITC caused some concern and so some HITC from another source was also tried, with similar results; the dye DDI (1, 1′ Diethyl - 2, 2′- Dicarbocyanine iodide) was also tried and found to lase with slightly worse performance than HITC at 790nm. Although the high (50%) reflectivity mirror used gave higher output in the forward direction, it was also found that a few mJ came out backwards off of the prism; this output was not utilised however because of the competition from ASE in this direction. The energy lost in this way was not measured for the visible dyes, preventing a quantitative comparison of efficiency. However, the high pump energy available for the near-IR dye meant that its efficiency was not a major consideration.

A comparison of the performance of the dye oscillator using the different dyes is presented in table 3.2

3.1.3 The Dye Amplifier

The dye amplifier comprised a 1 x 2 x 4cm cell containing dye solution pumped by the remaining 86% of the pump beam (somewhat less, due to aperturing by the optical components, for the ruby pumped HITC dye laser). As with the oscillator a 90^{o} prism was used to pump from underneath the cell when using 7D4MC and HITC; this may be seen in the photograph of the HITC dye laser in fig 3.6. The oscillator output had diverged somewhat by the time it reached the amplifier, thus a larger pumped region than that in the oscillator was in order; this was also necessary in order to avoid excessively high pumping intensities. As with the oscillator the tightness of the focussing and hence the size of the pumped region was optimised with respect to beam quality as well as energy output; the transverse and vertical position and orientation of the pumped region could be adjusted, ensuring good overlap between the oscillator beam

Dye	Tuning range	Osc pump	Osc output	Linewidth
7D4MC	443 - 489nm	12mJ at 347nm	1mJ	$< 0.2cm^{-1}$
Rh6G	570 - 603nm	12mJ at 347nm	1mJ	$< 0.2cm^{-1}$
HITC	770 - 815nm	100mJ at 694nm	2.5mJ	$0.7cm^{-1}$
			1.5mJ*	$< 0.17cm^{-1}$*

* with intracavity etalon

Table 3.2

Dye oscillator performance

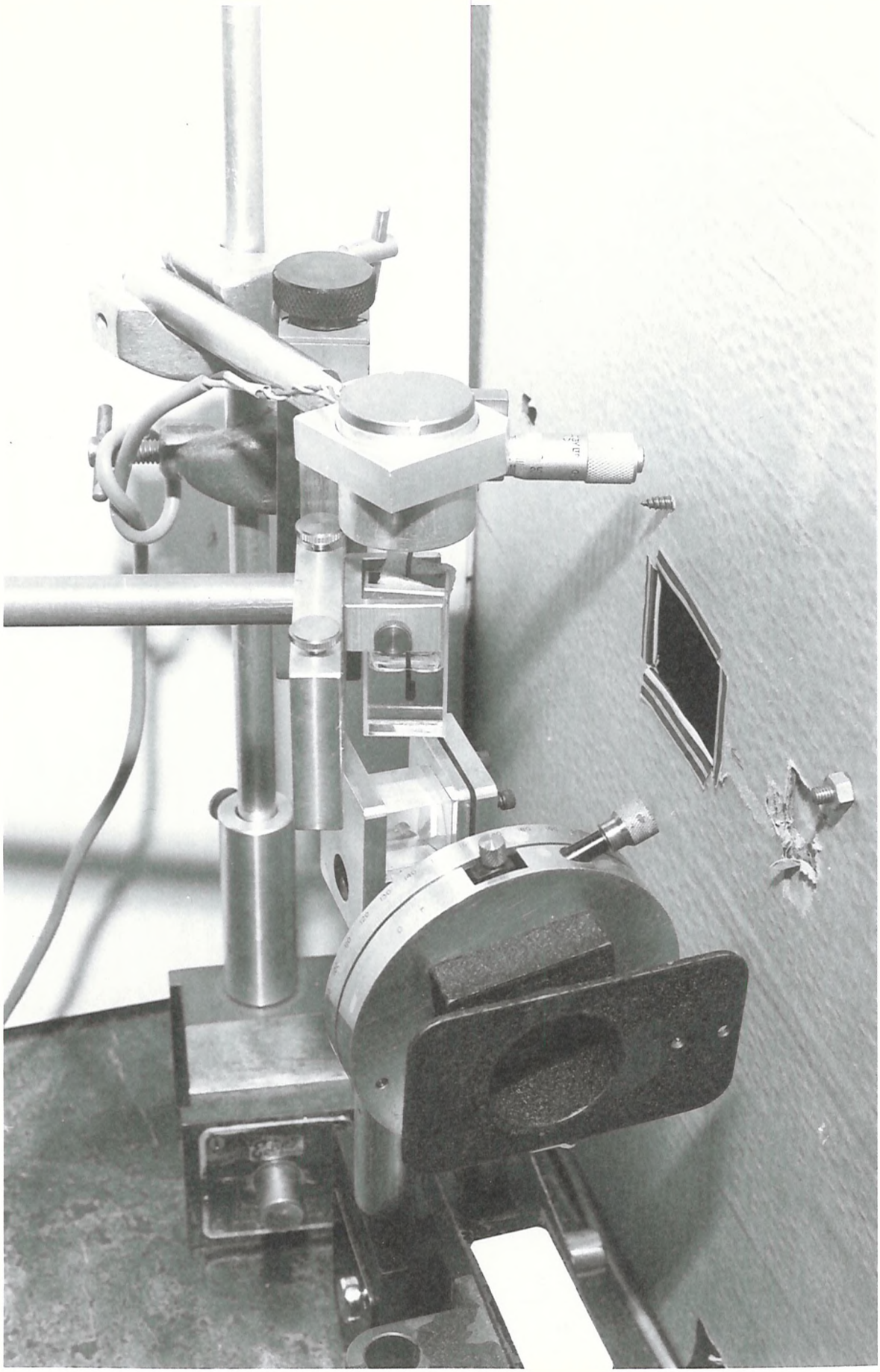

Fig 3.6 Dye laser amplifier

and the pumped region. The beam quality of the visible dye lasers was fairly good; the output of the 7D4MC system was investigated in some detail and found to be fairly gaussian in spatial distribution. From measured spot sizes and assuming gaussian beam theory the values inferred for the dye laser beam waist for various focussing conditions were fairly self consistent, again implying good spatial behaviour. The Rh6G laser appeared, by observation of polaroid burns, to be of similar quality. The pumped region of the HITC amplifier and its subsequent output beam were somewhat larger than for the visible dyes, due to the higher pumping energy available, thus making visual comparison of beam quality difficult; thermal distortion of the dye solution, expected at such higher pump energies, may have accounted for poorer beam quality observed on some occasions. Nevertheless, excellent beam quality was not essential for our purposes due to the high output energies available; normally the output was used unfocussed, but it was possible to attain fairly tight focussing when required. The performance of the dye amplifier is given in table 3.3 for the three dyes used; the energy and pulse length values listed there are typical ones.

It was sometimes found that during a day's work in the laboratory the performance of the overall system deteriorated from its optimum; variations in ruby laser output were sometimes the cause of this. Such variations may have been due to a measure of instability of the power supply and thermal and vibrational effects causing slight misalignment of the cavity; any small drop in performance of the ruby laser was obviously magnified in the subsequent frequency doubling and dye laser pumping stages. Fairly frequent monitoring and re-optimisation of the ruby output was therefore necessary. Pump beam wander and slight misalignment in the dye laser optics also on occasions resulted in a degraded performance.

Figure 3.7 displays the temporal behaviour of several consecutive shots from the HITC dye laser measured using a Judson InAs detector and fast oscilloscope; similar behaviour was observed with the visible dyes. As may be seen the pulse width varied somewhat; this may have been due to the variations in the Q-switched ruby pulse length. The effect of these variations was a fluctuation in pump power for the SERS processes. This together with the slow ruby repetition rate, made precise measurements sometimes difficult; nevertheless, averaging over several pulses, albeit slow, enabled such measurements

Dye	Dye concentration	Pump	Amp output	Pulse length	Output power
7D4MC	5×10^{-1} M/l in MeOH or EtOH	80mJ at 347nm	8mJ	16ns	500kW
Rh6G	10^{-3} M/l in EtOH	80mJ at 347nm	8mJ	16ns	500kW
HITC	5×10^{-5} M/l in EtOH	650mJ at 694nm	50mJ	30nS	1.7MW
			30mJ*		1MW*

* with intracavity etalon, dye osc output reduced

Table 3.3

Dye amplifier performance

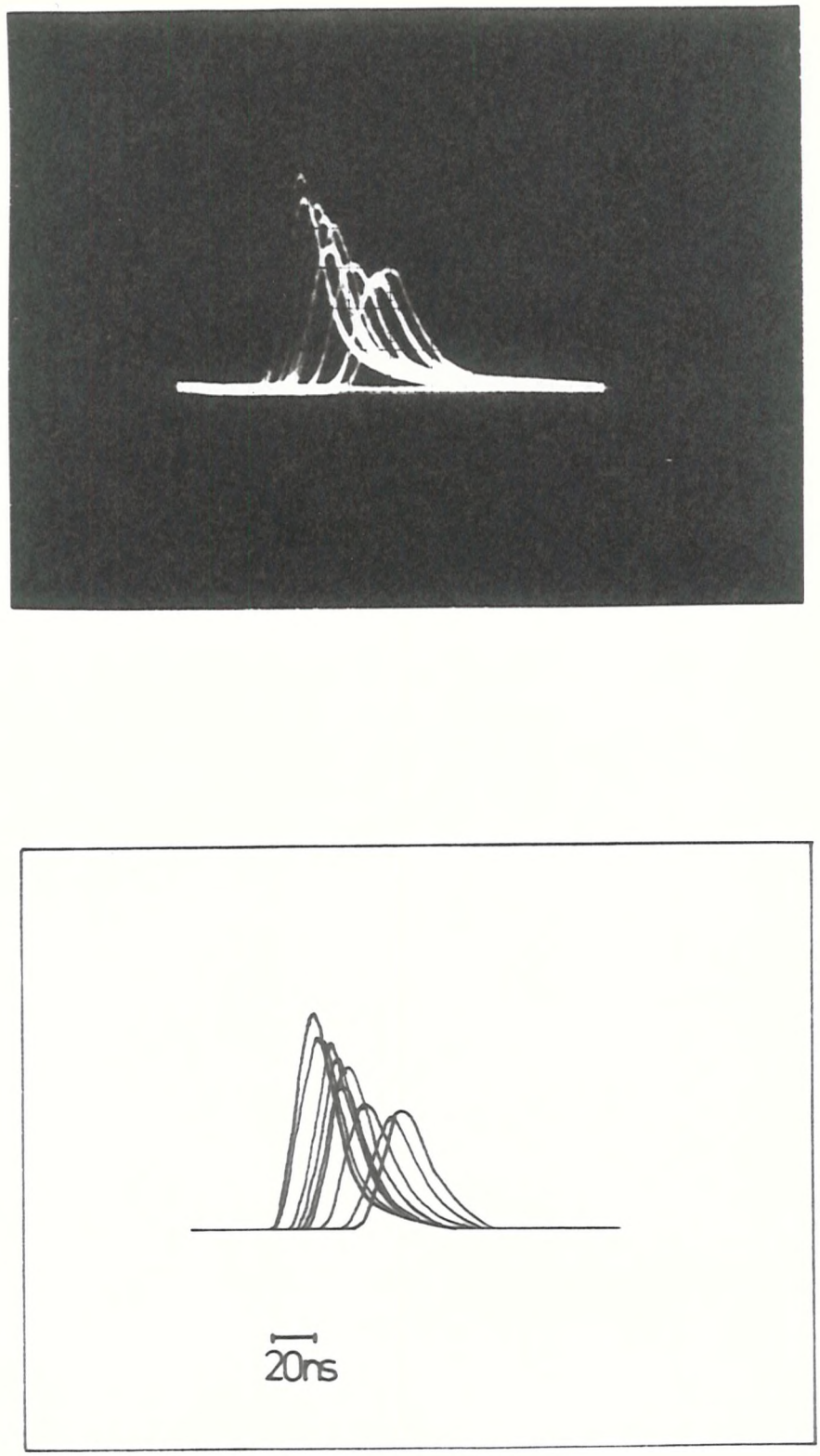

Fig 3.7 Ten consecutive pulses from the HITC dye laser

to be made. Despite its limitations, the high power narrow linewidth dye laser described has proved itself to be a very useful research tool.

3.2 Metal Vapours

We shall consider here both the physical and practical properties of the metal vapours used. The heat pipe ovens used for containing the metals will be described; some modifications to the design of the higher temperature oven are suggested for future work on the alkaline earths.

3.2.1 Alkalis and Alkaline Earths

The alkalis were the first elements in which stimulated electronic Raman scattering was performed and have also been used for a variety of other nonlinear optical experiments (eg Stappaerts et al 1976, Bjorklholm and Liao 1974, Bethune et al 1976 and many others). They are suited to such work in various ways - they have relatively simple one-electron spectra, low melting points and are readily available at modest cost. Considerable work has also been performed using the alkaline earths, notably in the fields of third harmonic generation, THG, and of four wave parametric mixing (eg Wynne and Sorokin 1977, Bjorklund et al 1977, Ferguson et al 1976, Wallace et al 1976); their much higher melting points can make operation somewhat less straightforward however.

Some of the parameters of relevance for SERS in the alkalis and alkaline earths are given in table 3.4. Cotter 1976b has adequately reviewed these properties for the alkalis and data is given in the table only for the elements Cs and Na, investigated in this work. For the alkaline earths data has been given for Mg and Ca as well as for Sr and Ba, on which experiments were performed. (No data has been given for the other alkaline earths Be and Ra, since the former's high melting point (1280^{o}C) and the latter's radioactive nature preclude their use for such work.) Mg and Ca have both been used at pressures of several torr in heat pipe ovens for investigating nonlinear optical processes (Wallace et al 1976, Ferguson et al 1976, Bloom et al 1975b).

The atomic number density N_A may be related to the temperature (K) and the vapour pressure (torr) of the element, assuming the ideal gas law, by

$$N_A = 9.66 \times 10^{24} \frac{p}{T} \qquad (m^{-3}) \qquad \ldots 3.1$$

		Cs	Na	Mg	Ca	Sr	Ba
Atomic weight		133	23	24	40	88	137
Ground state		$6^2S_{1/2}$	$3^2S_{1/2}$	3^1S_o	4^1S_o	5^1S_o	6^1S_o
Ionisation limit (cm^{-1})		31407	41450	61669	49305	45926	42032
Melting point (^oC)		28	98	649	839	770	729
Vapour pressure constants	a	8827	12423	16300	17658	17153	21414
	d	16.0	17.4	18.8	16.9	16.9	16.8
Temperature (^oC) for 10 torr		373	546	740	970	900	1203
Dimer concentration	at 1 torr	0.6%	3.3%	-	-	-	-
	at 10 torr	1.3%	5.8%	-	-	-	-
Oscillator strength data		Warner 1968	Warner 1968	-	Parkinson et al 1976 Friedrich et al 1969	Parkinson et al 1976 Kelly et al 1973	Miles and Wiese 1969
Energy level data		Moore 1958	Wiese et al 1969	Moore 1949	Moore 1949	Moore 1952	Moore 1958

Table 3.4 Relevant Data for some Alkalis and Alkaline Earths

The vapour pressure p depends on the thermodynamic properties of the element and its temperature and may be expressed as

$$p = \exp\left(-\frac{a}{T} + d\right) \qquad \ldots 3.2$$

where a and d are constants (table 3.4) . For the alkalis these constants have been taken from Miles and Harris 1973. For the alkaline earths the data of Schins et al 1971 has been tabulated; these measurements were made at somewhat higher pressures than we have used. For Ba, however, their results are in good agreement with those of Hinnov and Ohlendorf 1969 obtained at lower pressures; for Sr and Ca also their results are in fairly good agreement with other sources (Sax 1968, Weast 1971, Honig and Kramer 1969, Nesmeyanov 1963). Schins' data for the alkalis is also in good agreement also with that quoted by Miles and Harris. For Mg the vapour pressure constants tabulated have been calculated from the data of Honig and Kramer. It would appear from comparison of the literature that vapour pressure data for the alkaline earths is not as accurately known as for the alkalis; nevertheless the data of table 3.4 should serve to give reasonable estimates of pressure.

For the alkalis the percentage of dimers present in the vapour at the temperatures required for 10 torr and 1 torr vapour pressure are also given in the table, data taken from Lapp and Harris. For the purposes of SERS dimers may be ignored in the alkaline earths; Stull and Sinke 1956 (the source used by Lapp and Harris for the alkali data) do not note their existence, although Herzberg 1950, following Hamada 1931, ascribes some band spectra observed in Mg and Ca vapours to Van der Waal's dimers Mg_2, Ca_2.

Partial energy level diagrams for the elements investigated Cs, Na, Sr and Ba are shown in figs 3.8-3.11. Having fairly simple spectra, the alkalis have received much more attention, experimentally and theoretically, than the alkaline earths; the more complex electronic structure of the latter inhibits the use of the simple Bates-Damgaard method and other more complex methods for calculating oscillator strengths. Consequently the oscillator strength/matrix element data for the alkaline earths is somewhat more sparse than for the alkalis, although much of the information relevant to the experiments performed was located in the literature.

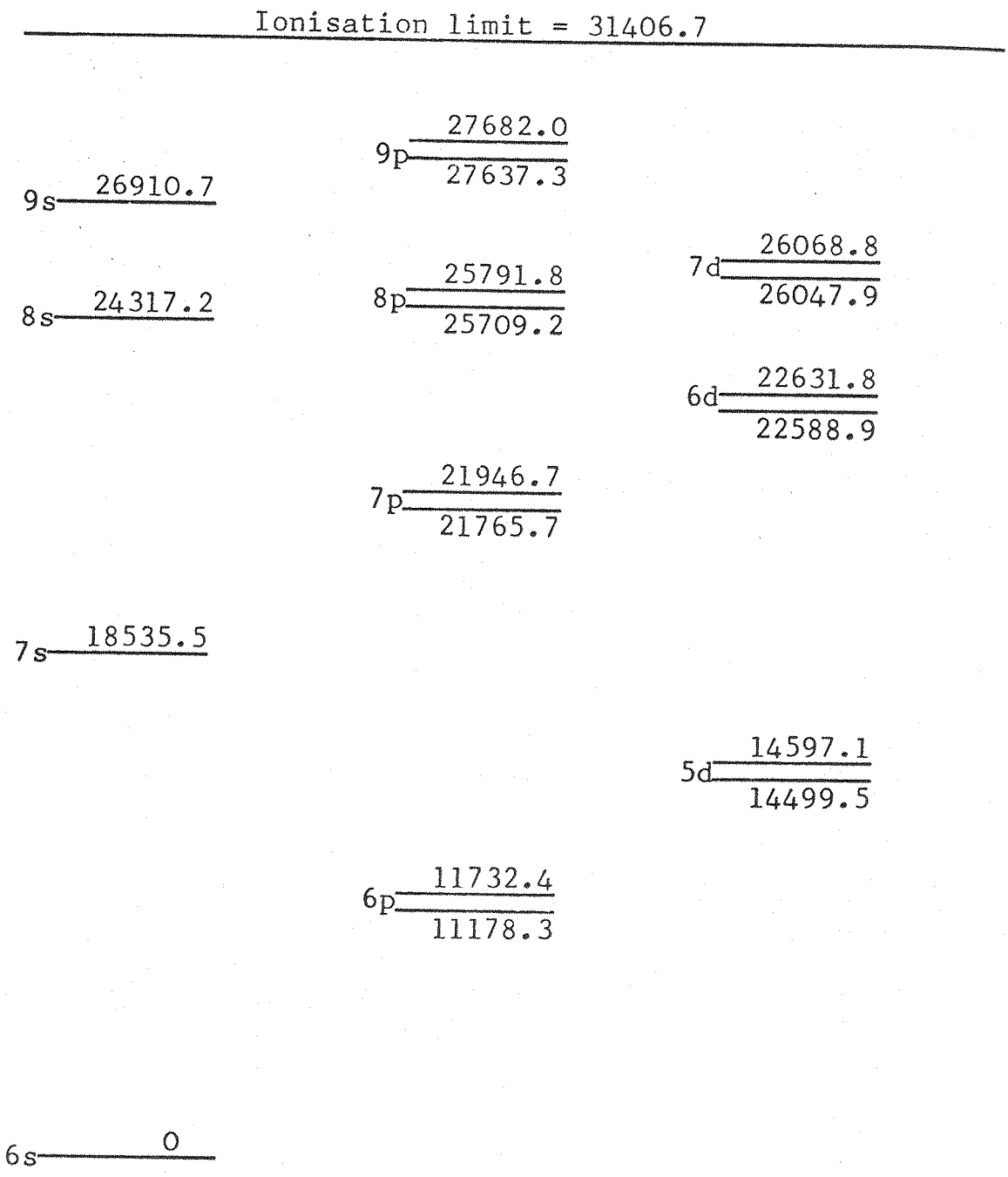

Fig 3.8

Energy level diagram (in cm^{-1}) of the neutral caesium atom

Data taken from Moore (1958)

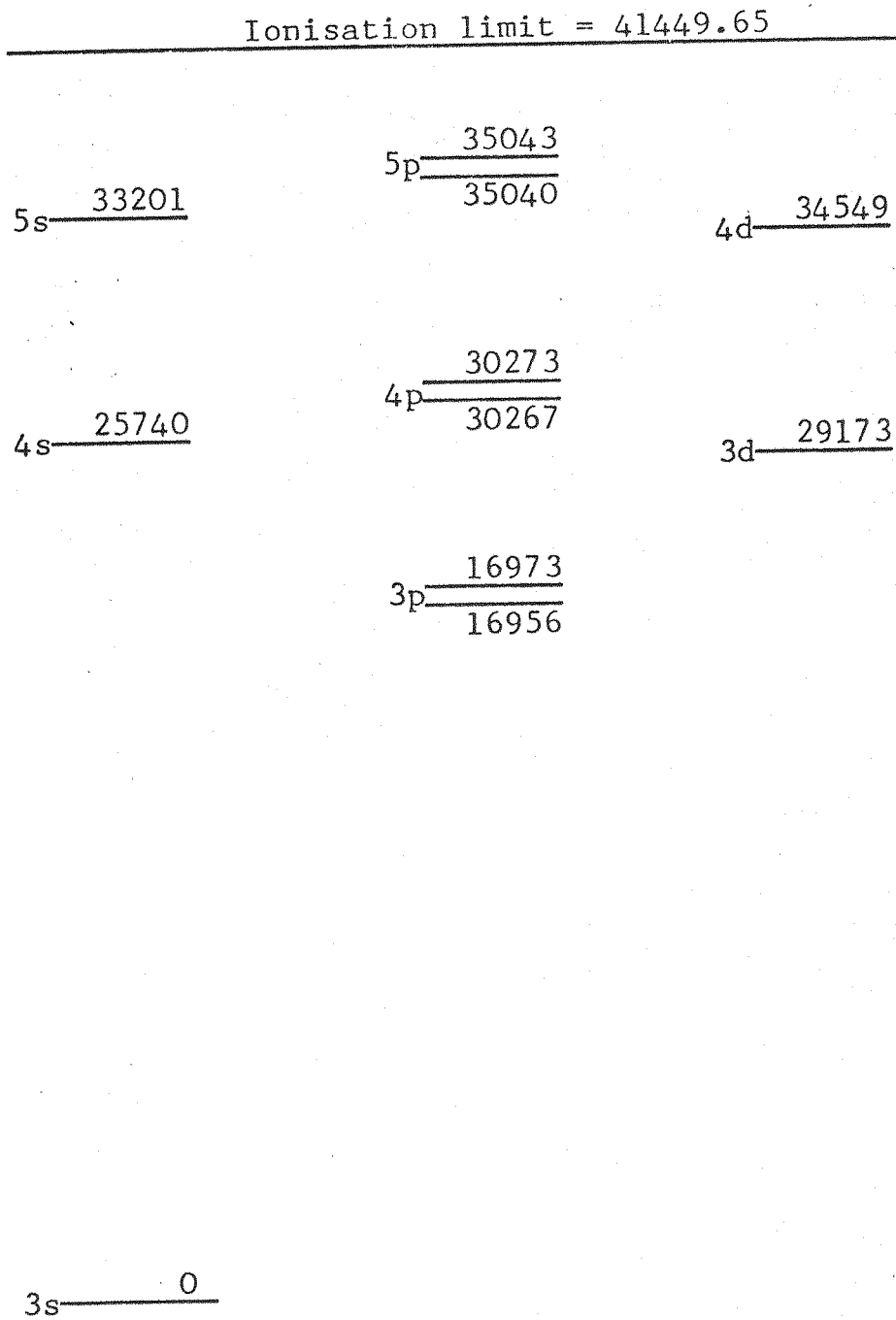

Fig 3.9
Energy level diagram (in cm^{-1}) of the neutral sodium atom
Data taken from Wiese et al. (1969)

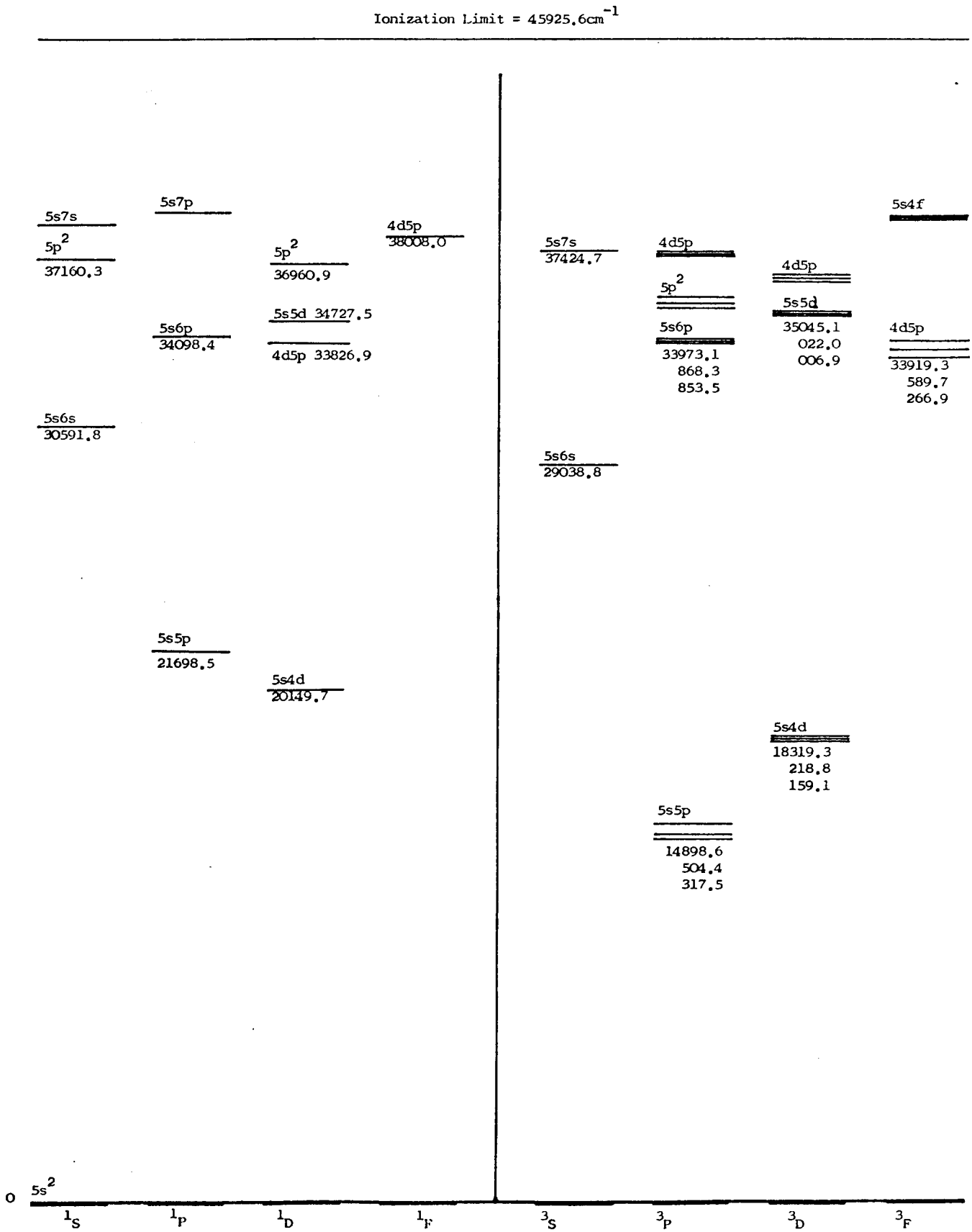

Fig 3.10 Energy level diagram (in cm^{-1}) of the neutral strontium atom
Data taken from Moore (1952)

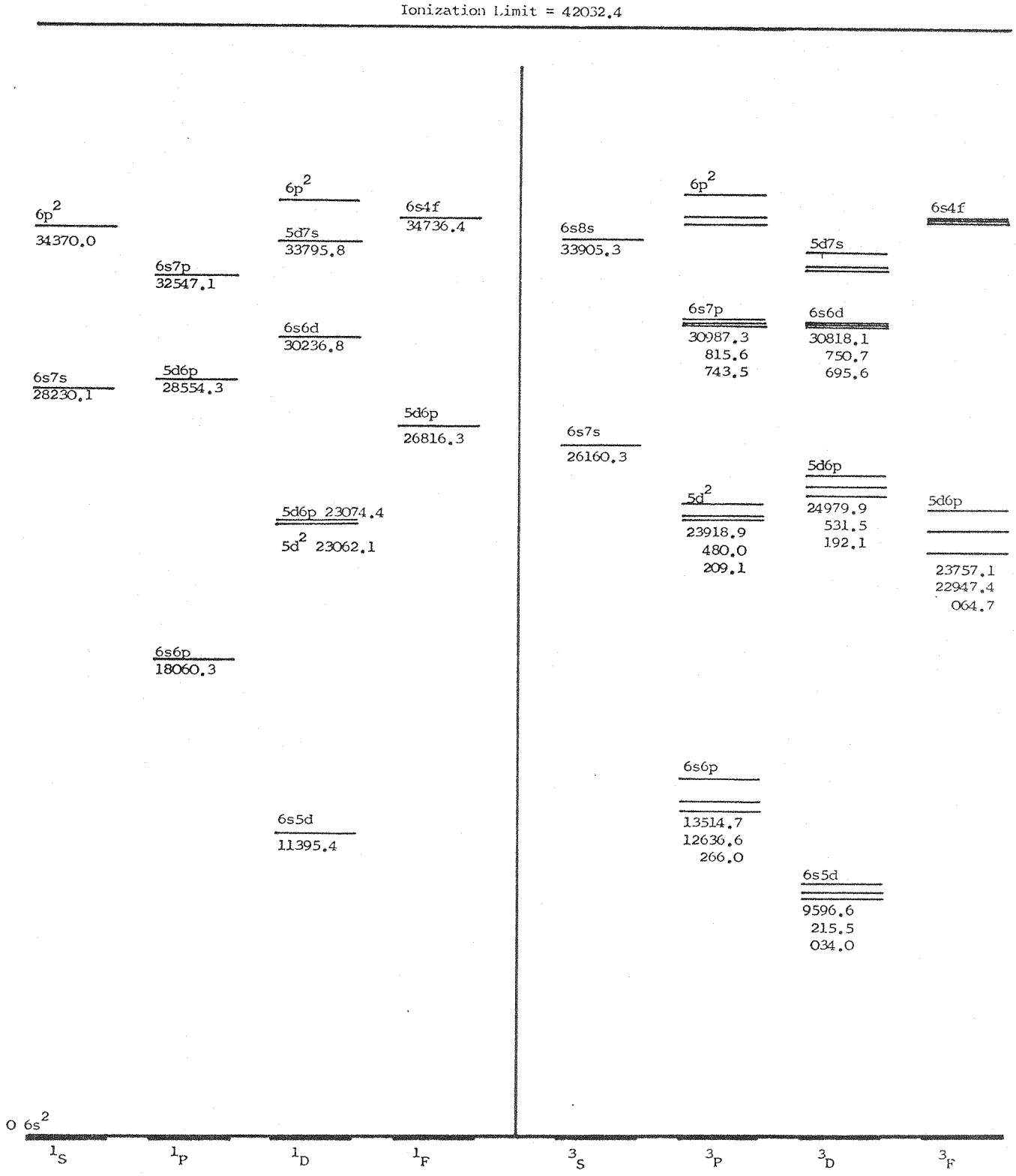

Fig 3.11 Energy level diagram (in cm^{-1}) of the neutral barium atom
Data taken from Moore (1958)

3.2.2 Heat Pipe Ovens

Increasingly over the past few years heat pipe ovens have found widespread acceptance as devices for containing metal vapours at pressures above 1 torr for optical experiments. The fundamental design and operation of the basic heat pipe oven are fully described by Vidal and Cooper 1969, its inventors, and will only be summarised here. In its simplest form the oven consists of a metal tube, heated over a central region and cooled at the ends, to which windows may be attached; inside the tube, extending over its length is a metal wick, typically a stainless steel mesh. A vacuum/gas handling system facilitates the initial evacuation of the whole assembly and subsequent introduction of a suitable inert buffer gas at the appropriate pressure. The metal required, loaded into the central region of the pipe, melts and then vapourises as the oven heats up, and diffuses toward the cooler regions inside the tube, where it condenses to form a liquid once more; the liquid metal is then transported back to the middle of the tube by capillary action of the wick. The metal vapour pressure attained in the tube is determined by the pressure of the buffer gas; in normal use, the heater is then adjusted to give a temperature corresponding to this pressure of metal vapour. The column of vapour produced effectively pushes the buffer gas to the ends of the tube whilst itself occupying the heated region. This buffer gas thus provides an inert cool region between the reactive metal vapour and the windows of the oven; this is a property of great significance for our application since the various IR transmitting output windows required would be damaged by direct exposure to the high temperature vapour. Another benefit of the heat pipe oven, not essential for SERS but useful for other applications is that the metal vapour column produced is uniform in temperature and density and well defined in length.

More complex heat pipe ovens have been developed for providing a homogeneous mixture of a metal vapour and an inert gas (Vidal and Haller 1971) or for providing a mixture of two metal vapours with independently controllable partial pressures (Vidal and Hessel 1972); whilst useful for other applications such as THG, such refinements are unnecessary for our purposes and the ovens we have used have been based on the original simple design.

Three different ovens have been used in this work, the first

two being 'low temperature' ones, operating with alkali metals up to 600°C, and the latter designed for use around 1000°C with the alkaline earths.

The first oven, used with Cs, was around 40cm in length with a very rapid transition between the heated and cooled regions; this resulted in the Cs vapour not only liquifying at the cooled regions, but also solidifying (!). Thus frequently it was necessary to push the accumulated metal back into the centre of the oven. The next design of oven allowed a larger distance between the heated region and the water cooling coils. Such a design had performed satisfactorily for several months operating with Cs; consequently the same design was adopted directly for use with Na at the somewhat higher temperatures used. Despite initial problems with accumulation of solid Na in the cooler regions it was found that after operating for a couple of weeks this problem disappeared and satisfactory operation ensued; this was tentatively ascribed to the Na taking time to adequately wet the wick. The Cs and Na ovens are shown in fig 3.12.

Both of these designs used grade 304 stainless steel $1\frac{1}{4}$" OD, $\frac{1}{8}$" wall thickness tube as the basis of the heat pipe; windows of spectrosil, infrasil or CaF_2, as appropriate, were mounted on flanges at the ends of the tube using standard O-ring seals. An electrical heating tape wound around the tube was then covered with 'Triton Kao-wool' fibre blanket to provide thermal insulation; closed circuit cooling water flowed through the copper coils near the ends of the tube. The wick consisted of several turns of 100mesh, 4.5 thou stainless steel mesh (250μm square mesh, 100μm diameter wire) rolled up and inserted as a tight fit inside the tube; before use the wick was cleaned with detergent in an ultrasonic bath and then also with aqua regia, as was the tube. When ready for use the oven was thoroughly evacuated and then buffer gas, argon, was introduced at slightly above atmospheric pressure; the windows could now be removed, an ampoule of alkali metal inserted into the heat pipe and then the ampoule broken in the inert atmosphere using a glass rod. The windows replaced at a lower argon pressure, the metal was distilled out into the heat pipe and the glass ampoule later removed. For normal use the heat pipe was evacuated using a rotary pump, the required pressure of buffer gas introduced and the power input to the heater

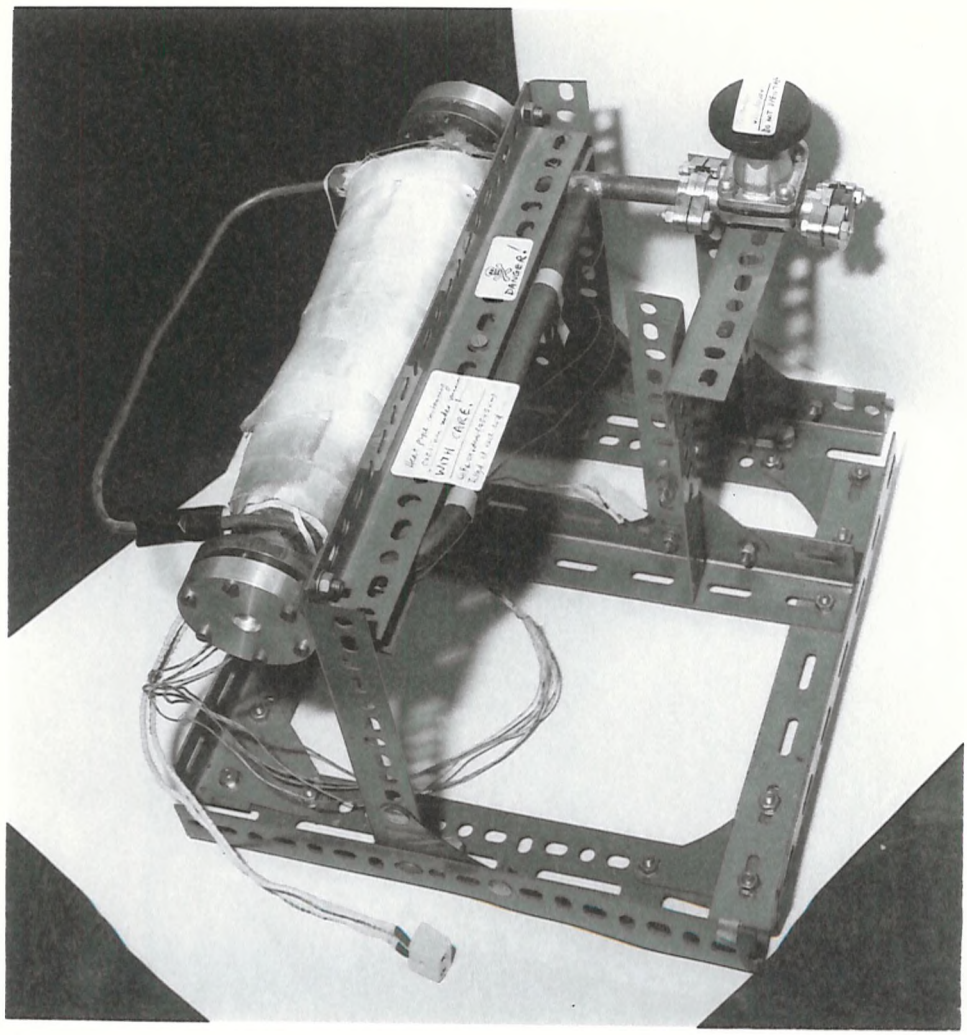

Fig 3.12 Cs (top) and Na (bottom) heat pipe ovens

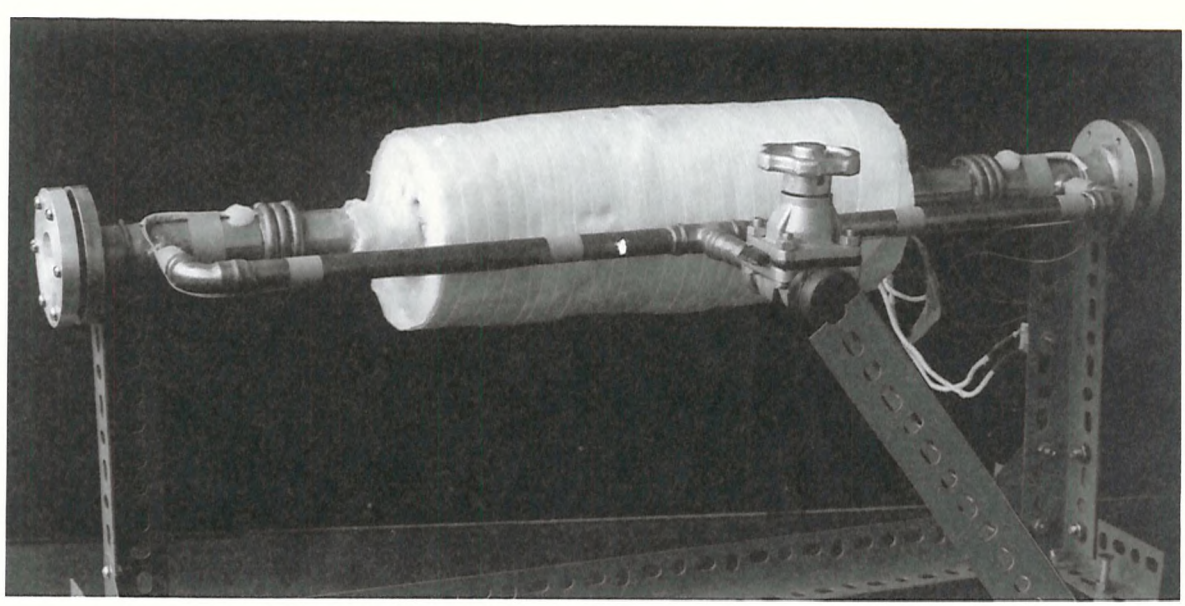

adjusted to give the appropriate temperature. The temperature of the Cs oven was monitored by three NiCr:NiAl thermocouples on the outside of the tube, whilst the Na oven was calibrated using a NiCr:NiAl thermocouple probe temporarily placed within the vapour column itself. A safety system monitoring cooling water flow and temperature near the end windows was interlocked with the heater and an emergency coolant reserviour. Further details of the modified alkali oven, the vacuum system and the safety system are given by Cotter (1976b, 1977b).

For the alkaline earths, it was apparent that considerable changes in design would be necessary to accomodate the higher temperatures required. Starting from the basis of the Na oven design several modifications were made. A higher temperature grade steel, no 310, was used for the basic tube; also, in view of the lower reactivity of the alkaline earths at room temperature, compared to the alkalis, it was decided to use a liner tube containing the wick and metal inside the main tube. In this way it was possible to use the same oven with different metals successively; a similar idea has been used by Wynne and Sorokin 1977, but they did not use a wick inside the liner tube and so could not operate in the heat pipe mode. A mesh of higher temperature grade steel appeared not to be readily available and thus we tried using the same wick material as before; in practise this worked without problems. A higher power heater was required and, in the absence of such a commercial device, a simple resistance wire heater was used. The main tube was initially wrapped with a high temperature paper insulation * which was available (from Morganite Ceramic Fibres), with a NiCr:NiAl and a Pt:PtRh thermocouple inserted between layers. This was then wound with 60turns of Kanthal Al resistance wire secured at the ends with stainless steel jubilee clips and the whole assembly covered with a considerable thickness of Kaowool insulation. Extra turns of cooling coils were also incorporated in this design. The thermocouples built into the oven

---

* The high temperature paper insulation used appeared somewhat fragile and the use of a woven material is recommended for future designs. Such a material suitable up to 1400^{o}C , is Refrasil, C1400 available from the Chemical and Insulating Co Ltd.

were calibrated against a high temperature rating NiCr:NiAl thermocouple probe placed within the vapour, thus providing a fairly accurate monitoring of the temperature .
The layout of the oven is shown schematically in fig 3.13 and a photograph is shown as fig 3.14.

The alkaline earths are delivered in large, 100g lumps stored under oil. Attempts to cut these up in an inert atmosphere proved in vain and it was found necessary to use a junior hacksaw to obtain amounts suitable for insertion into the heat pipe (10-20g). Thus a considerably greater degree of impurities was tolerated with the alkaline earths compared to the alkalis.

The initial performance of the oven with Sr was found to be satisfactory from the temperature aspect although some problems with accumulation of solid metal in the cooler regions were again experienced; unlike Na this situation did not improve with time. The accumulation behaviour was also different from that observed with the alkalis; instead of a steady build up of deposit over a period of days, the deposit was initially very slight but once it reached a certain amount the accumulation, crystalline in appearance, appeared to suddenly increase, growing across the whole aperture of the tube. Accumulation problems have been noted by other workers using Sr (Wynne and Sorokin 1977, Lee 1977). When such problems occured with the alkalis the oven was cooled, windows removed and the metal pushed back to the middle. Because of the frequency of this occurence with Sr, however, an alternative procedure was devised; this consisted of simply increasing the power input to the heater, thus melting the deposit and clearing the aperture. The heater was then returned to its normal power input. After many such cycles the amount of Sr in the central region might be expected to become depleted due to deposite of the metal further into the cool regions of the pipe, in fact during the time we used the oven with Sr in this way an adequate supply of the liquid metal could always be observed on the wick in the heated region indicating that such a depletion had not occured.

Replacement of the liner and wick enabled the heat pipe to be subsequently used with Ba. Requiring still higher temperatures, the

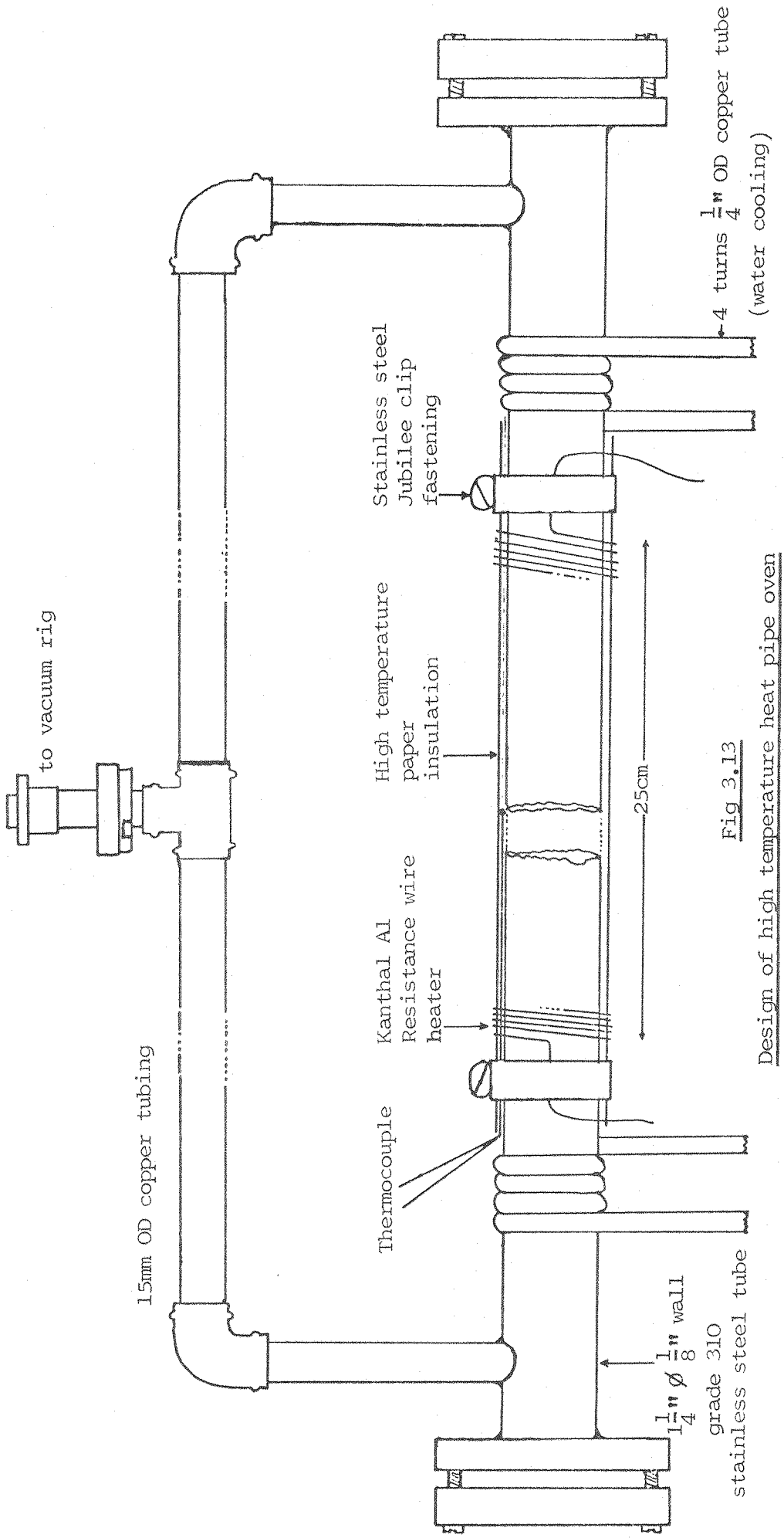

Fig 3.13

Design of high temperature heat pipe oven

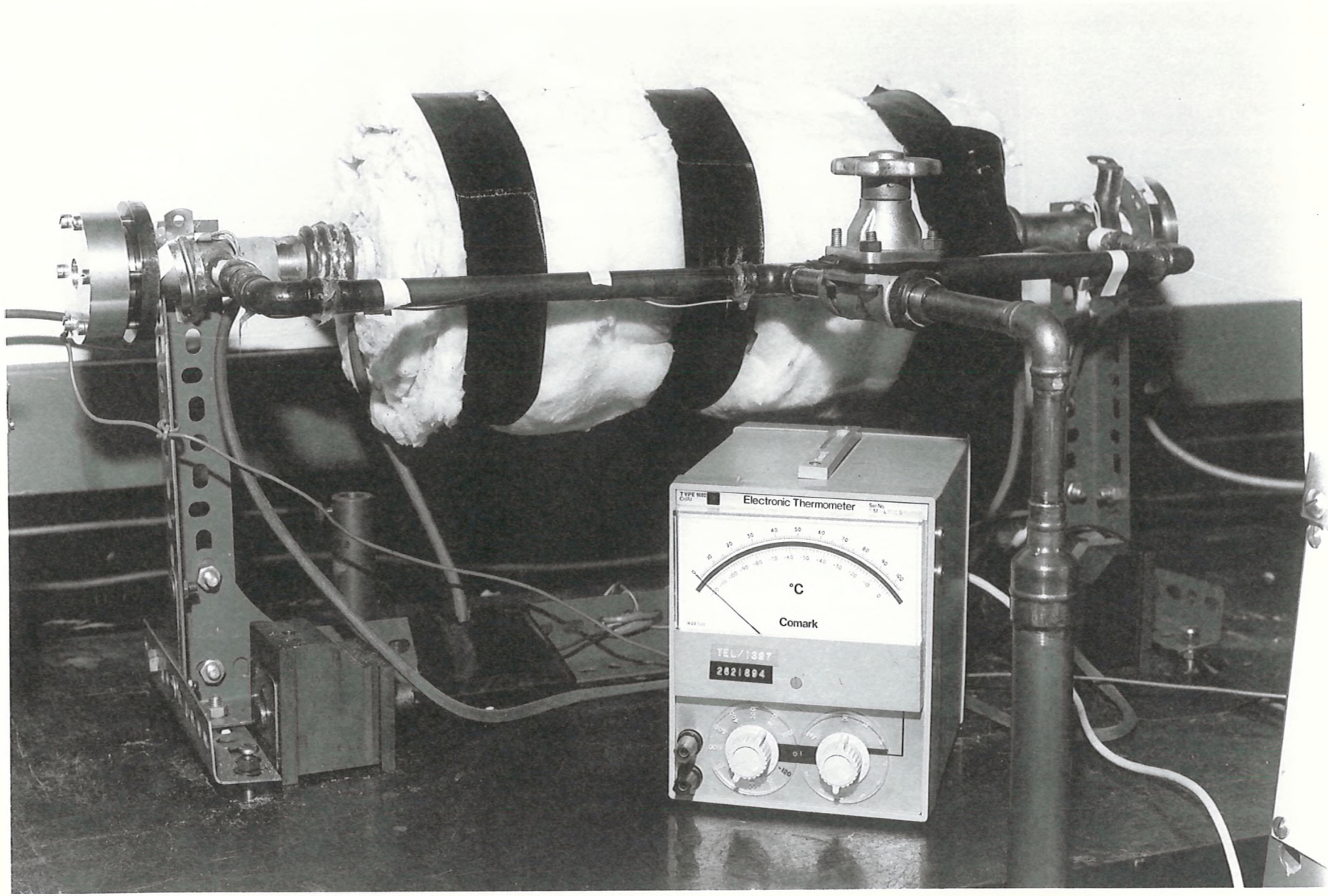

Fig 3.14 High temperature heat pipe oven for the alkaline earths

oven was operated at lower vapour pressures, $\leqslant$ 2 torr, and as might be expected at these pressures no trouble with metal accumulation was observed. Some potential and actual problems associated with the temperature now became apparent however, which should be circumvented in a future design. Firstly a high heater current (~ 5A) was necessary to reach the required temperatures; in future a higher resistance heater would be advantageous. Bifilar winding of the heater to eliminate the magnetic fields produced, which could prove troublesome under some conditions, would also be worthwhile. Secondly the cooling provided by the four turns of copper tube proved barely adequate; it is recommended that the degree of cooling be increased. A more immediate problem was encountered associated with the expansion of the steel tube at 1100^{o}C; the copper vacuum tubing linking the ends of the tube, necessary to equalise the buffer gas pressure, remains of course at room temperature. The net result is a slight bending of the ductile copper tube; however some softening of the steel tube was also apparent resulting in a bending of the main pipe, reducing its effective aperture. For a future oven at such temperatures a still higher temperature grade of steel should be sought or another metal used; nickel and tantalum have been used in this application (Wynne and Sorokin 1977). Also a flexible coupling should be introduced in the copper vacuum tubing.

Experience with ovens for the alkalis seems to indicate that heat pipe oven technology, like most things, is learnt by experience; thus it is anticipated that the next alkaline earth oven, when needed will overcome the snags outlined here. Nevertheless it is recorded that the oven constructed has succeeded in its goal of enabling us to perform some useful and new work on SERS in the alkaline earths.

CHAPTER 4

Experimental Investigations

The experimental work described in this chapter relates to the three aims mentioned in the introduction, viz to obtain increased tuning ranges, new tuning ranges, and narrower linewidth IR radiation. The work splits up into four distinct classes of stimulated electronic Raman process: SERS in an alkali, SHRS (stimulated hyper-Raman scattering), SERS from an excited initial state and SERS in the alkaline earths. The chapter is subdivided accordingly. In each section the aims of the experiment are initially outlined, the procedure and results described and discussed and conclusions drawn; related work, where appropriate, is also mentioned as are suggestions for future work.

4.1 SERS in Cs

The goal of the work in Cs was to extend the tuning range of the 6s-7s SERS transition by using some kind of feedback arrangement. To this end initial measurements were performed to discover the optimum pump focussing conditions, with the aim of extending the tuning range for the optimum focussing case. With the limited pump power and mirrors available it was in fact only possible to investigate the behaviour with feedback for the case of loose, non-optimum, focussing; some small increase in forward wave tuning range was in this way found. The significance of feedback to the backward SERS wave became apparent during this work in a dramatic increase of the backward wave tuning range and further work concentrated on characterising this effect; feedback of the pump and the SERS radiation were both shown to be significant. Although we were unable to investigate the full potential of these techniques at high power pumping the preliminary results obtained show great promise and indicate clear directions for future work using feedback/resonator techniques.

4.1.1 Focussing

Despite the desire to investigate these effects with a high power dye laser this was not possible due to the RDA crystal needing repair and also due to the low damage threshold of the mirrors available. Consequently the 7D4MC dye oscillator was used giving an output of ~ 1mJ in a

30ns pulse without a dye amplifier. Using a variety of lenses this pump beam was focussed to a waist at the centre of the heat pipe oven; by redirecting the beam a scanning slit and Si PIN diode could be used to measure the spot size at the waist. From these measurements the confocal parameter b_p was calculated. Calcium fluoride, CaF_2, windows were used on the heatpipe to transmit the generated SERS at around 3μm. A polished slice of germanium, Ge, was used to transmit the IR but block the dye laser after the heat pipe. A KBr lens then focussed the IR onto a Mullard pyroelectric detector either directly or sometimes via an IR grating monochromator. A value of 50nJ generated SERS energy, 1-10W, was arbitrarily defined as the tuning range limit; at this level the shot-to-shot energy stability of the output was still fairly good as was the S/N ratio and this enabled the tuning edge to be well defined. Comparative measurements performed with and without the monochromator before the detector confirmed the absence of ASE except under the following conditions:- (1) when ω_p was tuned within a few cm^{-1} of the $6s-7p_{1/2}$ resonance line, in which case $7p_{1/2}-7s$ ASE occured, and (2) when ω_p was tuned in the region $21050cm^{-1}$, in which case the $5d_{1/2}-6p_{3/2}$ and $5d_{3/2}-6p_{1/2}$ transitions were observed. The 5d levels are populated by 7p-5d ASE usually, but why this should occur at this detuning from ω_{7s7p} is not clear. This latter ASE was initially observed when pumping at high intensities; at the intensities used for the focussing measurements also this ASE appeared to occur under some focussing conditions at the low frequency end of the tuning range. It was desired to dispense with the monochromator in order to save time in aligning the optics in view of the low ruby repetition rate and problems experienced at the time with accumulation of Cs at the ends of the heat pipe. Consequently as focussing was varied the upper frequency tuning limit was measured, without the monochromator, in the absence of any ASE.

The effects of focussing on this upper tuning limit are shown in fig 4.1; similar behaviour was observed for the lower limit except for the case of $L/b_p = 0.45$, in which case ASE appeared at the lower pump frequencies. These results indicate an optimum tuning range for $L/b_p \simeq 0.55$, corresponding to a spot size of w = 160μm. Qualitatively we may explain this behaviour as follows. As L/b_p the tightness of focussing, is increased so is the pump intensity, and, hence, the Raman gain. However, an optimum pump intensity is reached beyond which other competing effects deplete the pump or in some other way reduce the

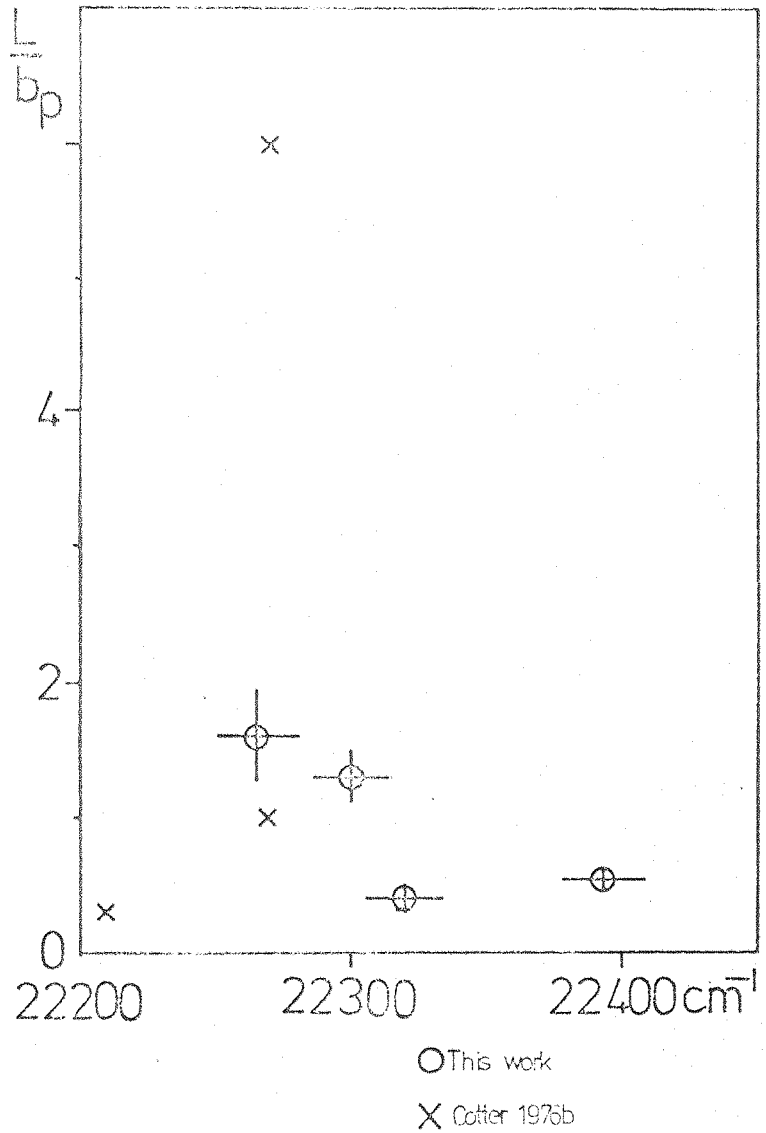

Fig 4.1 SERS in Cs: upper tuning limit as focussing is varied

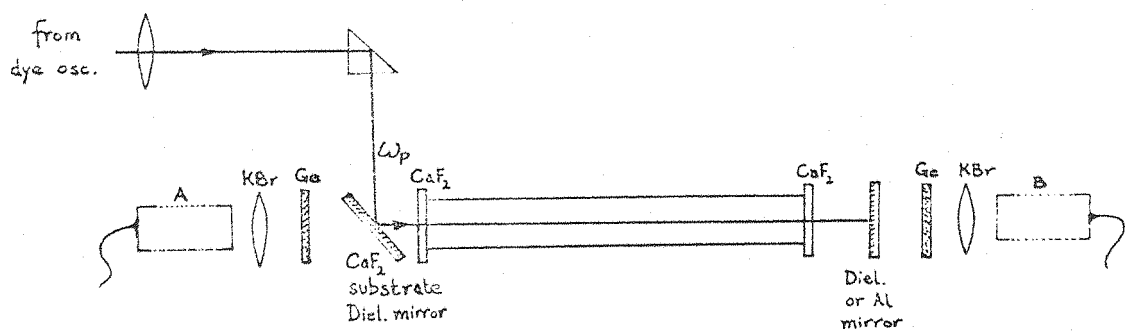

Fig 4.2 Experimental set up used for measuring tuning curves (Detector was either at A or B)

Raman gain once more, eg intensity dependent line broadening.

Also plotted on the figure are some data points of Cotter 1976b obtained using a 20kW, 7ns nitrogen pumped dye laser; his results do not show the pronounced optimum apparent in our measurements. Further measurements on a subsequent occasion again confirmed the trends displayed in fig 4.1. One possible explanation of this behaviour may be that the higher energy longer pump pulse used in our experiments results in a modification of competing effects; however with so few data points it is difficult to draw firm conclusions.

4.1.2 Feedback

Investigations were also performed to discover the effect of reflecting some of the pump radiation emerging from the heat pipe back on itself; this may be considered simply as resulting in an increased effective pump power. This higher intensity we would expect to result in a higher gain and hence larger tuning range. This is treated further in Appendix 1 as also is the idea of 'multipassing' the beam, ie reflecting it one or more times through the vapour cell, along different paths each time.

Our preliminary measurements used the same arrangement as previously with the addition of a plane dielectric coated mirror, $R_{blue} = 100\%$, on a CaF_2 substrate before the Ge filter. Comparative measurements of forward SERS were made with the mirror aligned and slightly misaligned perpendicular to the beam, ensuring that this misalignment did not displace the IR on the (large area) detector. Initial results using the same focussing arrangements as before revealed only a slight reduction in tuning range in fact under some conditions but, more generally, little change. This led us to consider if perhaps the backward generated Raman wave might be enhanced in this arrangement resulting in increased competition with the forward wave; this was subsequently investigated.

It was also appreciated that with the beam waist at the centre of the heat pipe the amount of pump radiation fed back on itself was fairly small, particularly for large L/b_p. In the absence of suitable curved mirrors the efficiency of pump feedback was improved by focussing loosely with a beam waist at the mirror rather than in the heat pipe. The dye laser, providing 10-20kW output, was thus focussed to a beam waist of $\sim 300\mu m$ at the mirror; at higher intensities than these mirror damage occured. Measurements of forward

wave tuning range were again obtained as before, with and without a monochromator, which this time revealed an increased tuning range of ~10%. Assuming a 50nJ tuning limit energy criterion, the tuning range increased from ~ 21675-22075cm^{-1}(400cm^{-1}) to ~ 21655-22100cm^{-1}(445cm^{-1}). The increased tuning observed is of the same order as would be expected from a simple calculation following Appendix 1; however it is stressed that this is a static analysis neglecting the backward wave which, as will be shown, plays an important role.

4.1.3 Backward Wave

As already noted the behaviour of the backward wave under such feedback conditions needs to be considered. The dielectric mirror used has a reflectivity of ~30% around 3μm; thus a significant amount of forward SERS was fed back and could act as a signal for backward amplification. This situation strictly requires a dynamic analysis, beyond the scope of the present work; instead the effect was investigated experimentally.

As a preliminary measurement, to see the possible importance of the backward wave, the dye laser was tuned to the edge of the backward wave tuning range and the backward SERS signal observed; alignment of the feedback mirror resulted in an increase of the signal by more than two orders of magnitude. This served to confirm the increased importance of the backward wave when the mirror was aligned.

Subsequently the tuning behaviour of the SERS was characterised using the arrangement of fig 4.2; to avoid mirror damage the dye laser was loosely focussed to a waist ~270μm about 10cms behind the feedback mirror, which was itself a distance of ~10cm from the end of the vapour column in the oven. (The large confocal parameter implied for this loose focussing reveals that our reflected pump intensity is not significantly different than if the waist were actually at the mirror.)

The normal forward wave tuning curve obtained without feedback is shown in fig 4.3a. One may observe that the tuning range around the $6s\text{-}7p_{3/2}$ resonance frequency is roughly twice that around the $6s\text{-}7p_{1/2}$ resonance, as would be expected from the ratio of the transition oscillator strengths. For the same reason the on-resonance dip due to SPA is more pronounced for the $6s\text{-}7p_{3/2}$ transition. This provides further independent confirmation of similar observations by Cotter 1976b.

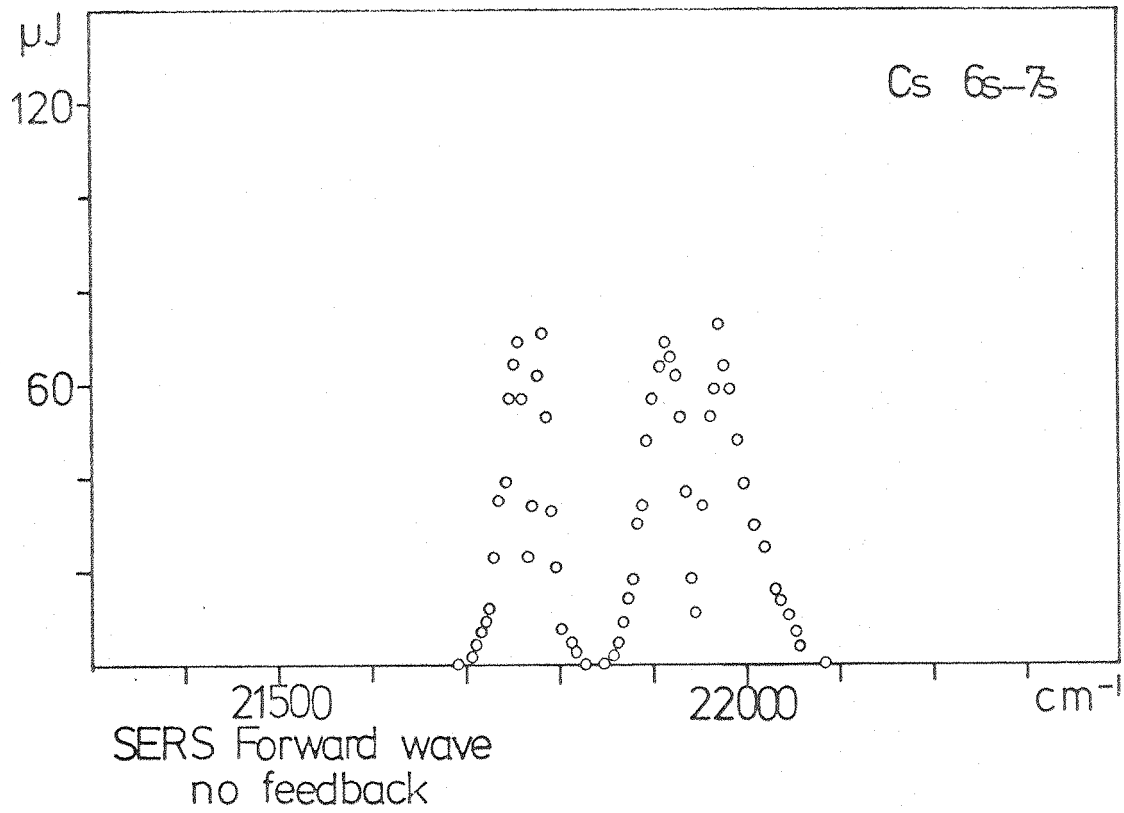

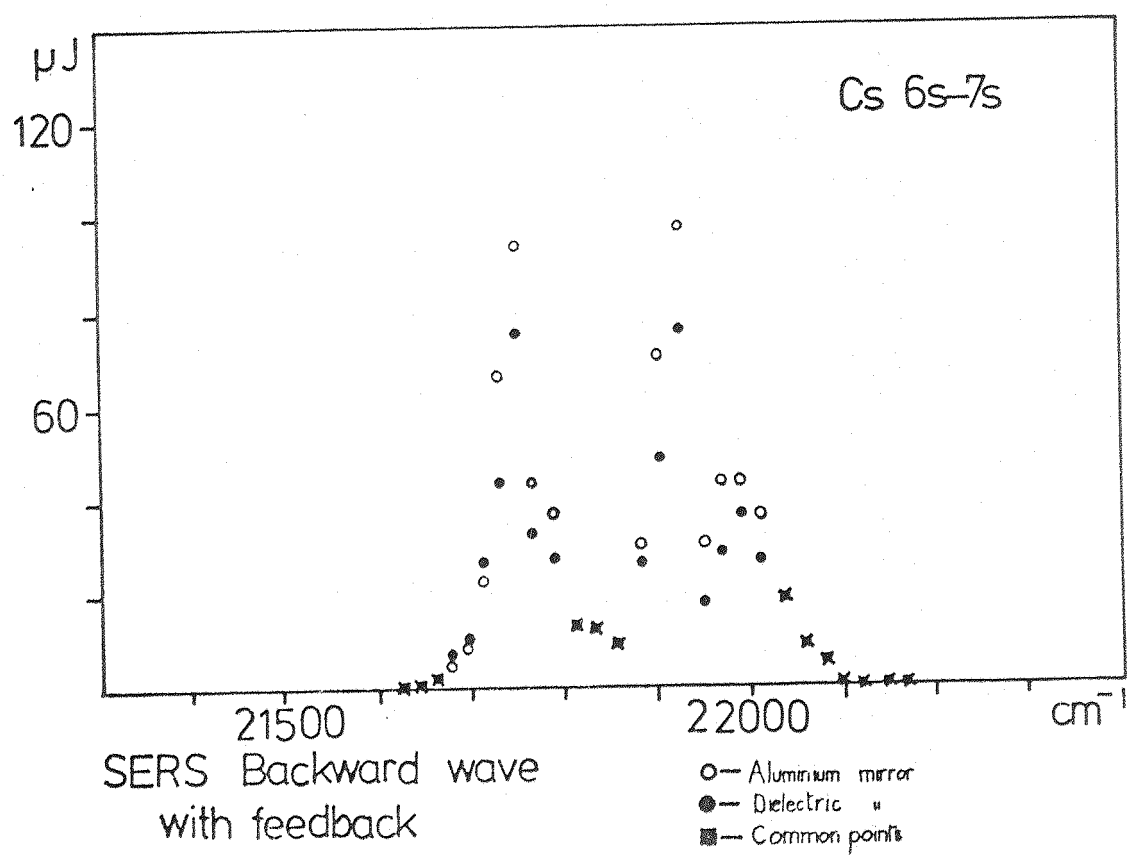

Fig 4.3 SERS in Cs - Tuning curves

The peak output energy near the resonances would apper to be limited by pump depletion and the output away from resonance by atomic depletion, as outlined in section 2.3.

Feedback could be applied in this arrangement by using either the dielectric mirror (R_{blue}= 100%, R_{IR}= 30%) or an aluminium coated mirror (R_{blue}= 90%, R_{IR}= 100%). Measurements were taken at a given frequency for each mirror alternately; in this way it was hoped that we might establish the relative importance of pump and SERS feedback. Window losses and beam divergence (diffraction loss) result in the actual feedback being less than these reflectivity values, being extimated as blue 90%, IR 2% for the dielectric mirror and blue 80%, IR 6% for the aluminium mirror. The backward wave tuning curve for such feedback is shown in fig 4.3b; comparing this with the forward wave behaviour reveals an overall increase in available tuning range. Around the $6s-7p_{1/2}$ resonance no on-resonance dip is observed; this anomalous feature was verified as being due to $7p_{1/2}-7s$ ASE; no such effect was seen near the other resonance $6s-7p_{3/2}$. At the peaks of the backward wave tuning curves a distinctly greater output is observed when using the higher IR feedback. This might be expected, since when pump depletion begins to occur the IR feedback becomes more important than pump feedback; thus the backward wave may compete more favourably for pump photons. Obviously this is a simplistic intuitive explanation and strictly the dynamic interaction of the two travelling waves needs to be considered.

It may be that higher peak photon conversion efficiencies than those generally observed, 50% may be attainable in this way although this has not been firmly established; precise measurements of photon conversion efficiencies were not attempted. Toward the edges of the tuning range the behaviour using either feedback mirror was very similar indicating the lesser importance of IR feedback. Nevertheless the importance of providing some IR feedback in this region was verified by the insertion of a water cell, absorbing around 3μm, before the mirror; this allowed some pump feedback to occur and still gave an increased signal compared to the no-feedback case, but a reduced signal compared to the pump and IR feedback case.

In these measurements no great care was taken as to the alignment or otherwise of the CaF_2 heat pipe windows; these could provide some small amount of IR feedback, of the order of only ~1% when allowance is made for the diffraction of the beam. In future work this factor should be checked. The tuning curves of fig 4.3 were obtained using the pyro-electric detector and have been normalised to account for the high losses in the Ge, KBr, CaF_2 and mirrors; thus the energies shown represent the generated SERS energy. Some of these losses could in practise be removed using anti reflection coatings. The energies measured by the detector were calibrated at a given frequency to the energy measured on a Laser Precision pyroclectric joulemeter which had itself been compared to a calorimetric energy meter and found to give reasonably good agreement. Some uncertainty however occured in this calibration for the backward wave curves, but the energies quoted are believed to be correct, certainly to within ± 50%; whilst in no way invalidating the tuning range results or feedback effects observed, this does however prevent a quantitative comparison of photon conversion efficiency.

Since this work, Cotter et al 1977a have also investigated such effects using a nitrogen pumped dye laser providing 20kW in 7ns, confocally focussed over a 20cm length of Cs vapour. Using a Ge filter, KBr lens and plane mirror, < 10% IR feedback and no pump feedback were applied; the heat pipe windows were skew to the optical axis to provide negligible feedback. This resulted in an increased backward wave energy compared to the no-feedback case; some slight increase in useful tuning range, compared to the no-feedback forward wave, may also be inferred from the results. These results are qualitatively in accord with our own.

4.1.4 Conclusions

Limited as we were by low damage threshold mirrors and by dye laser power it was not possible to investigate the effects of these techniques with high pump powers; however we should consider here what behaviour might be expected on the basis of these results. With the higher power dye laser system we would have available a higher energy beam in a shorter pulse, an intensity of, say, twenty times that used here. Thus looser focussing still could be used before we were limited by pump depletion; IR diffraction loss would then be less and higher IR

feedback could be achieved. Quite probably at higher pump intensities the conditions for optimum focussing would imply such a large beam waist; thus efficient pump and IR feedback could well be applied to the case of optimum focussing. Wyatt 1976 (see also Cotter et al 1976a) measured a tuning range for the Cs 6s-7s SERS process of 2.5-4.75μm using a 750kW dye laser; these tuning limits however corresponded to a signal level of ~25pJ, too low a level signal to allow much spectroscopic work to be performed. The use of such a feedback technique as outlined would probably increase the useful tuning range available from the system as well as extending the absolute range.

Thus we have demonstrated that, for loose, non-optimum, focusing at low pump intensities, the tuning range attainable can be considerably increased, relative to the forward wave tuning range , by providing efficient pump and IR feedback. Further work using higher powers and better mirrors would be expected to result in useful improvements to the Cs 6s-7s high power SERS system; a high power pump is necessary to take full advantage of these techniques by using slack focussing and consequent smaller diffraction loss. The possibility of using a 'multi-pass' arrangement is discussed in Appendix 1. From these preliminary results the use of such an arrangement, or a resonator, looks promising. It is anticipated that such a configuration would increase the useful tuning range and also modify the atomic saturation behaviour and hence the shape of the tuning curve.

4.2 Stimulated Hyper-Raman Scattering in Sodium

In ordinary Raman scattering a single pump photon scatters into a single Stokes photon, as illustrated already in fig 1.1; thus Raman scattering is a two photon process. Hyper-Raman scattering is the analogous three photon process where two pump photons (ω_p) are annihilated and one Stokes photon produced (ω_s), $\omega_s = 2\omega_p - \Omega$ where Ω is the Raman shift. Hyper-Raman scattering was first observed as a spontaneous process, like Raman scattering, and was observed in the stimulated regime initially by Yatsiv et al 1968. More recently Vrehen and Hikspoors 1976, 1977 have given the process some serious study using a fixed frequency Nd:YAG laser pumping near a fortuitous two photon resonance in Cs. Our interest in the process concerned the possibility of obtaining a tunable IR Stokes output in much the same manner as has been achieved from ordinary SERS using a tunable dye laser as the pump.

The process of 'three-photon scattering' has been studied by Carlsten, Szoke and Raymer 1976 and by Grynberg et al 1976; in this process an output at $2\omega_p - \Omega$ is observed when the pump is tuned near to a transition Ω. Only two levels are involved as the initial, final and intermediate levels and the generated frequency is close to the pump frequency; these features distinguish the three photon scattering process from hyper-Raman.

Vrehen and Hikspoors' 1976 initial results using stimulated hyper-Raman scattering, SHRS, in Cs indicated that despite being a fifth order nonlinear process considerable gain is possible for such a scheme. Consequently a search was made amongst the alkalis for an element with energy levels suitable for SHRS with dye laser pumping; the use of the Na 3s-(3p)-(4d)-$4p_{3/2}$ SHRS scheme pumped by a Rhodamine dye laser was adopted for investigation. With this scheme we anticipated a resonance enhancement of the hyper-Raman gain from the two-photon resonance (3s-4d) and further enhancement from the proximity of the single photon resonance (3s-3p); this scheme is shown in fig 4.4.

Calculations of the gain expected from this SHRS system in Na looked favourable; the experiment was therefore tried in order to evaluate SHRS as a technique for tunable IR generation. The essential results of this work have been published and are included as Appendix 2; in this section of the thesis however the work will be

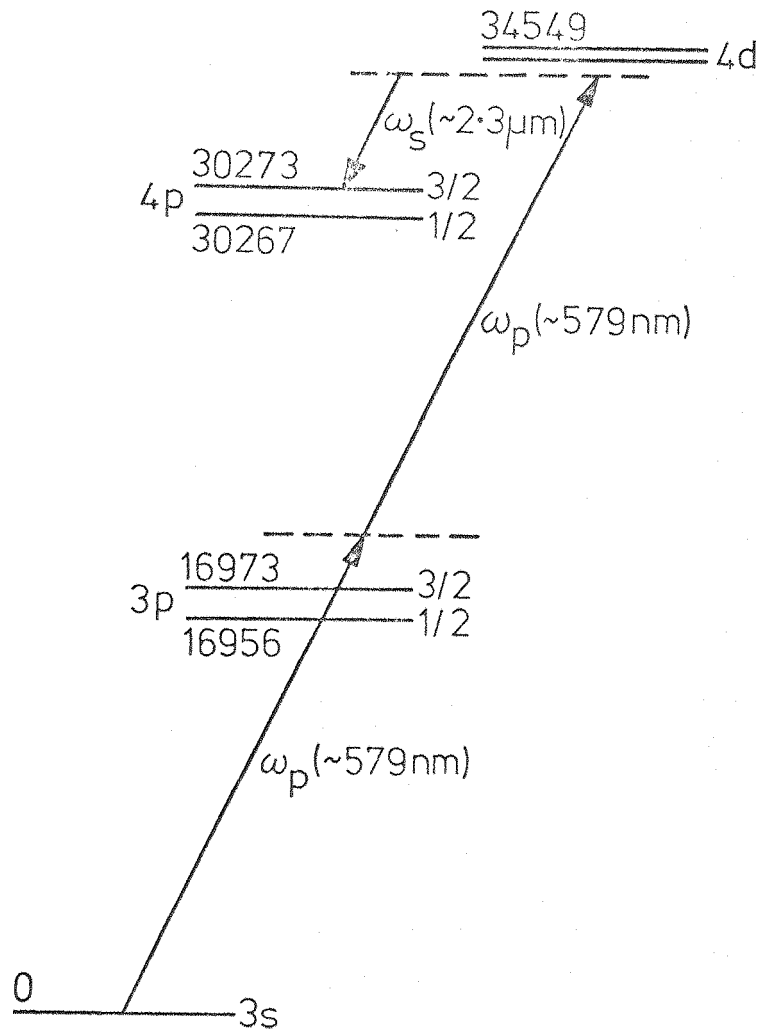

Fig 4.4 SHRS in Na Level Scheme

described in some greater detail. Initially the theoretical background is treated, followed by the experimental details and results; various points of interest raised by the results are discussed and some comments relating to the behaviour and potential of SHRS conclude the section.

4.2.1 Gain Calculation

A gain calculation for SHRS may be performed in an analogous way to that for SERS, described in chapter 2. In analogy to eqn 2.7 we find that

$$G_{HR} = \frac{15}{2}\frac{1}{c}(4\pi\alpha\hbar)^2\left(\frac{-\chi_{HR}}{e^4}\right) I_p^2 \omega_s \qquad \ldots 4.1$$

where χ_{HR} is the imaginary part of the fifth order nonlinear susceptibility $\chi^{(5)}(-\omega_s;\ \omega_p,\ -\omega_p,\ \omega_p,\ -\omega_p,\ \omega_s)$. χ_{HR} may be expressed as

$$\chi_{HR} = \frac{N}{\Gamma}\frac{4\pi\alpha}{5!}\frac{c}{e^2}\bar{\rho}_g\left\{\frac{1}{2J_g+1}\sum_{\substack{e\\ f,g}}\overline{|\beta_{HR}|^2}\right\} \qquad \ldots 4.2$$

where $\bar{\rho}_g$ is the fractional population of the ground level, J_g is the angular momentum of level g, $(2J_g+1$, its degeneracy), and β_{HR} is defined as

$$\beta_{HR} = \frac{2}{\hbar^2}\sum_{bc}\left\{\frac{\langle f|\underline{\varepsilon}_s^*\cdot\underline{Q}|b\rangle\langle b|\underline{\varepsilon}_p\underline{Q}|c\rangle\langle c|\underline{\varepsilon}_p\cdot\underline{Q}|g\rangle}{(\Omega_{bg}-2\omega_p)(\Omega_{cg}-\omega_p)} + \right.$$

$$\left. + \frac{\langle f|\underline{\varepsilon}_p\cdot\underline{Q}|b\rangle\langle b|\underline{\varepsilon}_s^*\underline{Q}|c\rangle\langle c|\underline{\varepsilon}_p\cdot\underline{Q}|g\rangle}{(\Omega_{bg}+\omega_s-\omega_p)(\Omega_{cg}-\omega_p)} + \frac{\langle f|\underline{\varepsilon}_p\cdot\underline{Q}|b\rangle\langle b|\underline{\varepsilon}_p\underline{Q}|c\rangle\langle c|\underline{\varepsilon}_s^*\cdot\underline{Q}|g\rangle}{(\Omega_{bg}+\omega_s-\omega_p)(\Omega_{bg}+\omega_s)}\right\} \qquad \ldots 4.3$$

where the matrix elements etc are as defined in chapter 2; these general equations are taken from Yuratich 1977a. Usually the last two anti-resonant terms contributing to β_{HR} may be neglected.

Applying these equations to the case of Na assuming a Stokes polarisation parallel to that of the pump and neglecting non-resonant intermediate levels we obtain for the susceptibility

$$\chi_{HR} = \frac{8}{5^3 3^4}\frac{N}{\Gamma}\frac{4\pi\kappa}{\hbar^4}ce^4\frac{\left|\langle f|r|4d\rangle\langle 4d|r|3p\rangle\langle 3p|r|3s\rangle\right|^2}{(\Delta\omega_1\Delta\omega_2)^2} \qquad \ldots 4.4$$

where $\Delta\omega_1 = \omega_{3s3p} - \omega_p$ and $\Delta\omega_2 = \omega_{3s4d} - 2\omega_p$ are the single-photon and two-photon resonance detunings. This expression neglects the spin orbit splittings of the 3p and 4d levels; this is valid since the respective detunings $\Delta\omega_1$, $\Delta\omega_2$ are large compared to the splittings. This is not the case for some of the other alkalis, eg Cs, and this simplification cannot be made. To consider a split final level f we may simply put $\left(\chi_{HR}\right)_{J_f = \frac{1}{2}} = \frac{1}{3}\left(\chi_{HR}\right)_{\text{spin free}}$; similarly $\left(\chi_{HR}\right)_{J_f = \frac{3}{2}} = \frac{2}{3}\left(\chi_{HR}\right)_{s.f.}$. Thus from equation 4.1 we may obtain an expression for the SHRS gain; it may be seen that since $G_{HR} \alpha\ \chi_{HR}$ the gain will be higher for scattering to the $J_f = \frac{3}{2}$ final state.

The angular dependence of the gain, contained in the $\underline{\varepsilon}.\underline{Q}$ factors of equation 4.3, has been lost by assuming the Stokes polarisation parallel to the pump polarisation; if this is considered in fact it is found that for pump and Stokes circularly polarised in the same sense the gain is increased by a further factor of 9/4. When generating a Stokes signal from noise, the Stokes wave will assume the polarisation for which the gain is greatest; thus for circularly polarised pump the SHRS will be similarly polarised and the gain it sees will by 9/4 x that which would occur if using linear polarisation.

As for ordinary SERS we find that it is possible to incorporate the effects of diffraction loss into the formalism. Starting from the wave equation for the growth of the hyper-Raman wave and proceeding as outlined earlier we arrive at an analogous expression to equation 2.24 for the threshold pump power at a given frequency.

$$P_{p_{th}} = \pi w_p^2 \cdot \frac{ce^2}{4\pi\alpha\hbar} \cdot \frac{1}{\omega_s \sqrt{15\,\chi_{HR}}} \cdot \left[1 + \left(1 + \frac{k_s w_p^2}{L}\right) \ln\left(P_s(L)_{th}/P_{so}\right)\right]^{\frac{1}{2}} \quad \ldots 4.5$$

A plot of $P_{p_{th}}$ versus ω_p is included in Appendix 2, displaying resonantly enhanced minima as ω_p approaches single- and two-photon resonance. Using parameter values $N = 10^{23}$ atoms m^{-3} (~10 torr), $\Gamma = 1 cm^{-1}$, L = 25cm, $L/b_p = 1$ ($w_p = 150\mu m$), $\ln\left(P_s(L)_{th}/P_{so}\right) = 30$ and assuming linearly polarised light leads us to expect a tuning range, with 500kW pump, of 2.25-2.77μm. For this calculation

matrix elements derived from Warner's 1968 gf-values were taken. A weakness in the calculation is the choice of Γ, bearing in mind our earlier comments regarding the linewidths observed for SERS; nevertheless even allowing for strong linebroadening these calculations suggest that significant tuning should be attainable from the process.

Thus far the effect of the 3s-3p single photon resonance has only been considered with respect to providing resonance enhancement of the susceptibility. However the large oscillator strength of this transition results in a large resonance-broadened linewidth and consequently in strong single photon absorption of the pump. Depletion of the pump by this mechanism thus tends to reduce the Raman gain near the 3s-3p frequency. Following the same approach as for equations 2.39-40, for the effect of SPA on SERS gain, we find that the hyper-Raman gain over the vapour length L becomes

$$G = G_{HRO} \quad \frac{1 - \exp(-2\sigma_A NL)}{2\sigma_A N} \qquad \ldots 4.6$$

where G_{HRO} is the gain per unit length calculated from equation 4.1 in the absence of SPA, and σ_A is the SPA cross section. In the limit of strong SPA this becomes $G = G_{HRO}/2\sigma_A N$ and in the limit of weak SPA it becomes $G = G_{HRO} L$, as would be expected. The importance of SPA for our particular case is apparent from fig 4.5 where the normalised hyper-Raman gain is plotted in the curves, one incorporating and the other neglecting the effect. In plotting this, σ_A has been calculated from equations 2.41-42 which strictly only apply in the impact region, ie near 3s-3p resonance, and not in the region of 3s-4d two photon resonance used for most of our experiments; fig 4.5 thus may only be taken as giving a guide to the behaviour of the gain. To this end one should note that the SPA cancels out any enhancement of the gain near the 3s-3p resonance and also lowers the gain significantly elsewhere.

The calculation of the threshold pump power incorporating diffraction loss is complicated somewhat by the introduction of SPA since the decrease of I_p with distance results in a z-dependent nonlinear polarisation $P_{NL}(\omega_s)$ occuring in the wave equation; this obscures the behaviour of the evolution of a 'matched mode'. This calculation has not been seriously attempted since the main features of the behaviour are already apparent and since the value of precise numerical solutions is questionable in view of the uncertainty over Γ.

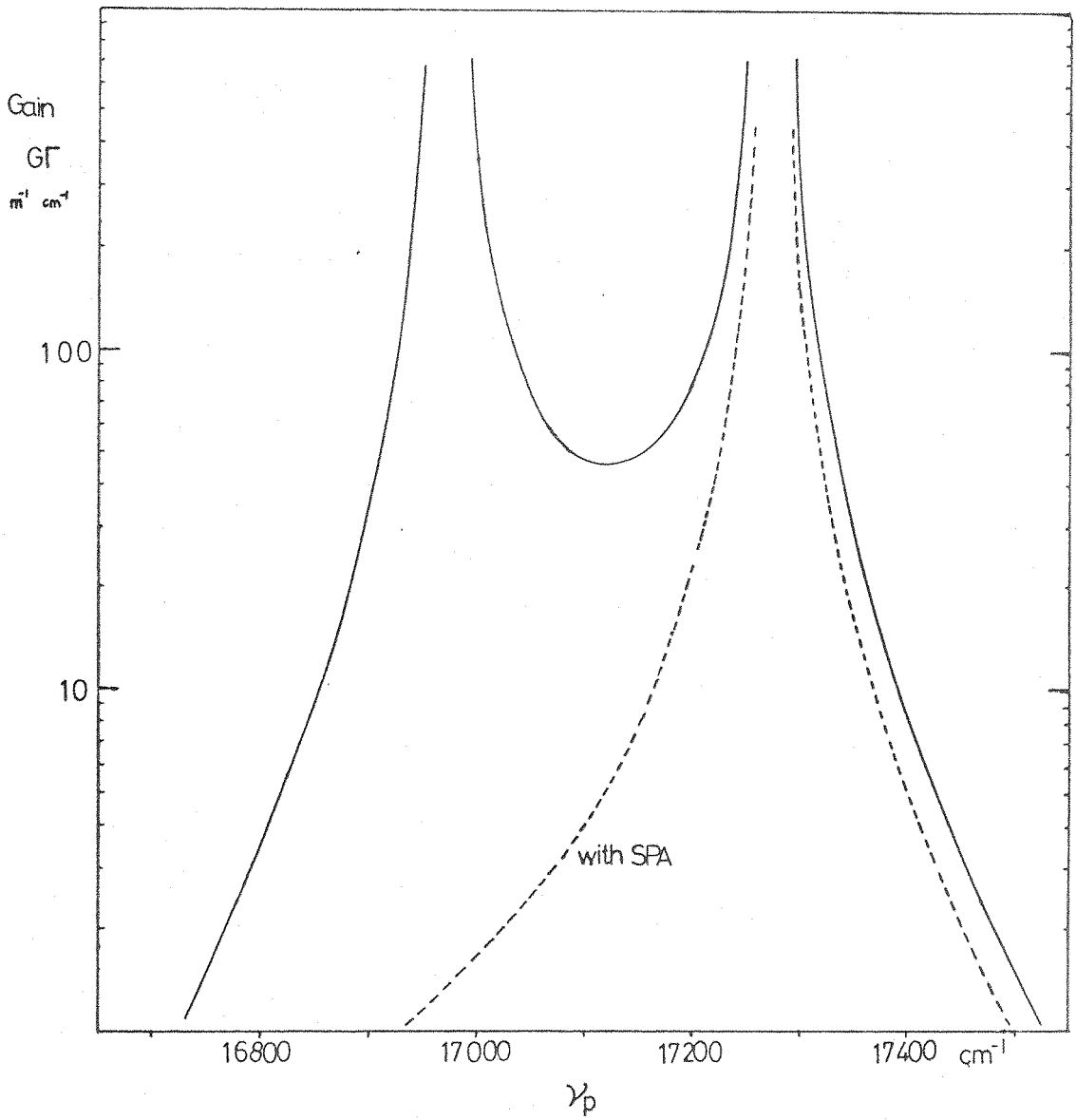

Fig 4.5 Normalised gain exponent for SHRS in Na with and without incorporating SPA

4.2.2 Observed Behaviour of SHRS

The Rh6G dye laser described earlier was used for this work. Use of a Fresnel Rhomb enabled us to convert the linearly polarised beam into nearly circularly polarised (60 ±40%) light, in order to take advantage of the predicted higher gain for a circularly polarised pump. This beam was focussed with a confocal parameter $b_p \simeq L \simeq 25$cms at the centre of the Na heat pipe oven containing 10 torr of Na. CaF_2 windows on the heat pipe oven transmitted the generated IR radiation which then passed through a Ge filter, a KBr lens and a 30cm monochromator before being incident upon a detector, either pyroelectric or InAs.

In this way we observed a strong tunable IR emission when the dye laser, circularly polarised, was tuned in the vicinity of the 3s-4d two photon resonance; the measured wavelength of the signal agreed to within experimental error ($\pm$ 2cm^{-1})with that calculated from $\omega_s = 2\omega_p - \omega_{3s-4p_{3/2}}$. Preliminary measurements indicated an energy exceeding 0.2nJ over a range of dye laser frequencies $\omega_p \simeq 17256 - 17336\text{cm}^{-1}$, ie $\omega_s \simeq 4240 - 4400\text{cm}^{-1}$; the more sensitive InAs detector was used for these measurements. A pyroelectric detector, possessing a greater dynamic range but poorer signal to noise ratio, was used to measure the variation in forward wave energy with dye laser tuning; this measurement was made for the case of circularly and linearly polarised pump and these results are shown in fig 4.6a. The energy measurements were calibrated, as for Cs SERS, by measurement with a pyroelectric energy meter, due allowance being made for other IR emissions observed (predominantly $4p_{3/2}$ - 4s ASE) and also for losses in the optics (windows, Ge, KBr). Other filters were also used in place of the Ge to block the dye laser beam to verify the absence of any free-carrier absorption in the Ge which might attenuate the IR. Various features should be noted from fig 4.6a and from the other measurements made.

(i) Saturation Mechanisms

Firstly, it would appear that a saturation mechanism may be occuring near the peak of the curve. The peak output energy of ~40μJ corresponds to ~6×10^{14} Stokes photons; estimates of the number of atoms in the pumped region and the total number of incident pump photons are ~2×10^{15} and ~2×10^{16} respectively. Using reasonable

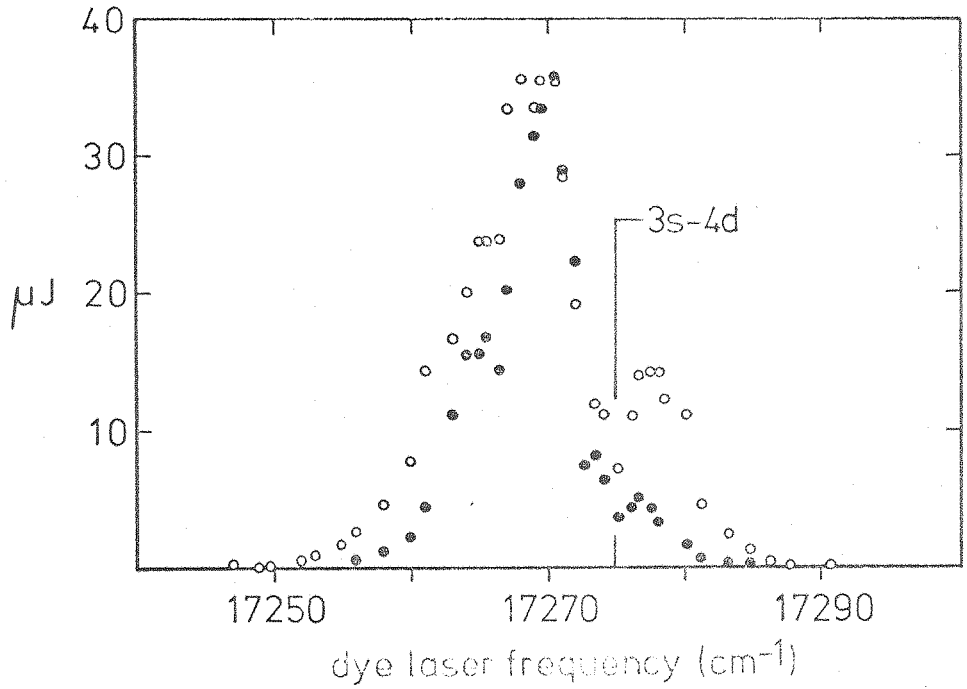

(a) 10 torr Na, linear (●) and circular (O) pump polarisation

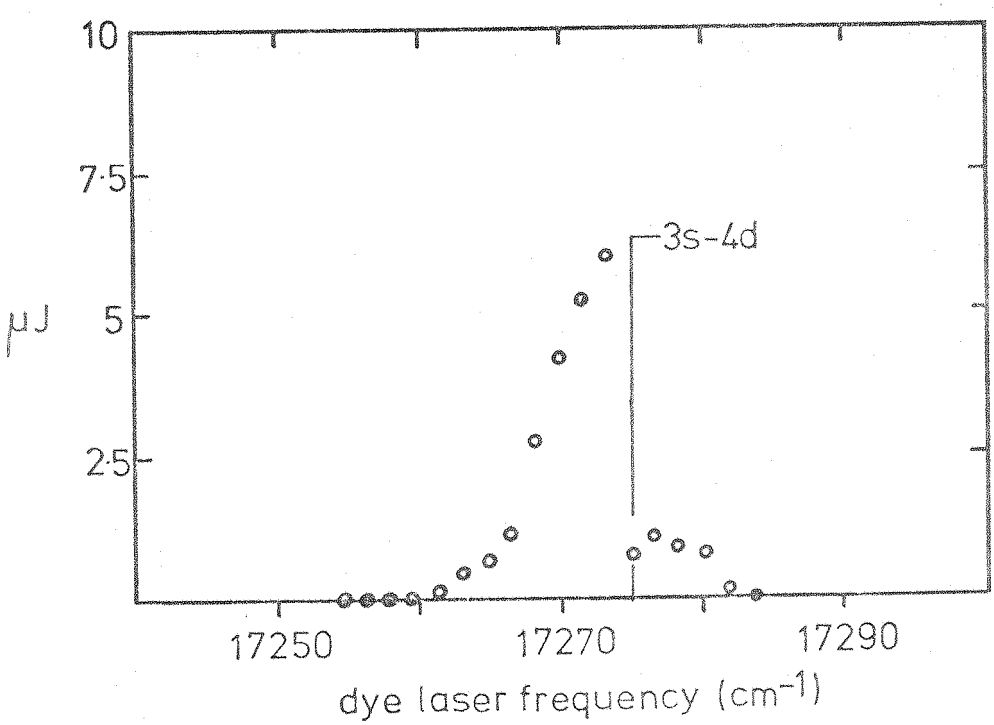

(b) 1 torr Na, circular pump polarisation

Fig 4.6 Observed SHRS energy as a function of tuning

estimates for the hyper-Raman gain coefficient, a simple calculation of saturation lengths, along the lines of section 2.3.3, indicates that atomic saturation might be expected to occur first; a detailed treatment of this is however complicated by the strong dependence of l_a, the atomic saturation length, on I_p ($l_a \propto I_p^{-2}$). From the above numbers we would not expect pump depletion to occur, or to in any way limit the output energy; however this neglects 3s-3p SPA which as already shown (fig 2.2) is still very appreciable at these frequencies. Measurements of pump transmission yielded values around 20-25% away from two photon resonance; such low values of transmission indicate that the pumped region may have been somewhat larger than estimated and/or that the pump may have been depleted by some strong multiphoton process. In the region of maximum IR signal, slightly below two photon resonance, a dip in the pump transmission of several percent was observed. Thus some measure of pump depletion was observed to occur which may have resulted in a reduction in Raman gain. It would seem however that atomic depletion was probably the mechanism limiting the peak output energy.

The peak output energy was observed to be the same for linearly or circularly polarised pump but a larger tuning range was obtained in the latter case; consideration of the atomic depletion mechanism incorporating the gain for the two cases lends us to expect such behaviour. As we tune away from two photon resonance the SHRS gain falls and the build up length increases. This results in reduced depletion of the atomic ground state and hence lower output energy. Since the build up length depends on the gain then, away from the peak of the curve, we expect to see increased output for the case of higher gain, as observed; the increased tuning range shown in fig 4.6a was obtained under essentially identical conditions, except for pump polarisation.

A measurement of the SHRS polarisation verified that for linearly polarised pump the Stokes wave was polarised similarly; likewise with a circularly polarised pump the Stokes wave was also observed to be circularly polarised.

(ii) Shape of the Tuning Profile

The asymmetry observed in the behaviour of the tuning curve above and below resonance is worthy of note. One possible explanation for this, suggested to us by New 1977, lies in the optical Stark shifts

experienced by the energy levels. When the pump is tuned below resonance, $2\omega_p < \omega_{3s4d'}$ the shifts of the ground state and the 4d state are both in the same direction, ie upwards. The shift of the latter state is strongly dependent on Stokes intensity and on the detuning from two photon resonance; the shift of the former is fairly constant, being determined by the pump intensity and detuning from single photon resonance. Thus it is to be expected that the exact two photon resonance condition may be fulfilled when the pump is tuned low of the expected value. When $2\omega p > \omega_{3s4d}$ the level shifts are such that the levels move closer together thus increasing the effective detuning from two photon resonance and decreasing the Raman gain. Qualitatively these effects could account for the observed asymmetry; quantitatively the magnitudes of the shifts may be calculated from eqns 2.52-53.

The direction of the shifts is such that if the field frequency is <u>less</u> than the frequency of the contributing transition then the levels are pushed <u>apart</u>, and vice versa. Thus the ground state experiences an upward shift due to its coupling with the 3p state via the pump; assuming $I_p = 6 \times 10^{12} Wm^{-2}$ and using matrix elements from Warner, we expect this shift to be $\sim 3cm^{-1}$, fairly constant over the range of dye laser frequencies of interest. The 4d state experiences an upward shift of $\sim 0.5cm^{-1}$ due to pump interaction with the 3p level and also a shift due to the SHRS coupling with the 4p level; these are the only significant contributions to the 4d level shift. The latter contribution is dominant over most of the range of interest, once the Stokes wave has reached a fairly high intensity; the magnitude of the shift, if Δ is the detuning from two photon resonance, is given for $\Delta > 8cm^{-1}$, by

$$\delta = \frac{P_s}{\Delta} \cdot \frac{1}{50} \quad cm^{-1} \qquad \ldots 4.7$$

where P_s is the Stokes power in Watts; for $\Delta \leq 8cm^{-1}$ we obtain

$$\delta' = \sqrt{\delta^2 + \left(\frac{\Delta}{2}\right)^2} - \frac{\Delta}{2} \qquad \ldots 4.8$$

δ being given by eqn 4.7. For $2\omega_p > \omega_{3s4d'}$ ie $\omega_s > \omega_{4p4d'}$ the shift of the 4d level is downward and for $2\omega_p < \omega_{3s4d}$ upward. Thus when the pump is tuned below the unpertubed two photon resonance frequency the 4d and 3s level shifts are in the same direction; eqn 4.7 and 4.8 reveal that they are of similar magnitude in the range

$\Delta \simeq 2\text{-}12 cm^{-1}$, in rough quantitative agreement with the frequency of peak SHRS output. When tuned above resonance the magnitude of the relative shifts of levels would also appear to be adequate to account for the reduced gain/output observed. The major uncertainty in evaluating the effect of this mechanism is the dynamic interaction of the Stokes wave and the level shifts, since the shift of the 4p level is only large for large Stokes intensities.

The dip in the output near resonance is believedto be due to 3s-4d two photon absorption accompanied by three photon ionisation. Estimates of the TPA rates assuming a Doppler broadened linewidth ($\Gamma \simeq 0.1 cm^{-1}$) indicate that over most of the tuning range TPA is less important than SPA to the 3p level; within a few cm^{-1} of two photon resonance the TPA may begin to become more significant. (These estimates were derived using the relationships

$$\frac{\partial I}{\partial z} = - KI^2 \qquad \ldots 4.9$$

where K, the absorption coefficient is given by

$$K = \frac{4\pi\alpha\hbar}{2ce^2} \cdot 3\omega \cdot \mathrm{Im}\ \chi^{(3)}_{TPA} \qquad \ldots 4.10$$

where $\chi^{(3)}_{TPA}$ was evaluated according to Yuratich and Hanna 1976)

A calculation of three photon ionisation adopting the transition rate approach, $P_i = \sigma^{(3)} F^3 \tau_p$ (notation as in chapter 2), and using theoretical values for $\sigma^{(3)}$, the 3PI cross section, calculated by Teague and Lambropoulos 1976 , indicates that complete ionisation should occur for intensities higher than $I_p \simeq 2 \times 10^{12} Wm^{-2}$ for the off resonant case and for lower intensities on resonance. This might suggest that 3PI was responsible for some of the pump depletion. At the peak of the output curve SHRS occurs over the length of the vapour column illustrating the fact that the SHRS cross section can under some conditions become comparable to or exceed the 3PI cross section. This would perhaps indicate that the 3PI rate as calculated may be an overestimate; empirical data on this process in Na appears as yet to be unavailable.

The interaction of the nonlinear processes occuring could perhaps be more fully explained using a dynamic analysis, since it is the generated IR radiation which contributes strongly to the shift of the 4d level, thus influencing the TPA and 3PI also, as

well as influencing its own evolution. Nevertheless this qualitative model does seem to give reasonable agreement with the observations, suggesting that optical Stark shifts, for this case, may be significant.

(iii) Spectral and Temporal Behaviour

The linewidth of the SHRS radiation was observed to be surprisingly broad, of the order of 2-3cm^{-1}. Linewidths measured under a variety of conditions are tabulated in table 4.1; these measurements were made using a 30cm IR grating monochromator and, usually, a pyroelectric detector. The instrumental resolution was measured as being 1.2cm^{-1} or less by observing the $4p_{3/2}$-4s ASE linewidth at 4533cm^{-1}.

As may be seen from the table, over most of the tuning range at high intensity, the linewidth was consistently fairly broad, 2.6 ± 0.5cm^{-1}; the ± 0.5cm^{-1} error probably represents the inaccuracies involved in manually scanning the monochromator. Towards the edges of the tuning range the signal to noise ratio deteriorated somewhat and the larger values of linewidth observed in these regions, marked with an asterisk in the table, are attributed to this cause. Some evidence of the line broadening being intensity dependent, at least near resonance, is apparent from table 4.1. At low intensities the IR signal might be thought to be 4d-4p ASE; this is believed not to be the case and is discussed further in section 4.2.2 (iv).

At high intensities no noticeable increase in linewidth was observed as we tuned towards two photon resonance. The calculations of the optical Stark shift suggest that it would be on the lower frequency side of the resonance that the ground state and final Raman state shifts would be additive; temporal variation of these shifts due to temporal intensity changes would be expected to lead to broadened linewidths increasing near two-photon resonance due to the increased $4p_{3/2}$ shift. That such behaviour was not observed may relate either to the magnitude of the effect being smaller than estimated or to the spectral evolution of the SHRS pulse.

The broad linewidth still observed at large detunings would indicate the presence of some other broadening mechanism, possibly plasma broadening. Using eqns 2.59-60 we find that the Stark constant for the 4p level is considerably larger than that for the ground state;

Table 4.1

Linewidth Measurements of SHRS

(at 10 torr Na pressure)

Pump Intensity (Wm^{-2})	Polarisation	Pump Frequency (cm^{-1})	SHRS Linewidth (cm^{-1})
6×10^{12}	Circ	17256	4.0*
"	"	17258	2.8
"	"	17260	2.3
"	"	17261	2.6
"	"	17263	2.4
"	"	17265	2.2
"	"	17267	2.4
"	"	17269	3.1
"	"	17270	2.5
"	"	17272	2.2
6×10^{12}	Lin	17262	3.6*
"	"	17270	2.8
"	"	17280	3.2*
3×10^{11}	Circ	17273	1.9
3×10^{10}	Circ	17273	1.5

* probably an overestimate - see text.

(at 1 torr Na pressure)

3×10^{12}	Circ	17273	2.1

thus we expect broadening of the 4p level to dominate. For the 4p level we find $C_4 \simeq 1.4 \times 10^{-55} Jm^4$, andso $\Gamma = 0.1 cm^{-1}$ for an electron density of $10^{21} m^{-3}$, ie an ionisation of ~2% of the atomic density; thus an ionisation of ~50% of the atoms present would be necessary to explain the broadening observed. Also, this ionisation would need to be present off-resonance, not just when ω_p is tuned to $2\omega_p = \omega_{3s4d}$. The presence of such strong ionisation might seem unlikely; certainly three photon ionisation or ordinary molecular ionisation could not account for this.

However, recent work by Lucatorto and McIlrath 1976 should be mentioned at this point. These workers used a $1MWcm^{-2}$ 500ns dye laser to pump the $3s-3p_{1/2}$ transition in Na at 1 torr and observed almost 100% ionisation, an unexpected result; various mechanisms were suggested for the anomalously high ionisation and a further experiment was performed in Li (McIlrath and Lucatorto 1977-ML) in order to clarify the situation. Again anamolously high ionisation was observed. The mechanism which has been invoked to explain the observations is that of superelastic heating of an initially small number of free 'seed' electrons, by collisions with excited atoms, followed by electron impact ionisation of excited state atoms by the heated electrons. Measures 1977 has treated this process analytically and has derived an estimate for the time required for complete ionisation of the atoms; these results applied to Lucatorto and McIlrath's experiment with Na provide sensible agreement. Measures' result for the ionisation time is

$$\tau_{ion} \simeq \frac{E/E_2^*}{2 N_{AO}^2 \bar{\sigma}_{12} R L (2E_{12}/m_e)^{1/2}} \ln\left(\frac{N_{AO}}{N_{eo}}\right) \qquad \ldots 4.11$$

where E represents the absorbed laser energy; $E_2^* = E_{12}E_1/E_2$ where $E_{1,2}$ are the ionisation energies from the initial (1) and excited (2) levels, and $E_{12} = E_1 - E_2$; N_{AO} is the initial ground state population, N_2 is the population of the excited levelland R the ratio $N_2/N_A(t)$ which for early times may be taken as N_2/N_{AO}; N_{eo} is the initial 'seed' electron density; L is the length of vapour; m_e is the electron mass; $\bar{\sigma}_{12}$ is the electron collision cross section for excitation of the $1 \rightarrow 2$ transition. Using this equation for ML's Li experiment again provides reasonable agreement if $\bar{\sigma}_{12}$ for Li is assumed to be a little smaller than for Na, which may not be an unreasonable

assumption. Applying this now to our situation, assuming only 10% population in the 3p level and taking $\bar{\sigma}_{12} = 8 \times 10^{-19} m^2$ (ML) we find τ_{ion} is of the order of 15ns. The 'seed' electrons necessary for this process are probably produced by off-resonant three photon ionisation at the intensities we have used, although other processes might be responsible for their production at lower intensities (Geltman 1977); for the above calculations N_{eo} was taken as $10^{11} m^{-3}$, although the dependence of τ_{ion} on N_{eo} is very weak.

Thus it would seem that this mechanism could explain our observed results. Further experimental investigations of the process, hopefully, will serve to test the theoretical approach of Measures; certainly it would seem that the process should be considered in SERS experiments involving the possible population of resonance levels.

In view of the usually small TPA it seems unlikely that significant resonance broadening of the 4p level will occur; we might expect lifetime broadening of the 4p level to occur however, resulting in a broadened SHRS linewidth. Taking an ASE intensity of $6 \times 10^{9} Wm^{-2}$ and assuming $\tau_{4p} = 350ns$ (Miles and Harris) we estimate from eqn 2.51 a lifetime broadening of $\sim 2.5 cm^{-1}$; this is also of the order of the broadening observed. The behaviour of the ASE output as a function of ω_p was not extensively studied, but certainly the ASE intensity decreased considerably as the SHRS output decreased; a decrease by a factor of ten would result in lifetime broadening of less than $1 cm^{-1}$. Thus it might be expected that lifetime broadening would decrease with detuning.

The effect of power broadening may be considered by using the analogous eqn to 2.58 for hyper-Raman ($I_p \rightarrow I_p^2$). From fig 4.5 we may take $G\Gamma_s = 300$, say, as a typical value; taking $\Gamma_s = 0.06 cm^{-1}$ (Doppler broadened) and $I_s = 6 \times 10^{10} Wm^{-2}$ (peak SHRS intensity) we find $\Gamma_p = 1 cm^{-1}$. In a realistic situation Γ_s may well be larger than the Doppler broadened value due to all the other mechanisms going on; if these other processes result in a $\Gamma_s = 0.3 cm^{-1}$ then we would expect the effect of power broadening to be an increase of Γ to $\Gamma_p = 2.5 cm^{-1}$. Thus power broadening may be expected to contribute significantly as a broadening mechanism when some other broadening is present but not very strong.

Also, since power broadening is dependent on Stokes intensity, the influence of this mechanism might be expected to decrease with detuning from resonance.

A feature of all of the mechanisms we have discussed except power broadening is that they invoke a broadening of the final Raman level as integral to the broadening of the Stokes wave. This would however result also in a broadening of the 4p-4s output yet, as already mentioned, the linewidth of this signal was noticeably smaller than that of the SHRS. It might be that the dynamic evolution of the SHRS and ASE is such that one experiences broadening due to some of the mechanisms proposed and the other does not, however this is by no means obvious and the behaviour remains incompletely understood.

The temporal behaviour of the SHRS pulse was observed using a fast InAs diode and Tektronix 7704 oscilloscope, the system having a rise time of perhaps 2ns or less. With the dye laser tuned to 17262cm^{-1} the SHRS pulse length was observed to be roughly 10ns. Generally the pulse was observed to be a fairly smooth pulse although occasionally additional structure in the form of secondary or subsequent peaks of lower amplitude was evident. Photographs were not taken of this behaviour, although qualitatively it was very similar to that observed for the backward wave (discussed later) shown in fig 4.7. Various mechanisms could be responsible for this temporal behaviour; we have not attempted to analyse it. A measurement of pulse length was also performed with the dye laser tuned to 17280cm^{-1}, but this time using narrow monochromator slits, thus sampling just ~1cm^{-1} of the hyper-Raman signal; the pulse length obtained in this way varied between 6-8ns apparently slightly shorter than the total pulse length. This might be considered as providing some indication of a frequency 'chirping'; however, the lack of full width pulse length measurements at the same frequency as these narrower linewidth measurements render this result inconclusive. More extensive measurements using a higher resolution instrument would be neccessary to provide useful data on this behaviour; these were not attempted.

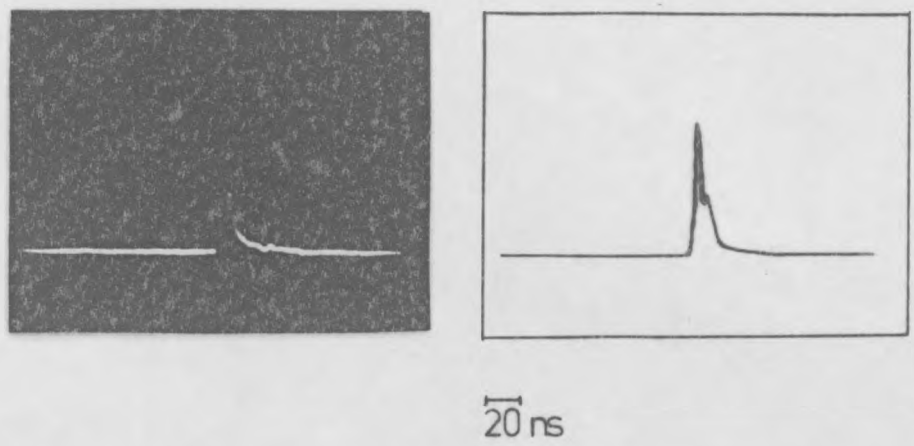

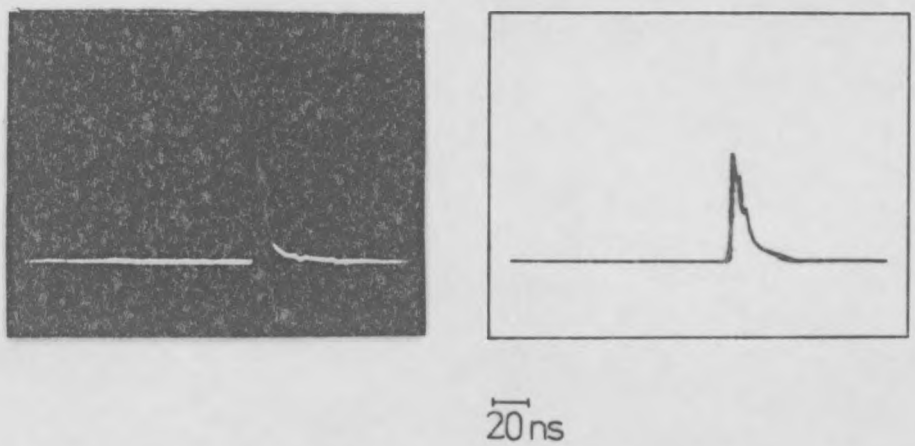

Fig 4.7 Backward wave SHRS in Na - temporal behaviour
(Conditions unchanged for both photographs)

(iv) Low Pressures and Low Intensities

The tuning profile was also measured at an Na pressure of ~1 torr using a circularly polarised pump at a slightly lower intensity than before; the observed behaviour is shown in fig 4.6b. The pump throughput was much higher in this case since the lower atomic density resulted in weaker SPA to the 3p level; the peak SHRS output was therefore certainly not limited by pump depletion. The peak output corresponded to 10^{14} photons; this is to be compared with the number of atoms in the pumped volume $N_A \simeq 2 \times 10^{14}$. These numbers imply that atomic saturation is the limiting mechanism in the region of high gain at this lower pressure. A dip in pump transmission corresponding to 1.5×10^{15} pump photons was observed in the region of resonance and maximum SHRS generation which would indicate that some processes other than SHRS are also occuring.

A linewidth of $2.1 cm^{-1}$ was measured under these conditions for $\bar{\nu}_p = 17273 cm^{-1}$; this might serve to suggest somewhat reduced plasma broadening at the lower atomic density but on its own is somewhat inconclusive.

Measurements of the tuning curve at 1 torr for a linearly polarised pump proved somewhat difficult. The peak signal appeared to be considerably down on that observed with circularly polarised light and a large jitter in signal amplitude was present over all of the tuning range. These observations suggest that under these conditions, with the lower gain for linearly polarised pump and lower gain due to the lower atomic number density, the length of vapour needed to reach detector threshold was approaching the length of the vapour column itself.

At 10 torr Na and tuned near the peak of the output curve the effect of attenuating the pump input was observed. Reduction of the pump intensity to $\sim 5 \times 10^{10} Wm^{-2}$ enabled us to still obtain an SHRS signal; we were able to verify that this signal was SHRS and not 4d-4p ASE in that as the dye laser was tuned we were able to observe a shift in the IR signal correspondingly, although the range of tuning was of course very small, $\sim 2 cm^{-1}$. The linewidth was sufficiently less than this for this tuning to be clearly observable. At lower intensities still we were able to observe a signal but without a higher resolution monochromator it was not possible to verify the presence of tuning and thereby to distinguish SHRS and ASE;

however, generally when SHRS was observed, no 4d-4p ASE occured. Thus the linewidth measured at low intensity in table 4.1 is ascribed to SHRS rather than ASE. In this way an IR signal was obtained for intensities as low as $2 \times 10^{10} Wm^{-2}$.

(v) Limiting Behaviour - The Possibility of Four Wave Parametric Mixing (see Fig 4.8)

Whilst much of the behaviour of the generated IR radiation was in accord with expectations for SHRS some unusual behaviour was observed and is reported here.

In the forward direction for $2\omega_p > \omega_{3s4d}$ the tuning range was observed, as expected, to be limited by the signal growing increasingly weaker and jittery as detuning increased; this behaviour is summarised in table 4.2. However on the low frequency side it was observed that as ω_p was tuned below ~17255cm^{-1}, at 10 torr pressure with circular polarisation, a broadband (several cm^{-1}) fixed frequency emission began to occur centred near 4220cm^{-1}. As ω_p was decreased so the amplitude of this signal increased remaining fixed in frequency and beginning to take over from the tunable IR output. As ω_p was tuned through and to the other side of the frequency corresponding to this emission no further tunable IR was found. Possibly this may indicate a transition between the SHRS and four wave parametric mixing processes. When linear polarisation was used the low frequency tuning limit was again observed to be limited by a similar fixed frequency signal, although this time it was nearer to the two photon resonance. The behaviour at 1 torr was not carefully investigated.

In order to further understand the possible role of the four wave process the backward emissions from the vapour were observed. For this a polycarbonate disc was placed between the focussing lens and the heat pipe, just before the entrance window, at 45° to the beams in such a way that the pump was transmitted and a few percent of any backward emission from the heat pipe was reflected from the disc through a Ge filter and KBr lens into the monochromator. A similar arrangement was also used to lodk for backward wave UV emissions, using a different filter instead of Ge. The backward IR emission observed in this way appeared to be limited in tuning at both extremes by fixed frequency emissions, this time closer in

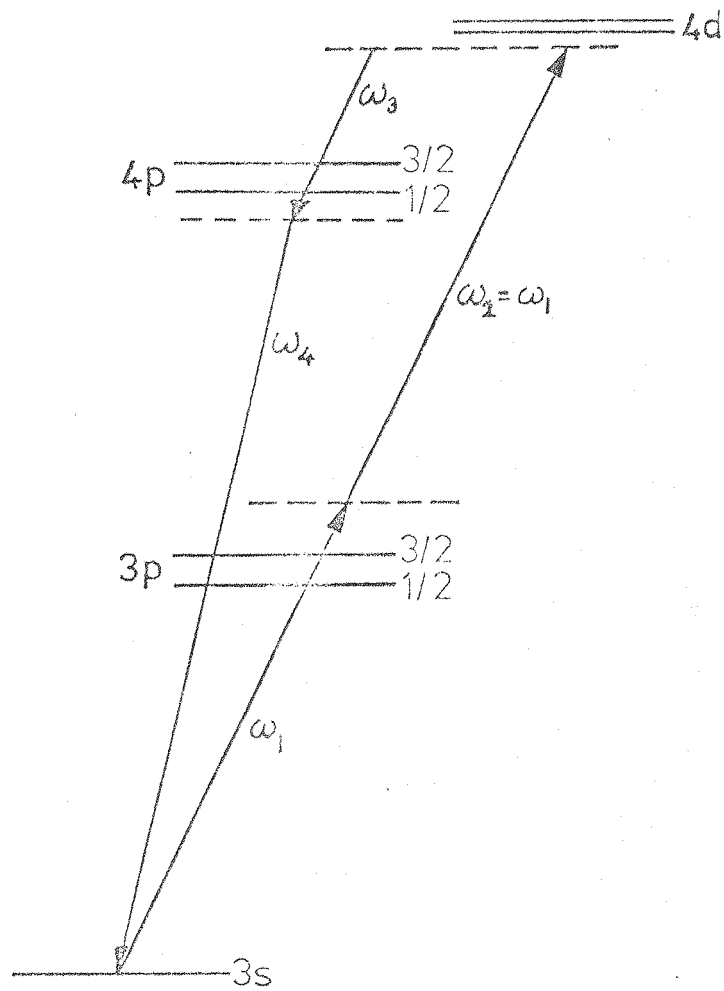

Fig 4.8 Parametric Four Wave Mixing Process in Na

Table 4.2

Behaviour of SHRS output energy towards the high frequency limit of tuning range

Pump Frequency	IR Energy (nJ)	% of Shots Present
17302	8	100
17306	0.8	80
17309	0.48	80
17313	0.32	60
17317	0.24	30
17321	0.2	20
17324	0.16	10

still to resonance. The IR was found to tune only over a very limited region, $\sim 4.5 cm^{-1}$ of pump tuning near resonance. Fairly wide slits were used on the monochromator in order to obtain sufficient signal to monitor giving a resolution of $\sim 3 cm^{-1}$; this was however sufficient to conclusively verify the tuning of the IR over a range of $9 cm^{-1}$. As the IR was tuned low in frequency the lower frequency limiting signal grew in amplitude to quite a large value until the two signals merged as ω_p decreased, upon further decrease in ω_p the fixed frequency signal gradually decreased in amplitude. As the IR was tuned high in frequency its amplitude decreased gradually and then it appeared to stop tuning, remain fixed in frequency and decrease in amplitude as ω_p continued to increase.

The absence of tunable SHRS over a more substantial tuning range in the backward direction might suggest that the forward wave was parametric in origin rather than true SHRS, since the coherence length in the forward direction would be much larger than in the backward direction. If this were the case however we would expect to see a forward wave $\omega_4 = 2\omega_p - \omega_{IR}$ accompanying the forward IR wave of energy $\frac{\omega_4}{\omega_{IR}} E_{IR}$; such an output was searched for but no UV signal of this magnitude was observed, although much weaker emissions near this frequency were found. This work was performed using a special glass filter to transmit ω_4, in the UV, but to block most of the dye laser light. The 30cm monochromator was again used, with a different grating, and a 9783R photomultiplier tube used to detect the signals. An energy calibration was obtained by measuring the peak UV output with the pyroelectric energy meter and relating that to the signals measured using the monochromator. Two UV outputs were observed in this way. One, fixed frequency at around $30366 cm^{-1}$, reached a peak energy of $\sim 2\mu J$ for $\bar{\nu}_p = 17268 cm^{-1}$ and decreased smoothly and symmetrically as $\bar{\nu}_p$ was tuned either side of this value. The other signal reached a peak value of $\sim 60nJ$ at $\bar{\nu}_p = 17266 cm^{-1}$ and tuned according to $2\omega_p - 4426 cm^{-1}$; a very weak signal $\sim 5nJ$ at $4426 cm^{-1}$ was just detectable on further investigation. This latter process is thus attributed to a four wave parametric mixing process. It is noted however that neither of the $30366 cm^{-1}$ and $4426 cm^{-1}$ emissions correspond to transitions between energy levels of the neutral Na atom; this same comment applies to the 'fixed frequencies' observed

to limit the IR tuning range.

With the IR forward wave energy observed of ~40μJ, we would expect, if its origin were purely in a four wave parametric process to observe a UV signal of energy ~250μJ. The absence of such a signal as the dye laser was tuned over all of the forward wave tuning range would strongly point to the IR being simply stimulated hyper-Raman scattering. However this does not explain the tuning limitations observed. An explanation of this behaviour might lie in the interaction of the four wave process with the hyper-Raman process in the small signal regime.

Thus, whilst the absence of strong four wave parametric would appear to have been verified, it would seem that some other process, possibly the parametric, may occur and interact with the SHRS to explain some of the features observed.

Observations of four wave processes have been reported by Bloom et al 1974 in Na pumped 3s-3d and by Vrehens and Hikspoors 1977 in Cs pumped 6s-7s; the parametric process involving the levels we have used in Na, shown in fig 4.8, has also been reported by Wynne and Sorokin 1977 and Hartig 1977. Wynne and Sorokin give no details of experimental conditions and so we cannot compare their results.

Hartig used 2 torr Na vapour pressure and intensities of the order of 10^{9} - 3 x 10^{10} Wm^{-2} in a $1cm^{-1}$ pump linewidth. In the forward direction he observed a broad ~$10cm^{-1}$ tunable signal, energy unspecified, accompanied by a UV signal near 330nm ($30300cm^{-1}$), peaking to 2μJ; this was with a pump energy of 80μJ (cf our pump energy of 6mJ). The $10cm^{-1}$ broad emission sounds to be of similar character to the emissions which we have observed to limit our IR tuning range; the UV signal, again, sounds similar to the fixed frequency emission which we have observed at $30366cm^{-1}$. Hartig also observed a signal near 333nm ($30030cm^{-1}$) which he ascribed to the four wave mixing process $\omega_{333} = 2\omega_p - \omega_{IR}$ where ω_{IR} is the Stokes wave generated in another Raman process 3s → (4p) → 4s pumped by the 330nm emission. This 333nm signal was an order of magnitude weaker than the 330nm emission, as was the signal we observed near this wavelength, so it might be that our signal has the same origin. Nevertheless our observed ω_{IR}, $4426cm^{-1}$, does <u>not</u> correspond to the Stokes frequency for 3s-4s Raman scattering pumped at $30366cm^{-1}$ (this would give ω_{IR} corresponding to $4626cm^{-1}$). In

a footnote to his work, commenting on ours, Hartig suggests the build up of the parametric process he observed from hyper-Raman noise.

An attempt has been made to consider the theory of the four wave mixing parametric process, although this is complicated by the role of 3s-4p SPA of the 'idler' which might be generated and also by the doublet splitting of the 4p level. This work is separately presented in Appendix 3 for clarity; without further numerical computations it is difficult to draw any definite conclusions from this approach.

4.2.3 Other Processes

As well as the results already discussed a variety of other processes were either considered or observed and these will be briefly outlined here. Initially we consider those not observed.

(i) Third Harmonic Generation

It is noted that the use of circularly polarised light should result in the suppression of any THG, since the electric dipole selection rules only permit $\Delta m_J = \pm 1$ for circularly polarised light (+ 1 for rhc, - 1 for lhc). Experimentally THG, at ~193nm, was not looked for.

(ii) SHRS in the Region of Single Photon Resonance (3s-3p)

As discussed earlier we expect SPA to neutralise the SHRS gain near the single photon resonance; nevertheless, bearing in mind the only approximate nature of the SPA calculations, it might have been possible for SHRS to have occured in this region. Careful observation however failed to detect its occurence and we conclude that the SPA is probably the cause of this.

(iii) Stimulated Three Photon Scattering

The process of stimulated three photon scattering mentioned at the beginning of section 4.2 was also looked for. In this process the levels 3p and 3s act as intermediates as the atom goes from the 3s to a 3p state; an emission at $2\omega_p - \omega_{3s3p}$ is expected. This process was only looked for in passing, at one spot frequency, 17262cm^{-1}; no emission at the expected 17547cm^{-1} was observed.

Considering the large detuning from single photon resonance this result is not surprising, but does however verify the absence of the process, which could otherwise have had some influence on, eg ionisation, hyper-Raman gain, etc.

We shall now turn our attention to processes which were observed under various conditions.

(iv) $4p_{3/2}$ - 4s ASE ($4533cm^{-1}$)

This signal was observed whenever strong SHRS was observed. At the peak of the SHRS output it was observed that 4-8% of the IR energy leaving the vapour originated in this emission; this corresponds to 2×10^{13} atoms undergoing a 4p-4s transition. The number of ASE photons is 0.1 times the number of Stokes photons. A calculation of the stimulated emission cross section leads us to expect a rapid build up of ASE; thus we might anticipate that most of the atoms promoted to the 4p level by the SHRS would undergo an ASE transition, resulting in the number of ASE photons equalling the number of Stokes photons. This simple calculation ignores the dynamics of the situation which might account for the observed factor of 0.1.

The behaviour of the ASE was observed at 1 torr in some detail. At its peak the ASE was only 1% of the IR output from the vapour; as we tuned away from 3s-4d two photon resonance so the 4p-4s ASE decreased. Off resonance a very small 'background' level signal was usually present, presumably due to multiphoton ionisation/excitation and subsequent cascades down the energy level ladder. As we tuned near ω_{3s3p} this also disappeared, probably due to self focussing/defocussing effects reducing the pump intensity and subsequent ionisation/excitation. When we tuned $2\omega_p \simeq \omega_{3s-5s}$ the ASE signal was observed to increase significantly; this was found to be due to population of the $4p_{3/2}$ level by $5s-4p_{3/2}$ ASE at $2928cm^{-1}$ subsequent to two photon excitation of ground state atoms to the 5s level. Attempts at observing the $5s-4p_{3/2}$ transition led us to the conclusion that this emission was indeed purely ASE, rather than SHRS 3s-(3p)-(5s)-4p. Our dye laser power was lower at this frequency and we were also at 1 torr pressure of Na; whether SHRS might go at higher power and pressures in unclear. Hartig also at low intensity and pressure observed 5s-4p ASE, but no tunable signals.

On a practical note, monitoring the ASE from the $4p_{3/2}$ level proved a sensitive indicator when attempting to tune the dye laser frequency close to a two photon resonance.

(v) 4f-3d ASE ($5414cm^{-1}$)

When tuned near two photon resonance, ω_{3s4d}, as well as SHRS and $4p_{3/2}$-4s ASE, an output was also observed at a frequency corresponding, to within experimental error, to the 4f-3d transition. Energies of the order of 0.8μJ (7×10^{12} photons) and 3nJ (3×10^{10} photons) were observed at 10 torr and 1 torr respectively. The two possible population mechanisms which immediately spring to mind are electric quadrupole excitation 3p-4f and collisional transfer from a population in the 4d level.

The magnitudes of these effects have been considered and it would seem that the former mechanism is too weak to account for the observed behaviour. Use of a 'typical' cross section for the collision process results in a much larger estimate for excitation of the 4f level and is therefore believed to be responsible for the observed results. The drop in 4f-3d energy with pressure is consistent also with this mechanism.

4.2.4 Discussion

(i) Conclusions From the Work Performed

From the work which has been described in this section it would seem that a number of useful conclusions may be drawn.

Initially we may deduce that fifth order nonlinear processes are indeed sufficiently strong for their occurence to be considered in nonlinear optical experiments; further physical insight and data for atomic systems may possibly be gathered using such processes. The potential for tunable outputs from such processes has also been demonstrated. As a practical IR source obviously SHRS is a poor competitor with SERS, nevertheless improvements in linewidth and photon conversion efficiency may be possible when pumping schemes with less SPA, although the concomitant decrease in G_{HR} may offset this; the importance of SPA as a limiting mechanism, initially unappreciated in our understanding of the hyper-Raman process, has been clearly demonstrated. We have also demonstrated that the four wave parametric mixing process generated through the third order

nonlinearity appears to play a role in such experiments, and it may in fact dominate the behaviour under some conditions; a simple and precise theoretical prediction of the interaction under experimental conditions would appear to be very difficult to make.

Various possible mechanisms have been suggested for the very broad linewidth observed, none of which totally and satisfactorily explains the observed behaviour, notably in view of the narrower 4p-4s ASE linewidth; as commented with respect to SERS, it is felt that a dynamic analysis of the situation may help to clarify this behaviour.

The mechanism of superelastic heating of electrons leading to subsequent ionisation of atoms is a very recently investigated process and its possible role in SERS type processes has not been previously considered. In having discussed it here it is to be emphasised that this process warrants consideration in any SERS process which may involve significant population of an excited (particularly resonance) level, since subsequent ionisation may account for poor efficiency or broadened linewidth. Experimental verification of the proposed quantitative theory of this mechanism is awaited with interest.

The collisional population transfer between the d and f levels which has been observed is an interesting feature, in that for the alkalis the energy differences between these nd-nf levels are small. Therefore the mechanism observed in our work would be expected to occur in any similar work in which high lying d states are populated.

(ii) Other Possible Schemes

We have considered a few SHRS schemes in other elements, our conclusions being briefly summarised in table 4.3. Our conclusions from the systems considered are not too promising; however, we have considered only a few elements and it would certainly be of interest to look at some others. Those considered in the table have fairly simple pumping requirements, of a visible dye laser, or, for the Vrehens and Hikspoors Cs case, an OPO. The Rb 5s-5p-5d-6p scheme was not initially considered due to the long wavelength dye pump required ~800nm; however since that time we have operated such a dye laser and thus this system, from the pump requirement point of view, is not as difficult as initially envisaged. Thus,

evaluation of other possible schemes is suggested.

The possibilities of using two separate dye laser pumps ω_1, ω_2 in order to gain additional enhancement of the gain from the single photon resonant level, (see eg Bjorkholm and Liao 1974), was briefly considered, but no experiment of this type was performed for Na 3s-3p-4d-4p scattering. The compromise between increased enhancement and loss due to SPA would need to be considered carefully in such a process in order to obtain optimum performance; this might require empirical optimisation. Nevertheless, some improvement in performance using such a system might be expected; this was not examined in detail.

Table 4.3

Other SHRS Schemes

Element	Transition	Estimated G_{HR} *	Effect of SPA	Comments
Cs	6s-7p-6s-7p	-	-	Vrehen and Hikspoors' scheme; they observed backward SHRS with ~250cm^{-1} detuning from resonance.
Cs	6s-6p-6d-7p	5000m^{-1}, for Δ=20cm^{-1} **	Very strong.	May or may not go, complicated by large doublet splitting. $\lambda_s \simeq 16\mu m$; high diffraction loss also.
Sr	5s-5p-5d-6p	8m^{-1} for Δ=20cm^{-1}	Weak. $\Delta\bar{\nu}_1$=4300cm^{-1}	Insufficient gain; $\lambda_s \simeq 14\mu m$
Sr	5s-5p-7s-6p	Similar to above	Weak. $\Delta\bar{\nu}_1$=2500cm^{-1}	Insufficient gain; $\lambda_s \simeq 2.3\mu m$

* for 'typical' experimental conditions, N 10^{23}m^{-1}, $I_p = 10^{12}$, Γ = 1cm^{-1}.

** for detailed gain calculation, see Yuratich 1977.

4.3 SERS from an Excited State

The concept of populating an excited state and then performing SERS from that state is not a new one; indeed the original observation of SERS in K by Rokni and Yatsiv involved this mechanism. Nevertheless until recently very little work had been published on such schemes. Korolev et al 1976 have probably achieved the best performance to date; optically pumping the $5p_{3/2}$ level in Rb vapour they obtained $\sim 60cm^{-1}$ tuning from $5p_{3/2}$ - $6p_{3/2,\ 1/2}$ SERS. Kung and Itzkan 1976 have obtained a few cm^{-1} tuning from $4p_{3/2}$ - $6p_{3/2}$, $4p_{1/2}$ - $7p_{1/2}$ SERS in K; their 4p populations were derived from a downward cascade of population after optically pumping the $5p_{1/2}$ level. Lau et al 1976 have also discussed optical pumping of processes from an excited state in alkali vapours.

Two main advantages may accrue from an excited state scheme. Firstly, since the initial Raman level is not the ground state, access may be obtained to several high lying and fairly closely spaced levels, which may serve as intermediate levels; thus a range of Stokes frequencies may be available, some at long wavelength. Secondly the possibility exists of recycling atoms back to the initial state; Grischkowsky et al 1977 have recently demonstrated this with a fixed frequency excited state system in K vapour. Such a system overcomes the atomic depletion problem and thus enables a long pulse high energy pump to be used, promising higher output energies. The first of these two features is apparent in fig 4.9 where the energy level diagram of Na is shown; the transitions indicated from the $3p_{3/2}$ level may all be reached using a single laser dye 7D4MC. With the potential of several new tuning ranges from this scheme and with an Na oven and suitable dye lasers available it was decided to try this experiment. For ease of detection we chose to investigate the shortest wavelength SERS transition of those indicated in the figure, that using the 6d intermediate level.

SERS was not in fact observed under the different conditions we tried; various possible reasons for this have been considered and are discussed, although insufficient evidence was collected to positively identify the cause of this behaviour. If, as suspected, superelastic collisional heating of electrons and subsequent ionisation is the limiting mechanism then a fundamental limitation on excited state processes when optically pumping at high vapour pressures must exist.

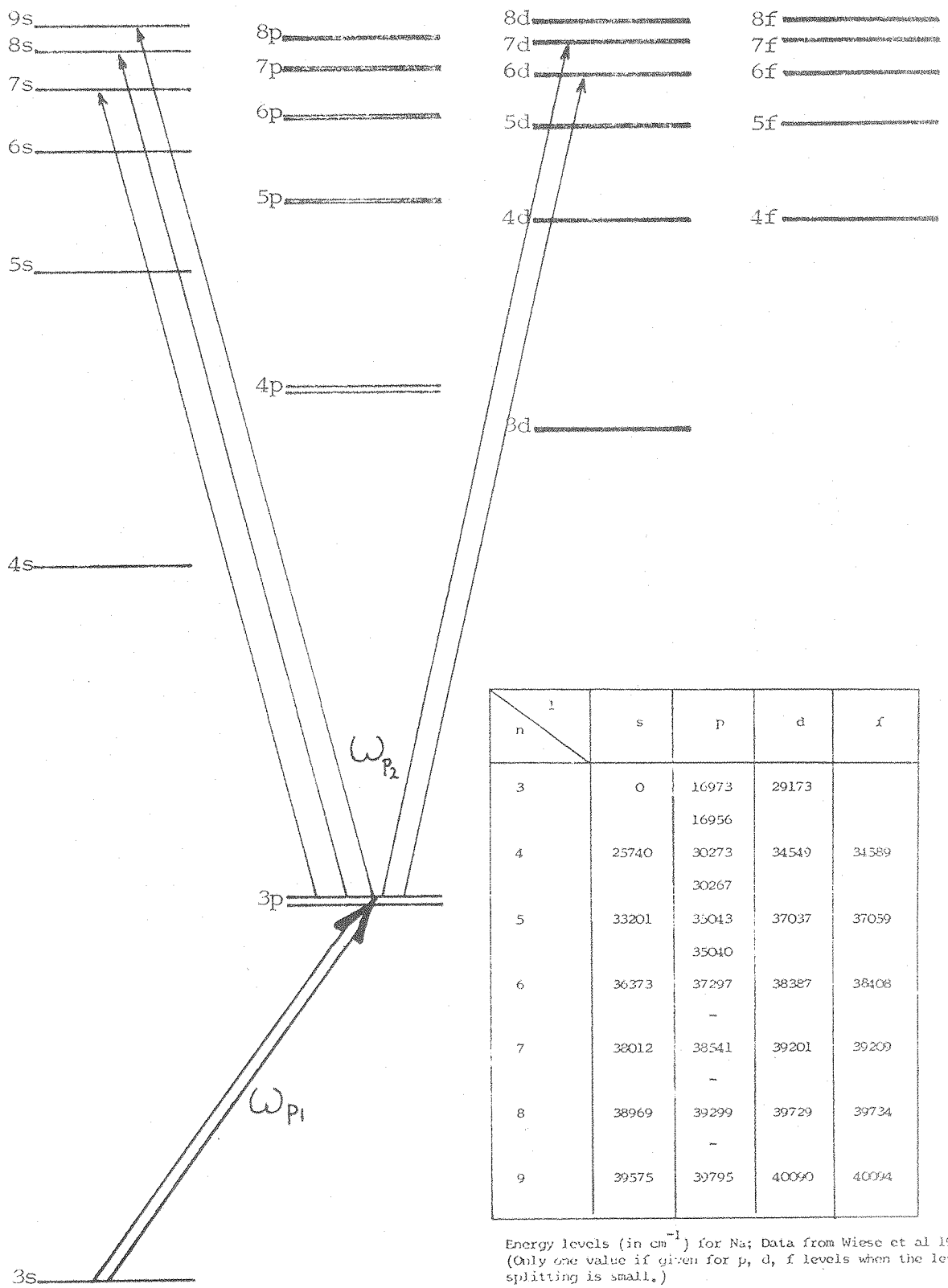

n \ l	s	p	d	f
3	0	16973 16956	29173	
4	25740	30273 30267	34549	34589
5	33201	35043 35040	37037	37059
6	36373	37297 –	38387	38408
7	38012	38541 –	39201	39209
8	38969	39299 –	39729	39734
9	39575	39795	40090	40094

Energy levels (in cm^{-1}) for Na; Data from Wiese et al 1969. (Only one value if given for p, d, f levels when the level splitting is small.)

Fig 4.9 Level scheme of Na used for excited state SERS experiment

4.3.1 Experimental Observations and Discussion

The dye lasers used were the Rh6G one described earlier (ω_{p_1}) and a nitrogen laser pumped 7D4MC dye laser (ω_{p_2}) producing a 120-300μJ, pulse in a 0.1cm^{-1} linewidth, described in fuller detail elsewhere (Cotter 1976b). The lasers were synchronised to within ± 50ns and a variable delay, τ_d, usually set as 50ns, could be introduced between ω_{p_1} and ω_{p_2}. The beams were combined with a dichroic mirror and aligned collinearly with the aid of apertures before and after the Na heat pipe. The CaF_2 windows on the heat pipe transmitted ~ 60% still at 9μm, ω_{6d6p}. The usual Ge filter, KBr lens and monochromator were followed, for this experiment, by a liquid nitrogen cooled CdHgTe detector; initial alignment was carried out using an IR signal generated by SHRS.

When using a resonance level as the excited state its lifetime is prolonged by radiation trapping, as briefly discussed by Kung and Itzkan; the work of Holstein 1951 may be used to estimate the effect of this. For our case we expect the 3p lifetime to be extended from its natural lifetime of 16ns to a value of the order of a micro-second.

Experiments were performed under a variety of conditions; Na pressures of 10 torr and 1 torr were used, the intensities of both lasers were independently varied over the range 10^{10} - 10^{12} Wm^{-2}. Different detunings of the two lasers from $\omega_{3s3p_{3/2}}$ and $\omega_{3p6d_{3/2}}$ were also tried. Initially we monitored the 6d-6p wavelength region around 9.2μm; a very weak signal of the order of ~20pJ corresponding to this ASE transition was the maximum observed.

At 10 torr with just the ω_{p_2} laser at full intensity an erratic signal at ω_{6d6p} was observed; with the ω_{p_1} laser also this signal was observed to be enhanced provided ω_{p_2} was close to ω_{3d6p}, otherwise the signal disappeared. At 1 torr no signal could be observed with just ω_{p_2}, although this could now occur with just ω_{p_1}. This behaviour was indicative of an ionisation process followed by atoms cascading down the energy level ladder, the fact that when both lasers were used the signal increased merely by a factor of at the most ten would seem to indicate that the role of the second laser may have been to increase the efficiency of ionisation.

With both lasers, at 1 torr, attenuation of the ω_{p_1} dye laser actually caused an increase in the 6d-6p signal; under such conditions the signal was observed for a range of ω_{p_2} detunings up to $20cm^{-1}$ from $\omega_{3p_{3/2}-6d'}$ peaking near resonance.

The possibility of 6d-5f ASE occuring was recognised but observations at ω_{6d5f} revealed only a signal of similar magnitude and behaviour to that already discussed. Measurements of the 6d6p signal as a function of τ_d the delay between laser pulses indicated an exponential fall off in signal with a time constant 0.15-1.5μsec under various conditions of focussing and intensity. This would be consistent with the expected radiation trapped 3p lifetime. How these measurements bear on ideas regarding possible depletion of the 3p level population, discussed later, remains unclear however.

From the lack of SERS, or even strong ASE, we may conclude that either (i) scattering from the 3p level was inefficient or that (ii) insufficient population was present in the 3p level.

(i) Various possibilities for inefficient scattering from the $3p_{3/2}$ level were examined.

The oscillator strengths of the transitions involved, $f_{3p_{3/2}-6d} \simeq 1.34 \times 10^{-2}$, $f_{6d-6p_{3/2}} \simeq 0.82$, were comparable to those involved in the other SERS transitions investigated by ourselves and others; thus the possibility of too weak a transition probability is ruled out.

The possibility of molecular absorption of the blue dye laser was considered; it was anticipated that the Rh6G laser would initially saturate this absorption, at least when using some small delay, τ_d, although it is possible that it did not. Assuming 10% of the molecules remain, a vapour pressure of 1 torr and an absorption cross section at 460nm of $1.5 \times 10^{-20}\ m^{-2}$ (derived from a low light level measurement) we estimate a $^1/_e$ absorption over the vapour length; the transmitted blue light did not appear to be seriously attenuated and this estimate may be regarded as a reasonable upper limit for the absorption. Such an effect would thus probably be insufficient to account for the observed behaviour.

Assuming reasonable 3p population, oscillator strengths and blue pump powers then the observed behaviour could be due to ionisation of atoms promoted to the 6d level either by photons or

by fast electrons. Three photon ionisation by three ω_{p_1} photons, estimated using the calculated cross sections of Teague and Lambropoulos 1976 , might be expected to produce 1% ionisation on single photon resonance at full intensity. A couple of orders of magnitude increase on this might be expected with photons of energy $\hbar\omega_{p_2}$ also present, for $\omega_{p_2} \simeq \omega_{3p_{3/2}-6d}$. Being very intensity dependent, this process would become far less important when the beams were attenuated. If this process were responsible for the ionisation one might expect the 6d-6p signal to be more sharply peaked as ω_{p_2} is detuned from $\omega_{3p_{3/2}-6d}$ than was observed; nevertheless, this process may well be important.

(ii) Insufficient population of the 3p level could be due to a collision or ionisation process.

Geltman 1977 has recently considered laser induced collisional processes of the form

$$X(n^2P) + X(n^2P) + \hbar\omega \rightarrow X(n^2S) + X^+ + e$$

which could lead to a depletion of 3p population in Na; this mechanism was one originally suggested by Lucatorto and McIlrath as a possible explanation of their results. Geltman's conclusions, valid for our situation also, are that such a process would be insufficient on its own to account for a significant depletion of 3p population.

Electrons produced by any of the processes considered already may gain energy by superelastic collisions with excited 3p state atoms, as discussed earlier, and then, colliding with other 3p state atoms, may result in ionisation; under our experimental conditions , Measures' calculation for this process would indicate the possibility of strong ionisation. At full intensity we calculate an ionisation time of ~ 100ns from eqn. 4.11.

From the observations and comments presented it would seem

that competing ionisation processes may be responsible for our negative results. For the three photon ionisation process discussed it should be possible to calculate an ionisation rate. Although the reliability of such a calculation might not be too good it would provide us with a better idea of the importance of this mechanism. The ionisation due to superelastic collisionally heated electrons is a process dependent upon atomic number density, $\tau_{ion} \alpha (N_{3s} N_{3p})^{-1}$. This may explain the results of Korolev et al who succeeded in observing SERS from an excited state using number densities one to two orders of magnitude smaller than ourselves; Kung and Itzkan's results however were under somewhat similar conditions to our own.

Unfortunately the equipment used was required for other work and so extensive measurements on this system were not performed. Whilst we may speculate on the possible mechanisms involved, a more reliable approach would be to monitor directly the 3p population and the ionisation of the vapour under various conditions; observation of the 6d-6p signal as a function of Na vapour pressure might also yield relevant data. If ionisation occurs by the route discussed by Measures then this would impose a fundamental limitation on optically pumping to an excited state at high densities; population by the use of an electric discharge might overcome this problem. Further work is needed in order to verify this possible limitation.

4.4 SERS in Alkaline Earths

Our interest in obtaining SERS in an alkaline earth system stemmed from the possibility of eliminating some of the possible line broadening mechanisms outlined in chapter 2; in this way we hoped to be able to identify the major causes of the broad linewidth previously observed.

Let us consider the various linebroadening mechanisms discussed earlier. In an alkaline earth we may Raman scatter to a metastable final level. This implies the elimination of lifetime broadening due to ASE from the level; it also implies a potentially greater importance of the resonance broadening of the final Raman level. The lack of dimers and the high ionisation limit for the alkaline earths together suggest a much lower degree of ionisation in the vapour, reducing the plasma broadening. The optical Stark effect and power broadening may also still occur.

The scheme originally considered was SERS $4^1S_o - 4^1P_1 - 3^1D_2$ in Ca; this idea was abandoned in favour of the analogous transition in Sr, $5^1S_o - 5^1P_1 - 4^1D_2$, see fig 3.10. The advantages of Sr were a higher vapour pressure for a given temperature and a simpler pump laser requirement $\lambda_p \sim 460$nm rather than 423nm. Sorokin et al 1969 had investigated this scheme using a 300kW $30cm^{-1}$ pump and failed to observe SERS; the reasons for this were still not appreciated even recently (Wynne and Sorokin 1977). Using a $0.1cm^{-1}$ dye laser of similar power we investigated this process, also failing to observe SERS. Further consideration has led us to identify SPA of the pump as the cause of this behaviour, with the conclusion that the singlet systems of the alkaline earths are unlikely to provide viable schemes for SERS from the ground state.

Consequently, to achieve our aim, we considered the possibility of performing SERS using an inter-system, singlet-triplet transition. The oscillator strengths for such transitions only become significant for the heavier elements, thus we were restricted to Sr or Ba. Of these, Sr has no convenient final Raman level below the 5^3P intermediate; Ba on the other hand has its 5^3D level lower in energy than the 6^3P intermediate and so may be used for SERS, see fig 3.11. Carlsten and Dunn 1975 have generated SERS in this way; in their experiment however a broad linewidth dye laser was used and so no information on SERS linewidth behaviour was obtained. Nevertheless their results

indicated the feasibility of the experiment; consequently the high temperature heatpipe was converted for use with Ba and a suitable dye laser worked up. We succeeded in obtaining similar SERS behaviour to that observed by Carlsten and Dunn under similar conditions and were able to measure the SERS linewidth under various conditions. A $0.2cm^{-1}$ dye laser/instrument limited linewidth was found indicating the feasibility of a narrower linewidth SERS source than has yet been obtained in the alkalis.

4.4.1 Sr

The initial experiments were conducted at 10 torr Sr pressure and used the 500kW 7D4MC dye laser already described, confocally focussed over the length of the vapour. The heat pipe, with CaF_2 windows, was followed by the usual Ge filter, KBr lens and monochromator; a room temperature InSb detector was used for most of the measurements. When tuned near resonance it was observed that very little pump was transmitted. Only a weak signal was observed at $\omega_{5^1P_1 - 4^1D_2}$, around 6.45μm. This signal was monitored as the pump, ω_p, was tuned; no great increase in signal was evident nor was there any trace of a tunable SERS output. At $100cm^{-1}$ detuning it was observed that still very little dye laser light was transmitted through the vapour. These observations led us immediately to consider the role of single photon absorption in this scheme.

For high Raman gain for a transition from a level g to a level f via an intermediate level i we require a large product $f_{gi}f_{if}$ (cf eqn 2.16). For the alkalis we find $f_{gi} < f_{if}$; eg for Cs $f_{6s-7p_{3/2}} = 0.03$ and $f_{7p_{3/2}-7s} = 1$. For the alkaline earths however this situation appears to be reversed, with $f_{gi} > f_{if}$; eg Sr $f_{5^1S-5^1P} = 1.9$ and $f_{5^1P-4^1D} = 0.01$. As discussed earlier, in the presence of strong SPA the Raman gain exponent over the vapour length becomes modified to $G_{RO}/\sigma_A N$ (eqn 2.43); using the formulae presented earlier for σ_A, assuming a resonance broadened s-p transition, we may express the gain exponent as over the vapour length L as

$$\frac{G_R}{\sigma_A N} = \frac{I_p}{\Gamma N} \frac{f_{fi}}{f_{gi}} \frac{\omega_s}{\Omega_{fi}} \frac{\sqrt{3}}{hc} \qquad \ldots 4.12$$

For our initial Sr experiments this gain exponent was about 15, assuming $\Gamma = 1cm^{-1}$, implying that there was insufficient gain for SERS to occur, a gain of at least e^{30} being necessary for SERS to occur. The calculation of the resonance broadened SPA cross section is strictly only valid for small detunings from line centre; nevertheless this eqn gives us some estimate of the likelihood of SPA preventing SERS and also suggests how we may adjust the various parameters in order to optimise the SERS gain.

Thus we set about investigating the effects of varying I_p and N experimentally. The pump focussing was tightened to give an intensity of the order of $10^{13}Wm^{-2}$ and the beam waist arranged to be at the entrance to the vapour, in order to more favourably compete with the SPA. Under these conditions at 10 torr we scanned, carefully looking for SERS, over a range of detunings from 0 to $+ 500cm^{-1}$ above the intermediate level; spot checks for SERS were also performed for $\Delta = -100$, -200 and $-300cm^{-1}$. For values of $\Delta = +100$, 200 and $300cm^{-1}$ we also looked for SERS as the number density was varied over the range $0.2 - 8 \times 10^{22}m^{-3}$. Various values of Δ were tried since G_R and σ_A may not be the ideal Lorentzian functions of Δ assumed. Under all these conditions, still no SERS was observed.

The $5^1P_1 - 4^1D_2$ ASE was also monitored as a function of pump frequency over the same ranges as for SERS. A slight dip was observed when pumping exactly on resonance; as ω_p was tuned above resonance an initial increase than a steady fall in signal was observed. Similar behaviour, but with a larger peak energy, was observed on the low side of resonance. Dips in the ASE energy were found for certain values of Δ. All this behaviour was qualitatively similar to that recorded by Wynne and Sorokin 1977, they attribute the dips observed in the ASE output to two photon resonantly enhanced ionisation. The peak ASE signal observed at 20 torr of ~12μJ was comparable to the number of atoms in the pumped region, indicative of atomic saturation of the process. Strong inter-system $4^1D_2 - 5^3P_{1,2}$ ASE was also found to occur, indicating that the 4^1D_2 level in Sr is not metastable. Weak $4^3D_3 - 5^3P_2$ ASE was also observed, the 4^3D_3 level probably being populated by a collision process; Sorokin et al 1969 also observed this feature. Allowance was made for these emissions in calibrating the $5^1P_1 - 4^1D_2$ ASE energy.

The 5^1P_1-4^1D_2 ASE was monitored for Δ= + 200cm^{-1} as the temperature of the oven was increased from 600-1000°C; the oven was not operating in the heat pipe mode over most of this range. The observations displayed as fig 4.10, show a clear N^2 dependence of ASE energy. (The apparent saturation of output at high densities may be due to the onset of heat piping, resulting in the number density staying constant as the temperature was increased.) Calculations of the stimulated emission cross section suggest that the ASE build up length is generally very small for the densities used and thus the ASE energy would be proportional to $N_{5^1P_1}$, the intermediate state population. If this population is derived from SPA of the pump we would expect $N_{5^1P_1} = N(e^{\sigma_A N l} - 1) \simeq \sigma_A N^2 l$, ie an N^2 dependence of output, as was observed. These results serve to indicate that SPA is still the dominant mechanism responsible for pump depletion and the lack of SERS under these modified experimental conditions.

It might be thought that other processes, enhanced by the strong single photon resonance, may also have been occuring; no evidence for such, eg ASE between higher lying levels, was however found.

Thus it appears that SPA dominates over the SERS process under the experimental conditions investigated, due to the high ratio of oscillator strengths, f_{gi}/f_{if}. Increase of pump intensity and decrease of atomic number density were expected to increase the effective Raman gain in the presence of SPA; changes in these parameters still did not however result in the observation of SERS. This behaviour is not fully understood; it may simply be due to an inaccurate model for the SPA. In the light of the oscillator strength ratios for the corresponding transition in Ca, Ba etc, it is unlikely that SERS in the singlets of the alkaline earths, from the ground initial state, will be possible. The ratio f_{gi}/f_{if} should also be considered in other potential SERS schemes.

4.4.2 Ba

For this work the Ba oven was maintained at temperatures of 910°C and 1080°C to give estimated vapour pressures of 0.25 and 2.5 torr respectively. For the 0.25 torr work, the oven was operated with a few torr of buffer gas simply as a Ba cell rather than as a heat pipe.

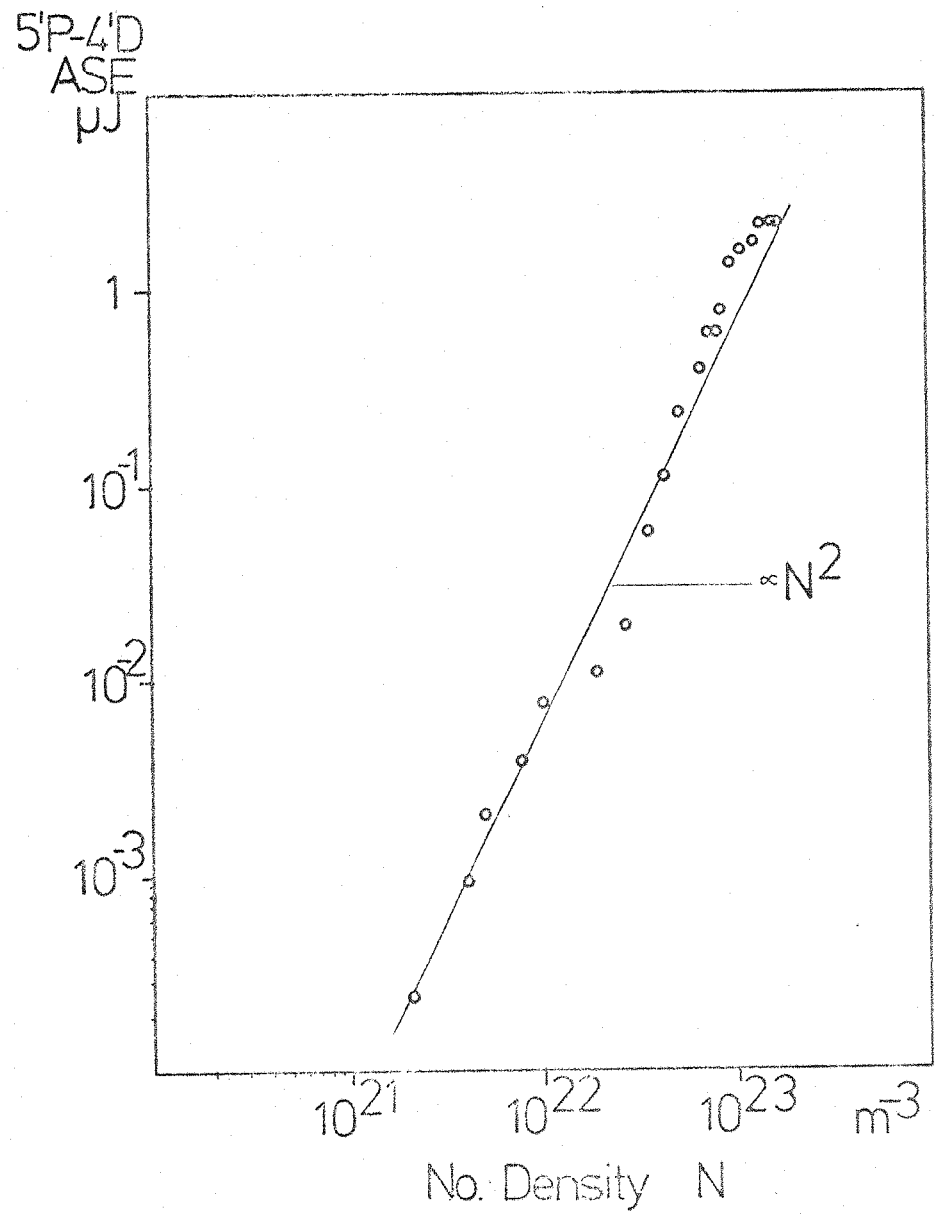

Fig 4.10 5^1P-4^1D ASE as a function of number density in Sr

The HITC dye laser was initially used unfocussed and without an intra-cavity etalon. The IR output from the Ba oven was incident upon a pyroelectric detector after passing though a Ge filter, KBr lens and monochromator.

At 0.25 torr initially a blue output was observed to occur; measurement of its wavelength, ~457nm, identified this emission as originating in the four wave parametric process (CARS) $\omega = 2\omega_p - \omega_s$. This process has been previously observed by Carlsten and McIlrath 1973 and was not investigated by ourselves in detail; it is recorded however that blue output was noticeable for wide tuning of the pump indicating the strength of the process. The blue output was also observed when operating at 2.5 torr.

(i) SERS Tuning Behaviour

Two SERS outputs were observed corresponding to scattering to the 5^3D_1 and 5^3D_2 final levels; the gains for the two transitions (calculated from eqn 4.13 and the oscillator strength data) are in the approximate ratio 1:2. Carlsten and Dunn 1975 also observed these two SERS outputs. The tuning behaviour of these emissions was investigated and is shown in fig 4.11 for both 0.25 and 2.5 torr. At 0.25 torr both SERS signals increase as the pump is tuned towards resonance. At 2.5 torr it may be observed that an on resonance dip has developed in the $\rightarrow {}^3D_2$ SERS signal. Carlsten and Dunn observed similar SERS tuning behaviour and tentatively attributed the dip to SPA of the pump by the intermediate level; however we have shown that this dip is accompanied by a corresponding increase in $\rightarrow {}^3D_1$ SERS. Thus it would seem that near resonance the competition between the two SERS lines becomes modified in favour of the, normally weaker, $\rightarrow {}^3D_1$ line; the reason for this behaviour is not apparent, although the observed parametric process may play some role in this. Solution of the coupled equations using an approach similar to that of Appendix 3 might yield some information on this. The ratio of the peak $\rightarrow {}^3D_1$ to minimum $\rightarrow {}^3D_2$ signals was noted as being generally 1.0-1.5 independent of pump intensity over the range $5 \times 10^8 - 10^{11} Wm^{-2}$. Investigation of the tuning behaviour at higher pressures would be interesting but such measurements were not performed due to the

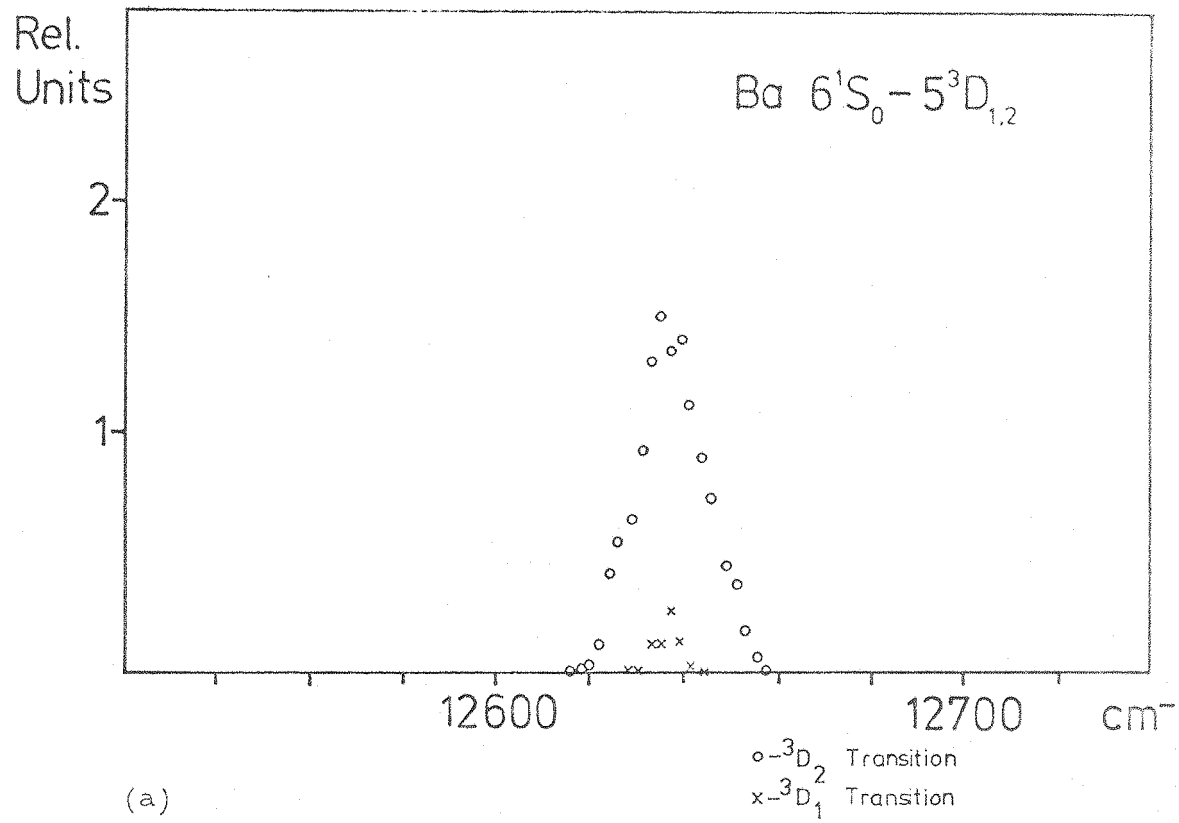

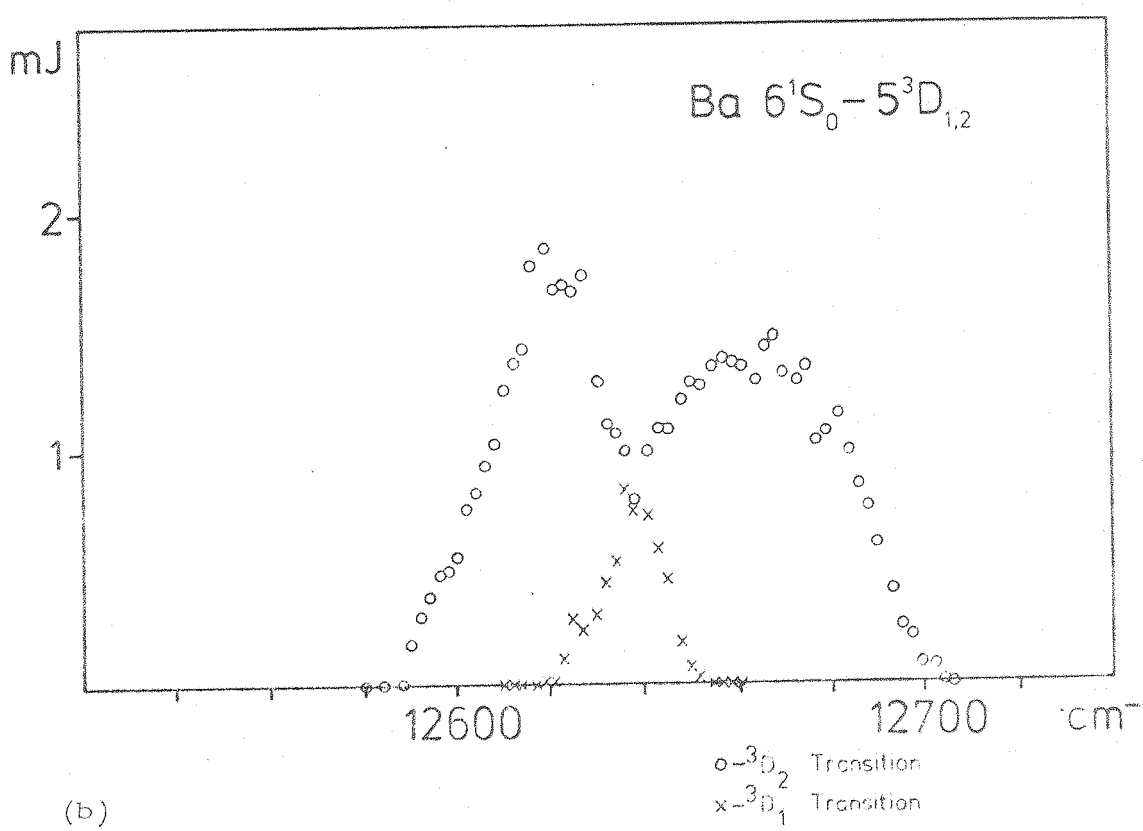

Fig 4.11 SERS in Ba tuning curves (a) 0.25 torr, (b) 2.5 torr

temperature limitations of the heat pipe oven. The assymetry* in the peak $\rightarrow {}^3D_2$ SERS output for ω_p above or below $\omega_{6{}^1S_o - 6{}^3P_1}$ was also observed by Carlsten and Dunn; the cause of this is not known. Energy calibration of the 2.5 torr tuning curves was carried out with a pyroelectric energy meter, as in other cases; no IR outputs other than the SERS ones were observed as the monochromator was scanned.

The use of a lens enabled us to focus the pump beam tightly in the heat pipe, increasing the intensity by a factor of around 20; under these conditions a significant, but not dramatic, increase in tuning range of the $\rightarrow {}^3D_2$ SERS was observed. Reliable quantitative measurements of this were however not pursued.

(ii) Linewidth Investigations

Linewidth measurements were performed on the $\rightarrow {}^3D_2$ SERS emission using a Hilger-Watts Monospek 1000 f/10 1 metre grating monochromator; a 16μm blaze 60 l/mm grating was used in fourth order. The frequency resolution of the instrument was checked for various slit widths using a narrowband 3.39μm cw HeNe laser; the chopped 3.39μm radiation was monitored using a liquid nitrogen cooled InSb detector. A resolution of $0.11cm^{-1}$ was verified using 40μm slits, the slit width used for the linewidth measurements.

An initial measurement of linewidth using the dye laser without an intracavity etalon revealed a dye-laser-limited $0.7cm^{-1}$ linewidth. Subsequent use of an etalon improved the dye laser linewidth to $\lesssim 0.17cm^{-1}$, as already described, and measurements of the SERS linewidth under the various conditions used are given in table 4.4. These linewdiths were obtained by automatically scanning the Monospek through the SERS line whilst the dye laser was operating at a fixed repetition rate; an example of such a scan is shown in fig 4.12 (the spread in

---

* In order to gather sufficient data points it was necessary to scan the tuning range in two halves on subsequent days; changes in the dye laser output between the two occasions account for the observed apparent assymetry in width of tuning range above and below resonance. Further measurements confirmed that the assymetry in peak output was not due to this.

Table 4.4

SERS in Ba-Linewidth Measurements

Pump Frequency (cm^{-1})	Detuning from intermediate resonance (cm^{-1})	Pressure (torr)	Peak Intensity (Wm^{-2})	Linewidth (cm^{-1}) FWHM
12630	- 6	0.2	7×10^{10}	0.2 ± 0.03 *
		2.0	7×10^{10}	0.21 ± 0.05
			4×10^{9}	0.24 ± 0.04
			10^{12}	0.19 ± 0.03
12616	- 20	2.0	7×10^{10}	0.21 ± 0.04
12606	- 30	2.0	7×10^{10}	0.23 ± 0.04

* Errors quoted are standard deviation of a series of at least eight measurements for each specified case.

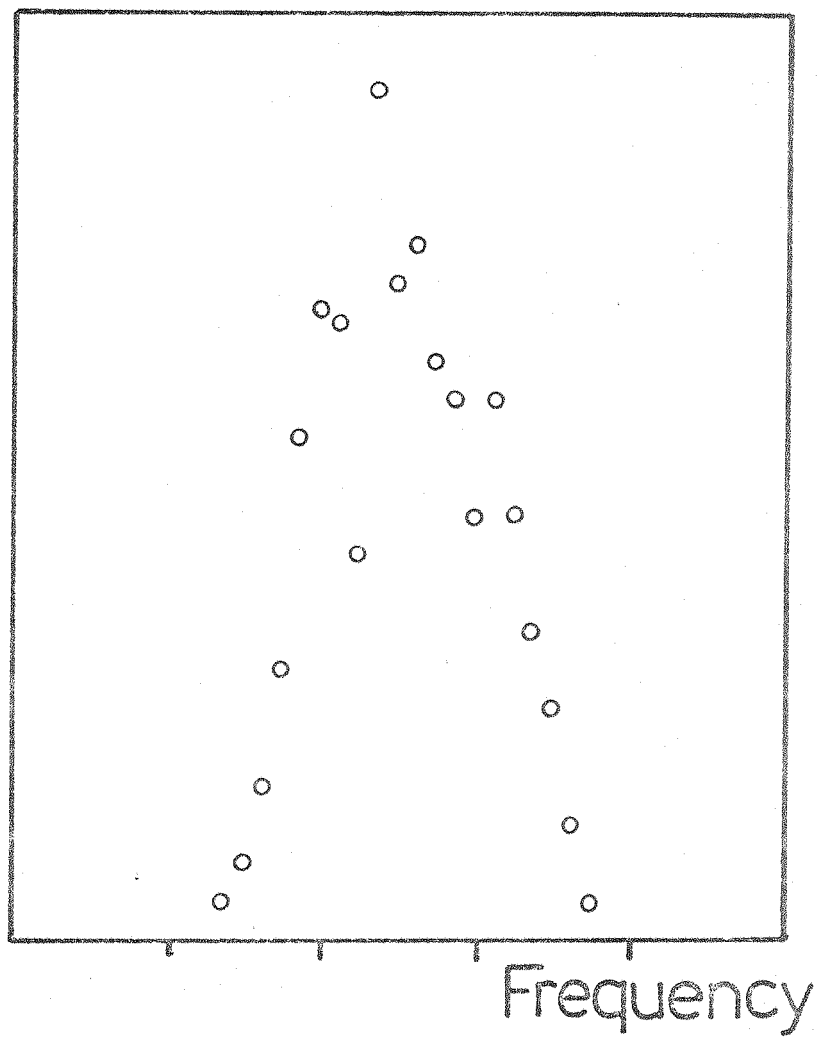

Fig 4.12 Typical SERS linewidth scan in Ba experiment

amplitude of points is believed to be due to shot to shot variations in dye laser power). Generally four scans in each direction (increasing and decreasing frequency) were performed and the results averaged. The Monospek was also manually scanned across the SERS line, several values of the signal being measured at each point; such results agreed with those obtained with the automatic scanning procedure generally used. The FP fringes from the dye laser were checked before and after linewidth scans in order to detect any drift in dye laser frequency or etalon mode hopping, but no problems were in fact encountered in these areas.

(iii) Discussion of Linewidth Behaviour

From table 4.4 it may been seen that for all the experimental conditions used the SERS linewidth did not differ significantly from $0.2cm^{-1}$. If we consider our overall frequency resolution to be the convolution of the dye laser linewidth and monospek resolution, assuming the lineshapes to be gaussian, we expect a resolution of $\sqrt{(0.17)^2+(0.11)^2} \simeq 0.19cm^{-1}$. Thus we interpret the measured IR linewidths as being system-limited. These linewidths are narrower than we have previously observed for any SERS process; narrower output still may perhaps be attained using a narrower linewidth dye laser.

The magnitudes of the various linebroadening mechanisms discussed in chapter 2 have been estimated for our Ba experiment. Resonance broadening we expect to be of little influence due to the low atomic density and oscillator strengths. Calculations of the optical Stark effect suggest that the shift would be $<0.2cm^{-1}$ under our unfocussed conditions, but should be of the order of $0.7cm^{-1}$ at the higher intensities used. A calculation of power broadening is complicated by the uncertainty in Γ used in the calculation of g, the Raman gain; nevertheless this mechanism would certainly be expected to produce strong linebroadening, at least $1cm^{-1}$, in our high intensity case.

The fact that narrow system-limited $0.2cm^{-1}$ linewidth was still observed for our high intensity measurement would suggest that the optical Stark effect and power broadening do not significantly influence the linewidth behaviour of the SERS. This is reasonable if one accepts that the spectral properties of the SERS are determined whilst still in the small signal regime. The indications would thus

seem to be that either plasma broadening or lifetime broadening, both eliminated in this Ba scheme, may be the predominant SERS broadening mechanism; the plasma broadening effect is operative in the small and large-signal regimes.

A further interesting feature relating to the linewidth behaviour is found if a gain calculation is performed for the $6^1S_o - (6^3P_1) - 5^3D_{1,2}$ SERS transitions. We obtain an expression for the gain coefficient

$$G_R = K \cdot \frac{NI_L \omega_s}{\Gamma(\Delta\omega)^2} \left(\frac{\pi\alpha}{m}\right)^2 \hbar \frac{f_{dp} f_{ps}}{\Omega_{pd} \Omega_{sp}} \qquad \ldots 4.13$$

where K is a numerical factor equal to 9 for the $^3D_1$ final state and 12 for the $^3D_2$ final state. Using the values of oscillator strength, known to reasonable accuracy, given by Miles and Wiese 1969 and our experimental conditions we may estimate the value of detuning for which the gain over the vapour length, G_RL, drops to the value of 30 (necessary for the SERS to reach detector threshold). Conversely, from our observed tuning range, we may infer a Raman linewidth Γ consistent with this; in this way we find Γ to be of the order $0.01cm^{-1}$ or less. This may be contrasted to the earlier analogous calculations for SERS in Cs where the calculated thresholds for the process were 2 orders of magnitude lower than the experimental ones when using such values for Γ.

(iv) Conclusions

Comparison of experiment with theory for SERS in Ba may be seen to differ significantly from previous work in the alkalis; for the first time a system-limited SERS linewidth as narrow as $0.2cm^{-1}$ has been achieved. Examination of the gain calculation suggests that a linewidth significantly narrower still may be attainable. The observation of a narrow linewidth at high pump intensity suggests that the effects of optical Stark shifts and power broadening may not be as severe as our simple calculations have indicated.

Further work is recommended using a narrower linewidth dye laser in order to discover the inherent linewidth limitations of this alkaline earth system and to futher investigate the roles of the optical Stark effect and power broadening. Further investigation into the

competition between the two SERS outputs would also be of interest whilst not of direct relevance to linewidth behaviour.

CHAPTER 5

Concluding Remarks

We begin this final chapter by relating the results achieved to the initial goals of the work; we also indicate the main areas where it is felt that further work would be productive and helpful as well as considering briefly the role of SERS as a tunable IR source in the light of our results.

Our first aim was to extend the tuning ranges in an existing SERS system. Whilst not having achieved an absolute increase in tuning range, the potential of pump and SERS feedback to achieve this end has been demonstrated in Cs 6s-7s scattering under non-optimum conditions. Further work in this area using a higher power pump system together with various feedback and multipass arrangements could yield the desired improvements in tuning range.

Generation of tunable IR in new regions of the spectrum has been achieved over the limited region 4240-4400cm^{-1}, using the process of stimulated hyper-Raman scattering in Na. Perhaps the greater significance of this result is that it represents the first demonstration of a tunable output from such a fifth order nonlinear process. The theoretical basis presented combined with our experimental work with Na enables us to predict in some measure the expected performance of other SHRS candidates. Some facets of the SHRS behaviour do remain incompletely understood however, notably the possible interaction with the four wave mixing process discussed.

Consideration of generation of SERS from an excited initial state has indicated the possible advantages of such a scheme; preliminary experiments in Na failed however to yield SERS. Examination of the possible causes of this behaviour has led us to realisation that a limitation of such schemes using optical pumping at high densities may exist due to ionisation; further investigations by other workers of the mechanism discovered by Lucatorto and McIlrath (ionisation following superelastic collisional heating of electrons) should yield further clarification of this. The use of an electric discharge to populate an excited level might be feasible instead of optical pumping, although further complications might thereby be introduced. The potential advantages of SERS from an excited state may therefore be limited by these features.

Generation of SERS within the singlet system of an alkaline earth would not appear to be a viable scheme due to the unfavourable ratio of oscillator strengths resulting in strong SPA of the pump; this factor may also need consideration in some excited state schemes. The generation of SERS using intersystem transitions in the alkaline earths is limited to the heavier elements; thus far fewer SERS schemes exist in the alkaline earths than in the alkalis.

Efforts to obtain a narrower linewidth IR output have resulted in the observation of a $0.2cm^{-1}$ system-limited linewidth from SERS in Ba. Comparison of theory with experiment for Ba is in contrast with similar previous work in the alkalis and may indicate the potential of still narrower linewidths. Further work using a narrower linewidth dye laser with the Ba SERS scheme is needed to verify this; this could also result in further understanding of the linebroadening mechanisms at work in the alkalis.

These mechanisms are still not fully understood, although the Ba experiments have indicated that the optical Stark effect and power broadening are both less important than our rough calculations have suggested. This would seem to point to plasma broadening and/or life-time broadening as the dominant linebroadening mechanisms. The tentative explanation of the assymetry in the Na SHRS tuning curve involving AC Stark shifts would thus perhaps seem in doubt in the light of this; it may be that some other mechanism is responsible for this assymetry.

The role of SERS as a tunable IR source has been well assessed by Cotter 1976b; the major limitation of the process has been the broad linewidth observed. The current work has indicated the potential of a narrower linewidth source, attainable using an alkaline earth. The system investigated however, in Ba, is limited in tuning range and has a higher threshold, in comparison to schemes in the alkalis; these factors limit its usefulness as a practical source. The lack of suitable energy levels and/or oscillator strengths for such systems in the alkaline earths would suggest that a narrow linewidth, wide tuning range device will probably not be realisable in this way, unless perhaps some suitable excited state scheme exists. Even so, inherent limitations of such a scheme may exist.

To positively identify the roles of the various line broadening

and shifting mechanisms must remain a high priority in any attempts to further the development of SERS as a tunable source; further work in Ba promises to yield such information.

APPENDIX 1

Feedback and Multipass Effects

In this appendix a simple explanation is presented of the physical mechanisms responsible for an increase in tuning range when a feedback or multipass scheme is used, the approach used enabling estimates of the effects to be made. The model described neglects competing mechanisms, saturation and backward wave effects, all of which may be of significance under certain conditions. Nevertheless a rough estimate of the expected behaviour may be obtained.

The starting point for this section is eqn 2.23 for the field gain of the SERS wave which is rewritten here:

$$\frac{A(L)}{A(0)} = \exp\left[\tilde{P}_p - 2\sqrt{\tilde{P}_p} / 2K\right] \arctan {}^{L}/_{b_p} \quad \ldots \text{ A1.1}$$

A.1.1 Effect of Pump Feedback

The case of pump feedback on itself may be considered to result simply in an increased pump intensity in the vapour; thus we may treat this as an effective increase in P_p or, equivalently, $\tilde{P}_p$. We may define our tuning limits as those points where the output SERS power has fallen to $P_{s_{th}}$ = 10W, which corresponds roughly to a power gain of exp (30). Without pump feedback, solving eqn A1.1 with the field gain A(L)/A(0) = exp (15) gives us the normal tuning range limits; replacing $\tilde{P}_p$ by $\tilde{P}_p(1 + x)$, where x is the fraction of pump feedback, gives us the modified tuning range limits.

Using values of χ_R for Cs for the 6s-7s transition and values of N = 1.5 x 10^{23} m^{-3} (10 torr) and Γ = 1 cm^{-1}, fig A1.1 shows the fractional increase in tuning range as a function of the amount of pump feedback for different conditions of pump power and focussing; a maximum increase of ~30% is evident in these cases. An increase slightly smaller than this was observed for our experimental case which, however, used somewhat different focussing conditions. It may be seen that the % increase in tuning range is slightly greater for larger ${}^{L}/_{b_p}$. Under tighter focussing conditions, however, competing effects such as ionisation may have to be considered.

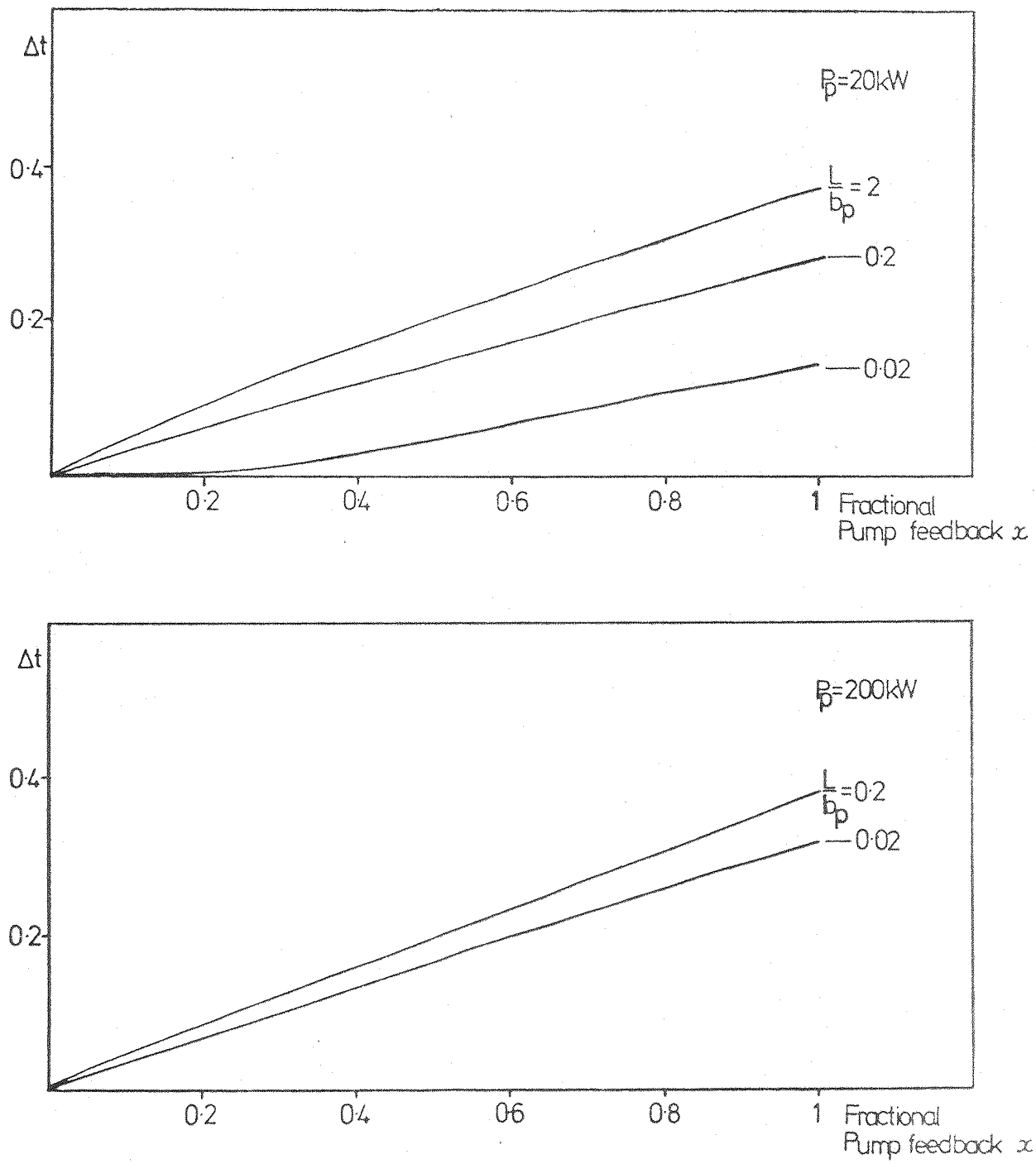

Fig A1.1 Calculated fractional increase of tuning range, Δt, as a function of degree of pump feedback. ($\Delta t = \frac{\text{increase in}}{\text{tuning range}}$ under conditions specified/tuning range under identical conditions but with zero pump feedback.)

These calculations suggest that by using pump feedback a maximum increase in tuning range of a few tens of percent might be attained.

A.1.2 Multipass

In the multipass scheme we consider the pump and IR reflected back through the vapour along a different path to its first transit; by a suitable use of reflectors it may make n such transits. Assuming 100% reflection of the pump each time and no pump depletion and also assuming the beam to be refocussed to give the same L/b_p for each transit, (this may be circumvented if a large b_p is used), then we may write the total field gain after n transits as

$$\left\{\frac{A(L)}{A(O)}\right\}^n \cdot f^{(n-1)}$$

where f is the fractional IR feedback at each reflection. Again setting this equal to exp (15) enables us to solve for the modified tuning range. Figure A1.2 displays a plot of increase in tuning range over the single pass , no feedback, case against number of transits calculated in this way. From this it may be seen that there is a significant increase gained by going to a 2-pass scheme ; as the number of passes is increased so the increase in tuning range is seen to saturate . The dependence of increase in tuning upon degree of IR feedback can be seen from fig A1.2 and is plotted explicitly in fig A1.3 for a 2 pass scheme. From this it may be seen that the degree of IR feedback can vary over orders of magnitude with little effect upon tuning range; this might be expected comparing the actual feedback signal to the spontaneous noise power.

In practice it should be borne in mind that a small amount of IR feedback would probably occur from the windows even when misaligned from the beam. The role of such window reflections has not yet been studied by ourselves; our calculation for the tuning ranges does not take this into account. Thus the analysis here may be taken as showing the qualitative behaviour of the tuning ranges as parameters are varied rather than as giving reliable absolute values.

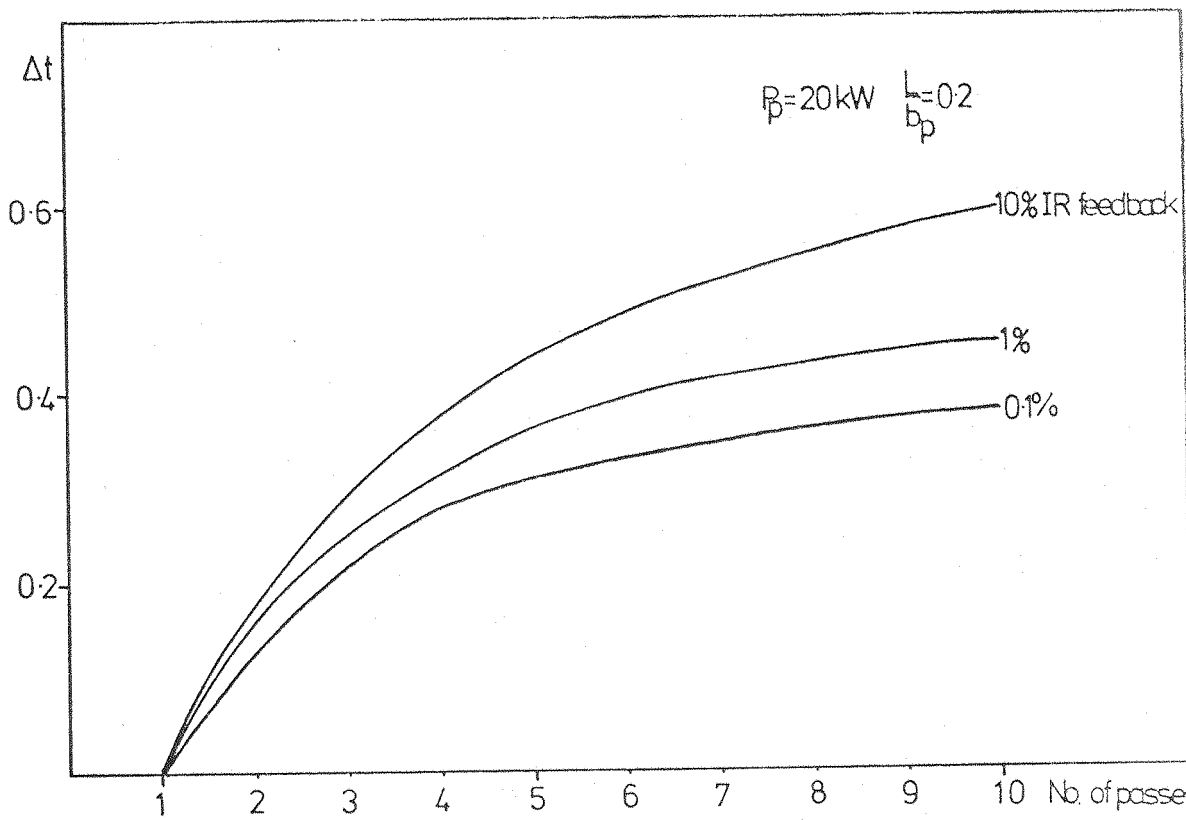

Fig A1.2 Calculated fractional increase of tuning range for a multipass scheme as a function of number of passes. ($\Delta t = \frac{\text{increase in tuning range}}{\text{tuning range}}$ under conditions specified/tuning range under identical conditions but single pass.)

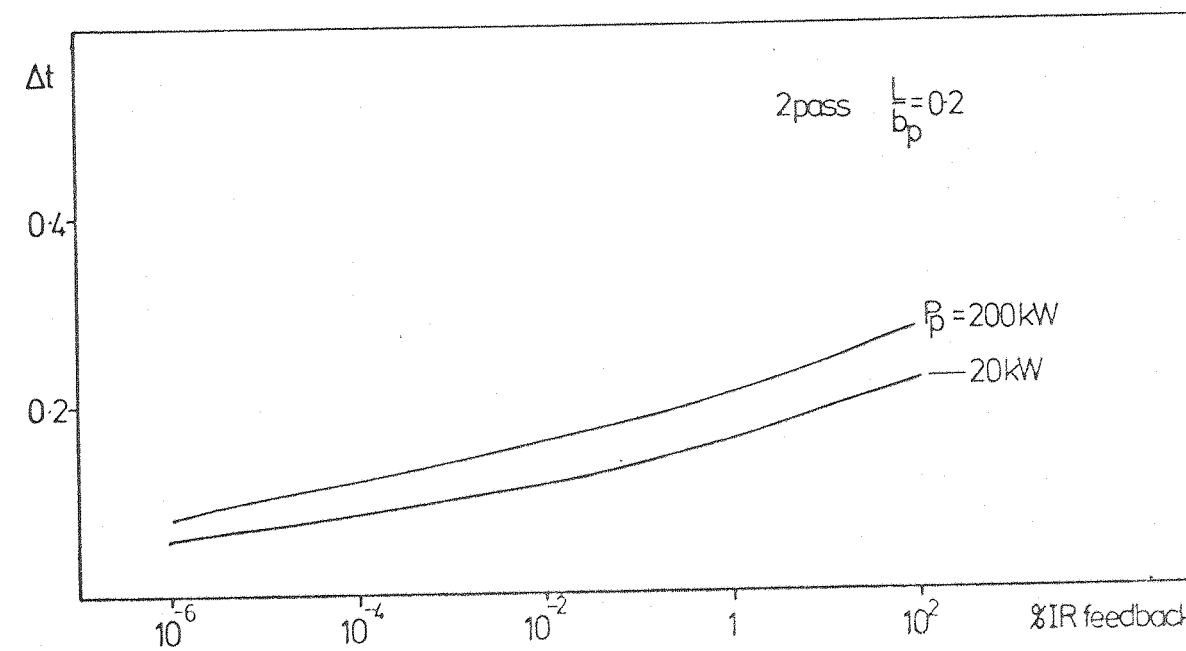

Fig A1.3 Effect of IR feedback in 2-pass scheme. ($\Delta t = \frac{\text{increase in tuning range}}{\text{tuning range}}$ under conditions specified/tuning range under identical conditions but zero IR feedback.)

From experiments we may find the optimum focussing conditions for the largest single pass tuning range, ie the optimum intensity I_p, $\propto (P_p) \times (L/b_p)$. Thus we may, by keeping this product constant at this optimum value calculate the effect of scaling the power of the pump at constant intensity for these various processes. Such a calculation would be worthwhile in any future work involving such techniques.

In order to obtain worthwhile improvements in tuning range it would be necessary to provide efficient coupling of the pump back into the vapour over several transits; possibly the easiest way of achieving this would be to use a high power loosely focussed beam with plane reflectors.

An estimate of the increase in the backward wave tuning range over the forward wave, as observed experimentally, may perhaps be obtained by considering this situation as a double pass scheme with IR feedback; obviously this neglects the dynamics of the interaction of the forward and backward travelling waves, but at the limits of the tuning range the forward SERS wave will in any case be small. From fig A1.2 we would expect an increase in tuning of ~15%, not that dissimilar from that observed. A small charge in amount of the IR feedback would not be expected to result in much change in tuning range on the basis of this model; such behaviour was in fact observed.

Figure A1.2 illustrates the saturation of improvement in tuning range with number of passes; nevertheless it is evident that a many-transit scheme is preferable to, say, a double pass one. Thus it is possible that an oscillator configuration might be beneficial. In order to obtain several round trips the pump pulse in this case might need to be longer; difficulties in attaining high power at long pulse length obviously exist. Nevertheless, use of curved mirrors to provide tight focussing of the pump in the vapour might permit the operation of such a scheme.

In conclusion, elementary calculations have indicated the possible advantages of pump feedback, multipass and oscillator schemes. Low power experiments using pump feedback (chapter 4) have indicated some improvements in tuning range; the effects of using looser focussing with higher pump powers would be of interest.

With high pump powers there would also appear to be potential for significant increases of tuning range using multipass schemes; experimental investigation of such ideas is recommended.

APPENDIX 2

Stimulated Hyper-Raman Emission from Sodium Vapour

(reprinted from Optics Communications,
vol 22, no 2, August 1977)

The following published papers were included in the bound thesis. These have not been digitised due to copyright restrictions, but the links are provided.

https://doi.org/10.1016/0030-4018(77)90017-7

APPENDIX 3

Four Wave Parametric Mixing in Na - Competition with SHRS in Na

In this appendix the behaviour of the four wave parametric mixing process, discussed in section 4.2, is examined. It is found that the single photon absorption of the parametric ω_4 wave may necessitate a consideration of the process based on the coupled wave equations. From these the behaviour of the gain for the parametric process may be assessed as a function of the frequencies involved.

A3.1 Phase Matching

In a parametric process, for high gain, a phase matching condition must be satisfied, generally $\Delta k=0$ (unless focussing is used - Bjorklund 1975). The phase mismatch, $\Delta k = 2k_1 - k_3 - k_4$, neglecting any absorption, may be expressed as

$$\Delta k = \frac{N}{2(\varepsilon_o hc)} \left(\frac{2\omega_1 \mu_1^2}{\Delta_1} - \frac{\omega_4 \mu_4^2}{\Delta} \right) \qquad \ldots \text{A3.1}$$

where $\mu = e \langle |z| \rangle$, $\Delta_1 = \Omega_{3s3p} - \omega_1$, $\Delta = \Omega_{3s4p} - \omega_4$; this is the normal Sellmeier type equation. The contribution to Δk from k_3, taken above as zero, is in fact much smaller than the k_1, k_4 terms, assuming all the population remains in the ground state.

Solution of A3.1 for $\Delta k = 0$, then, should give a value of ω_4 for which the parametric gain is highest as a function of ω_1; neglecting other influences we would expect the parametric wave to be generated at this frequency. However, performing this algebra results in a value of ω_4 within a few cm^{-1} of Ω_{3s4p} for the values of ω_1 actually used; under these conditions we find that strong SPA of the ω_4 wave is expected by the 3s-4p transition. Consequently, the frequency for optimum parametric gain might be expected to occur at some other value, further from Ω_{3s4p}. To calculate this effect we must resort to the basic gain equations of the system.

A3.2 General Approach

Starting from expressions for the respective nonlinear susceptibilities $\chi^{(5)}$ and $\chi^{(3)}$ we may write down expressions for the nonlinear polarisations induced at frequencies ω_3 and ω_4,

$$P_{NL}(\omega_3) = \frac{15}{8}\ \varepsilon_o \chi^{(5)}\ |E_1|^4\ E_3 \exp(ik_3 z)$$

$$+ \frac{3}{4}\ \varepsilon_o \chi^{(3)} |E_1|^2\ E_4^*\ \exp(i(2k_1 - k_4^*)z)$$

... A3.2a

$$P_{NL}(\omega_4) = \frac{3}{4}\ \varepsilon_o \chi^{(3)} |E_1|^2\ E_3 \exp(i(2k_1 - k_3)z) \qquad \text{... A3.2b}$$

These may then be inserted into the appropriate coupled wave equations, of the form

$$\frac{\partial E(\omega)}{\partial z} = \frac{i\mu_o \omega c}{2\eta_\omega}\ P_{NL}(\omega) \exp(-ik_\omega z) \qquad \text{... A3.3}$$

Writing this equation for $\omega=\omega_3$, ω_4 and then substituting the latter into the former we obtain a quadratic differential equation for E_3

$$\frac{\partial^2 E_3}{\partial z^2} - \left(\frac{g}{2} + i\Delta k\right) \frac{\partial E_3}{\partial z}$$

$$+ \left(i\,\frac{g}{2}\,\Delta k - \frac{\alpha}{4} \exp(-2\Delta k'' z)\right) E_3 = 0 \qquad \text{... A3.4}$$

which may be solved by standard techniques. In deriving this we have made the following definitions in order to simplify the algebra

$$g = i\,\frac{15}{8}\,\frac{\omega_3}{c}\ \chi^{(5)}\ |E_1|^4 \qquad \text{... A3.5a}$$

$$\alpha = \frac{9}{16}\,\frac{\omega_3 \omega_4}{c^2}\ \left|\chi^{(3)}\ E_1^{\,2}\right|^2 \qquad \text{... A3.5b}$$

$$\Delta k = \Delta k' + i\Delta k'' \qquad \text{... A3.5c}$$

(We generally denote a complex number by $z = z' + iz''$.)

We now consider an initial starting noise to be present at ω_3, $E_3(0)$, and define our power gains at ω_3, ω_4 as $R_{3,4}(z) = \left|\frac{E_{3,4}(z)}{E_3(0)}\right|^2$.

Pursuing the algebra gives us equations for these gains

$$R_3 = \frac{1}{|\gamma|^2} \exp\left(\left(\frac{g'}{2} - \Delta k''\right)z\right) \left|\cosh\left(\frac{\gamma z}{2} + \phi\right)\right|^2 \qquad \ldots \text{A3.6a}$$

where $\phi = \tanh^{-1}\left(\frac{\frac{g}{2} - i\Delta k}{\gamma}\right)$

and

$$R_4 = \frac{\alpha\mu}{|\gamma|^2} \cdot \exp\left(\left(\frac{g'}{2} - \Delta k''\right) z\right) \left|\sinh\left(\frac{\gamma z}{2}\right)\right|^2 \qquad \ldots \text{A3.6b}$$

where we have defined $\mu = \omega_4/\omega_3$ and

$$\gamma = \sqrt{\left(\frac{g}{2} - i\Delta k\right)^2 + \alpha} \qquad \ldots \text{A3.7}$$

The sinh and cosh terms may be expressed as a product of exponential and oscillatory terms. The equations may be compared to those describing other parametric interactions; the oscillatory behaviour is seen to dominate in the early growth of the waves, giving way, for large z, to exponential growth. In this region we may re write eqn 3.6 as

$$R_3 = \frac{1}{4|\gamma|^2} \exp\left(\left(\frac{g'}{2} - \Delta k'' + \gamma'\right) z\right) \left|\frac{g}{2} - i\Delta k + \gamma\right|^2 \qquad \ldots \text{A3.8a}$$

and

$$R_4 = \frac{\alpha\mu}{|\gamma|^2} \exp\left(\left(\frac{g'}{2} - \Delta k'' + \gamma'\right) z\right) \qquad \ldots \text{A3.8b}$$

For these equations the root γ of A3.6 has been chosen such that $\gamma' > 0$. The approximations are valid for $\gamma' z >> 1$ which is satisfied for a typical $z = L$ and for gains of the order exp (30), or even smaller in fact, and these equations may thus be used to examine the dependence of the parametric gain upon frequency.

It is hoped, by comparing the hyper-Raman and parametric gains under various conditions, to thus obtain information on the competition behaviour. Further work aimed at numerical solution of these equations is continuing.

REFERENCES

ANLIKER P, LUTHI H R, SEELIG W, STEINGER J, WEBBER H P, LEUTWYLER S, SCHUMACHER E and WOSTE L, IEEE J Quant Electron, QE13, 547, 1977.

BASTING D, OUW D, and SCHAFER F P, Optics Comms, 18, 260, 1976.

BEBB H B, Phys Rev, 149, 25, 1966.

BETHUNE D S, SMITH R W and SHEN Y R, Phys Rev Letts, 37, 431, 1976.

BJORKHOLM J E and LIAO P F, Phys Rev Letts, 33, 128, 1974.

BJORKLUND G C, IEEE J Quant Electron, QE11, 287, 1975.

BJORKLUND G C, BJORKHOLM J E, FREEMAN R R and LIAO P F, Appl Phys Letts, 31, 330, 1977.

BLOOM D M, YARDLEY J T , YOUNG J F and HARRIS S E, Appl Phys Letts, 24, 427, 1974.

BLOOM D M, BEKKERS G W, YOUNG J F and HARRIS S E, Appl Phys Letts, 26, 687, 1975a.

BLOOM D M, YOUNG J F and HARRIS S E, Appl Phys Letts, 27, 390, 1975b.

BONCH-BRUEVICH A M and KHODOVOI V A, Sov Phys Usp, 10, 637, 1968.

BROSNAN S J, FLEMING R N, HERBST R L and BYER R L, Appl Phys Letts, 30, 330, 1977.

BUCHER H and CHOW W, Appl Phys, 13, 267, 1977.

BYER R L and HERBST R L, 'Parametric Oscillation and Mixing'in SHEN 1977.

CARLSTEN J L and McILRATH T J, J Phys B, 6, L80, 1973.

CARLSTEN J L and DUNN P C, Optics Comms, 14, 8, 1975.

CARLSTEN J L, SZOKE A, and RAYMER M G, Phys Rev A, 15, 1029, 1977.

COLLES M J and PIDGEON C R, Rep Prog Phys, 38, 329, 1975.

CORNEY A and GARDNER K, 'Coherent Anti-Stokes Raman Scattering in Caesium Vapour', paper 51 presented at the 3rd National Quantum Electronics Conference, Southampton, September 1977.

COTTER D, HANNA D C, KARKKAINEN PA and WYATT R, Optics Comms, 15, 143, 1975a.

COTTER D, HANNA D C and WYATT R, Appl Phys, 8, 333, 1975b.

COTTER D, HANNA D C and WYATT R, Optics Comms, 16, 256, 1976a.

COTTER D, PhD Thesis, Southampton University, 1976b.

COTTER D. and HANNA D C, IEEE J Quant Electron (to be published) 1977a.

COTTER D, and HANNA D C, Optical and Quant Electron, 9, 509, 1977b.

EICHER H, IEEE J Quant Electron, QE11, 121, 1975.

ELGIN J, private communication (via M A Yuratich), 1977.

FAWCETT B C, IEEE J Quant Electron, QE6, 473, 1970.

FERGUSON A I and ARTHURS E G, Phys Letts, 58a, 298, 1976.

FRIEDRICH H and TREFFTZ E, J Quant Spectrosc Radiat Transfer, 9, 333, 1968.

FREY R and PRADERE F, Infrared Physics, 16, 117, 1976.

FREY R, PRADERE F, LUKASIK J and DUCUING J, Optics Comms, 22, 355, 1977.

GELTMAN S, J Phys B, 10, 3057, 1977.

GRANNEMAN E H A and VAN DER WIEL M J, J Phys B, 8, 1617, 1975.

GRANNEMAN E H A, KLEWER M, NYGAARD K J and VAN DER WIEL M J, J Phys B, 9, 865, 1976.

GRASYUK A Z, Sov J Quant Electron,4, 269, 1974.

GRIEM H R, 'Spectral Line Broadening by Plasmas', pub Academic Press 1974.

GRISCHKOWSKY D R, LANKARD J R, and SOROKIN P P, IEEE J Quant Electron, QE13, 392, 1977.

GRYNBERG G, BIRABEN F, BASSINI M and CAGNAC B, Phys Rev Letts, 37, 283, 1976.

GUSEV Y U L, MARENNIKOV S I, CHEBOTAYEV V P, Appl Phys, 14, 121, 1977.

HAMADA M, Phil Mag, 12, 50, 1931.

HANNA D C, LUTHER-DAVIES B, RUTT H N and SMITH R C, Appl Phys Letts, 20, 34, 1972.

HANNA D C, LUTHER-DAVIES B, SMITH R C and WYATT R, Appl Phys Letts, 25, 142, 1974.

HANNA D C, KARKKAINEN P A and WYATT R, Optical and Quant Electron, 7, 115, 1975.

HANSON R K, Appl Optics, 16, 1479, 1977.

HARTIG W, Appl Phys (to be published).

HERZBERG G, 'Spectra of Diatomic Molecules', pub Van Nostrand, 1950, et subseq.

HINDMARSH W R, in 'Atoms, Molecules and Lasers', pub Int'l Atomic Energy Authority, 1974.

HINKLEY E D, 'Laser Monitoring of the Atmosphere', pub Springer-Verlag, 1976.

HINNOV E and OHLENDORF W, J Chem Phys, 50, 3005, 1969.

HOLSTEIN T, Phys Rev, 83, 1159, 1951.

HONIG R and KRAMER D, RCA Review, p 285, June 1969.

KARKKAINEN P A, PhD Thesis, Southampton University, 1975.

KARKKAINEN P A, Appl Phys, 13, 159, 1977.

KATO K, IEEE J Quant Electron, QE10, 622, 1974.

KATO K, Optics Comms, 19, 18, 1976.

KELLY F M, KOH T K and MATHUR M S, Can Jnl Phys, 52, 795, 1973.

KILDAL H and DEUTSCH T F, 'Optically Pumped Gas Lasers' in MOORADIAN et al, 1976.

KILDAL H and BRUECK S R J, Phys Rev Letts, 38, 347, 1977.

KLEWER M, BEERLAGE M J M, GRANNEMAN E H A and VAN DER WIEL M J, J Phys B, 10, L243, 1977.

KOROLEV F A, ODINTSOV V I, FAKHMI A O, Opt Spectrosc, 40, 242, 1976.

KUHL J and SCHMIDT W, Appl Phys, 3, 251, 1974.

KUNG R T V and ITZKAN I, Appl Phys Letts, 29, 780, 1976.

LAMBDA-PHYSIK Gmbh and Co, Gottingen, Germany, private communication, 1977.

LAMBROPOULOS P and TEAGUE M R, J Phys B, 9, 587, 1976.

LAPP M and HARRIS L P, J Quant Spectrosc Radiat Transfer, 6, 169, 1966.

LAU A M F, BISCHEL W K, RHODES C K and HILL R M, Appl Phys Letts, 29, 245, 1976.

LAYCOCK L, private communication, 1977.

LEE C, private communication, 1977.

LETOKHOV V A and CHEBOTAYEV V P, 'Nonlinear Laser Spectroscopy', pub Springer-Verlag, 1977.

LIAO P F and BJORKHOLM J E, Phys Rev Letts, 34, 1, 1975.

LIAO P F and BJORKHOLM J E, Optics Comms, 16, 392, 1976.

LIN C, STOLEN R H, and COHEN L G, Appl Phys Letts, 31, 97, 1977.

LOUDON R, 'The Quantum Theory of Light', pub OUP, 1973.

LOY M M T, SOROKIN P P and LANKARD J R, Appl Phys Letts, 30, 415, 1977.

LUCATORTO T B, McILRATH T J, Phys Rev Letts, 37, 428, 1976.

MAX E and ENG S T, Optical and Quant Electron, 9,411, 1977.

McILRATH T J and LUCATORTO T B, Phys Rev Letts, 38, 1390, 1977.

McFARLAND B B, Appl Phys Letts, 10, 208, 1967.

MEASURES R M, J Appl Phys, 48, 2673, 1977.

MILES B M and WIESE W L, Atomic Data, 1. 1, 1969.

MILES B M and WIESE W L, 'Bibliography on Atomic Transition Probabilities', NBS Special Publication no 320, US Department of Commerce, 1970. Also Supplement 1 to the above, FUHR J R and WIESE W L, 1971.

MILES R B and HARRIS S E, IEEE J Quant Electron, QE9, 470, 1973.

MIYAZOE Y and MAEDA M, Appl Phys Letts, 12, 206, 1968.

MOLLENAUER L F and OLSEN D H, J Appl Phys, 46, 3109, 1975.

MOORADIAN A et al (eds), 'Tunable Lasers and Appliciations', Proceedings of the Loen Conference, Norway, 1976, pub Springer-Verlag, 1976.

MOORE C E, 'Atomic Energy Levels', NBS circular no 467, vol 1, 1949; vol 2, 1952; vol 3, 1958; pub US Department of Commerce.

NESMEYANOV A N, 'Vapour Pressure of the Chemical Elements', pub Elsevier, 1963.

NEW G H C, private communication, 1977.

OETTINGER P E and DEWEY C G (JNR), 'Lasing Efficiency and Photochemical Stability of Infrared Laser Dyes in the 710-1080nm Spectral Region', IEEE Journal of Quant. Electron., QE12, 95, 1976.

PARKINSON W H, REEVES E M and TOMKINS F S, J Phys B, 9, 157, 1976.

PATEL C K N, CHANG T Y and NGUYEN V T, Appl Phys Letts, 28, 603, 1976.

POLIAKOFF M, DAVIES B, McNEISH A, SMITH K P and TURNER J J, 'Infrared Laser Induced Photochemistry at Low Temperatures', in WEST 1977,p 222.

ROKNI M and YATSIV S, Phys Letts, 24a, 277, 1967.

ROMANEK K M, HILDEBRAND O and GOBEL E, Optics Comms, 21, 16, 1977.

RULLIERE C and RAYEZ J, Appl Phys,11, 377, 1976.

RULLIERE C, MORAND J P, and DE WITTE O, Optics Comms, 20, 339, 1977.

SARJEANT W J, ALCOCK A J and LEOPOLD K E, Appl Phys Letts, 30, 635, 1977.

SAX N I, (ed), 'Dangerous Properties of Industrial Materials', pub Van Nostrand Reinhold, 1968.

SCHAFER F P, (ed), 'Dye Lasers', pub Springer-Verlag, 1973.

SCHAFER F P, in MOORADIAN, 1976.

SCHIMITSCHEK E J and TRIAS J A, Optics Comms, 16, 313, 1976.

SCHINS H E J, VAN WIJK W M and DORPEMA B, Z Metallkde, 62, 330, 1977.

SHEN Y R,(ed), 'Nonlinear IR Generation', pub Springer-Verlag, 1977.

SOROKIN P P and LANKARD J R, IBM J Res Devel, 10, 162, 1966.

SOROKIN P P, SHIREN N S, LANKARD J R, HAMMOND E C and KAZYAKA T G, Appl Phys Letts, 10, 44, 1967a.

SOROKIN P P, LANKARD J R, HAMMOND E C and MORUZZI V L, IBM J Res Devel, 11, 130, 1967b.

SOROKIN P P and LANKARD J R, Phys Rev, 186, 342, 1969.

SOROKIN P P, WYNNE J J and LANKARD J R, Appl Phys Letts, 22, 342, 1973.

STAPPAERTS E A, HARRIS S E and YOUNG J F, Appl Phys Letts, 29, 669, 1976.

STULL D R and SINKE G C, 'Thermodynamic Properties of the Elements', Advances in Chemistry Series,v18, pub Amer Chem Soc, USA, 1956.

TEAGUE M R and LAMBROPOULOS P, J Phys B, 9, 1251, 1976.

VIDAL C R and COOPER J, J Appl Phys, 40, 3370, 1969.

VIDAL C R and HALLER F B, Rev Sci Instrum, 42, 1779, 1971.

VIDAL C R and HESSEL M M, J Appl Phys, 43, 2776, 1972.

VREHEN Q H F and HIKSPOORS H M J, Optics Comms, 18, 113, 1976.

VREHEN Q H F and HIKSPOORS H M J, Optics Comms, 21, 127, 1977.

WALLACE S G and ZDASIUK G, Appl Phys Letts, 28, 449, 1976.

WALTHER M, 'Atomic and Molecular Spectroscopy with Lasers', pub Springer-Verlag, 1975.

WANG C C and DAVIS L I (JNR), Phys Rev Letts, 35, 650, 1975.

WARD J F and SMITH A V, Phys Rev Letts, 35, 653, 1975.

WARNER B, Mon Not R astr Soc, 139, 115, 1968.

WEAST R C,(ed), 'Handbook of Chemistry and Physics', pub The Chemical Rubber Co, 1971, (52nd edition).

WEST M, (ed), Digest of the 'Lasers in Chemistry' Conference , 31 May - 2 June, London, 1977, pub Elsevier, 1977.

WIESE W L, SMITH M W and MILES B M, 'Atomic Transition Probabilities', vol 2, NSRDS-NBS 22, pub US Department of Commerce, 1969.

WYATT R, PhD Thesis, Southampton University, 1976.

WYATT R, TURNER A J and SMITH R C, 'Performance Characteristics and Applications of a Lithium Niobate Optical Parametric Oscillator', in WEST, 1977, 383 .

WYNNE J J, SOROKIN P P and LANKARD J R, 'Laser Spectroscopy', Proceedings of the Laser Spectroscopy Conference, Vail, Colorado, June, 1973,p 103, pub Plenum, 1973.

WYNNE J J and SOROKIN P P, 'Optical Mixing in Atomic Vapours', in SHEN, 1977.

YURATICH M A and HANNA D C, J Phys B, 9, 729, 1976.

YURATICH M A, PhD Thesis, Southampton University, 1977a.

YURATICH M A, private communication, 1977b.

YATSIV S, ROKNI M, BARAK S, IEEE J Quant Electron, QE4, 900, 1968.